Machine-learning interatomic potentials

an automated tool of accelerating ab initio materials modeling

Alexander Shapeev, Skoltech

USPEX SCHOOL 2020,

organized with support from:

RSF | Russian Science Foundation

I am a mathematician

- 1997-2014: BSc, MSc, PhD, 2 postdocs in Mathematics (Computational Fluid Mechanics, Numerical Methods)
- Since 2014: application of (ideas of) Machine learning to interatomic interaction models (mostly, materials)

My interest:

- technology (“the how”) of machine-learning interatomic potentials (as opposed to the science /“the what and why”/ of atomistic simulations)

Molecular modeling

- ~40% of supercomputing time is spent on Molecular Modeling

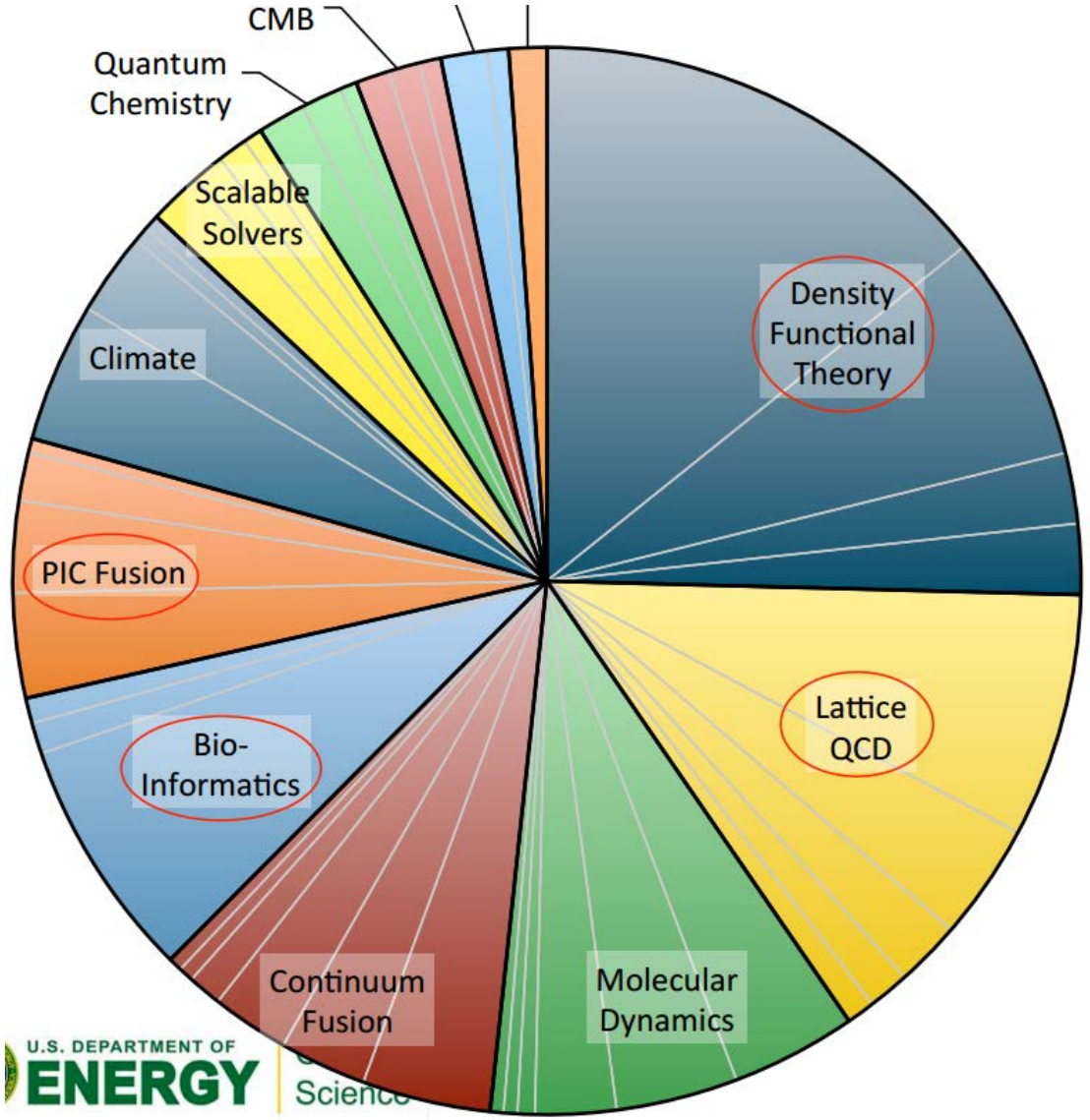

[Adopted from nersc.gov]

Motivation:

more and more materials properties
can be computed with DFT

Ab initio Melting point calculation

Aluminum (8x8x8 k-point mesh):

Zhu, Körmann, Ruban, Neugebauer, Grabowski (2020):

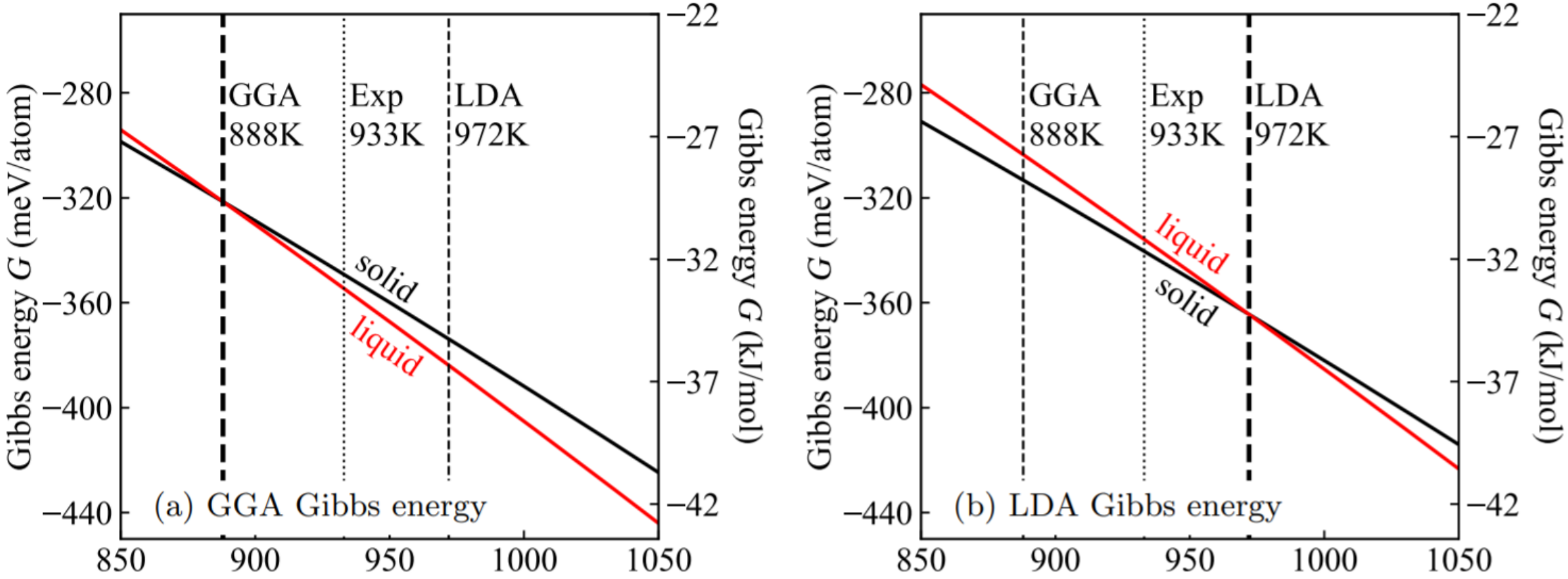

From rapid prototyping to high performance computing

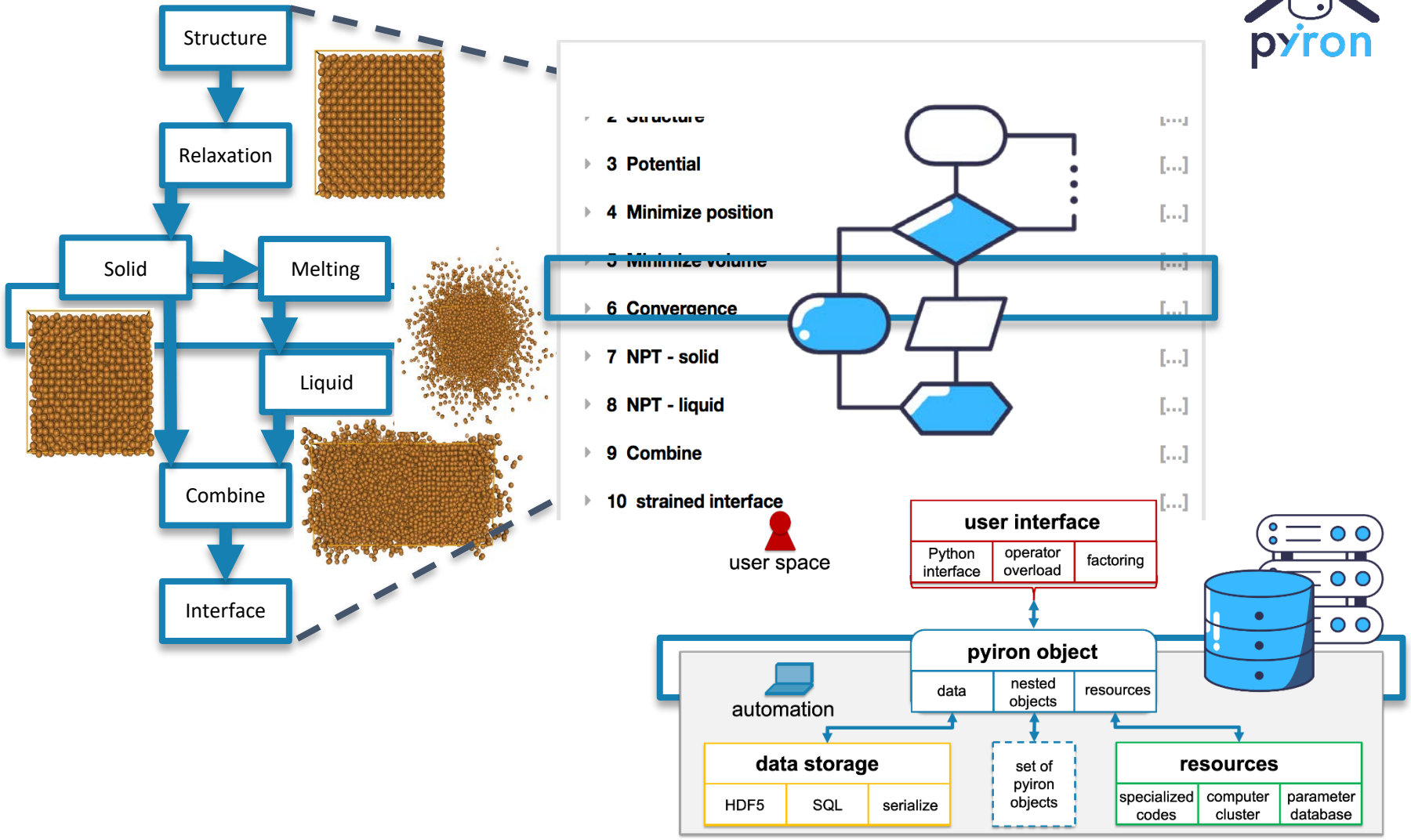

J. Janssen, et al., Comp. Mat. Sci. 161 (2019) - http://pyiron.org - https://github.com/pyiron/

www.aflowlib.org/superalloys/

46. AlInNi
47. AlIrNi
48. AlLiNi ▲
49. AlMgNi
50. AlMnNi ▲
51. AlMoNi
52. AlNbNi ▲
53. AlNiOs ▲
54. AlNiPd
55. AlNiPt ▲
56. AlNiRe
57. AlNiRh ▲
58. AlNiRu ▲
59. AlNiSb ▲
60. AlNiSc ▲
61. AlNiSi ▲
62. AlNiSn
63. AlNiSr
64. AlNiTa ▲
65. AlNiTc
66. AlNiTi ▲
67. AlNiTl
68. AlNiV ▲
69. AlNiW
70. AlNiY ▲
71. AlNiZn ▲
72. AlNiZr ▲
73. AuBeNi
74. AuCaNi
75. AuCdNi
76. AuCoNi
77. AuCrNi
78. AuCuNi
79. AuFeNi
80. AuGaNi

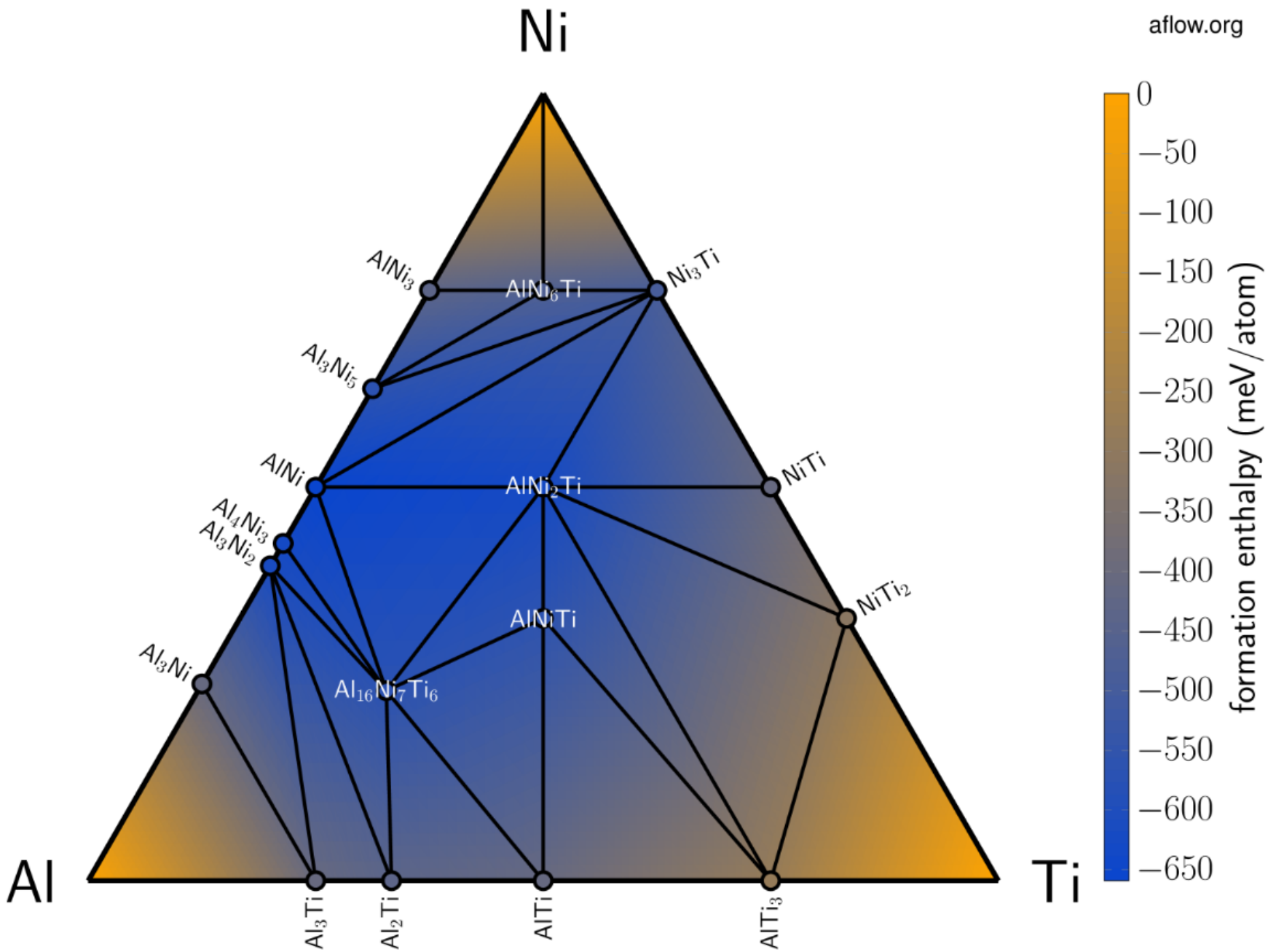

Prediction of convex hull of stable alloys

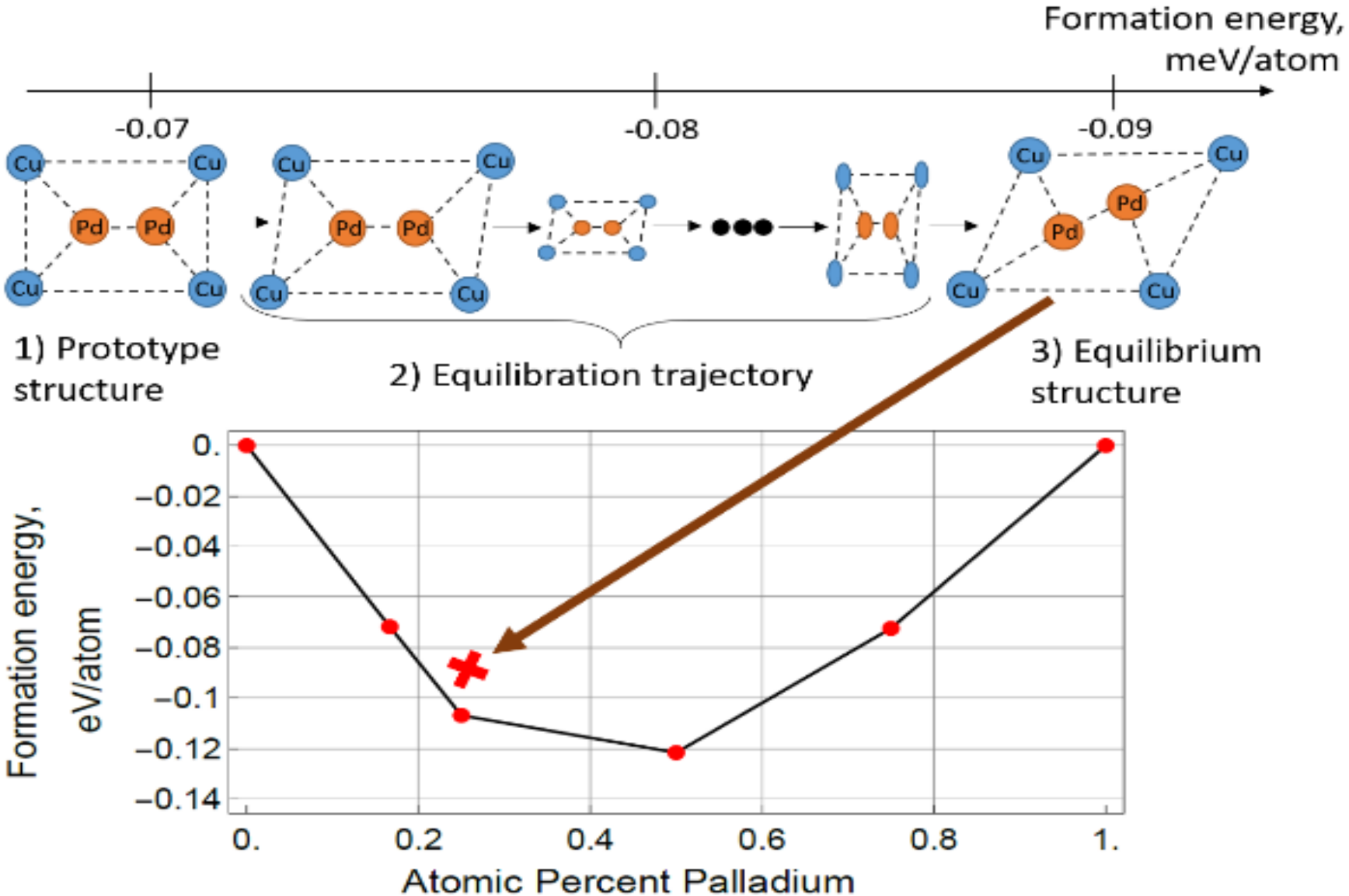

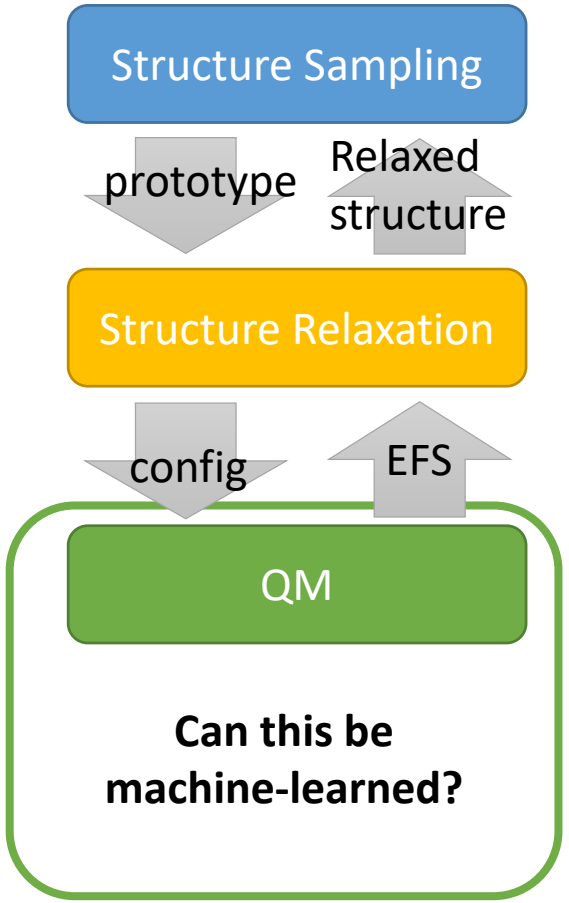

Machine-learning interatomic potentials

My perspective

Machine learning as interpolation,

… data-driven and multidimensional.

- Problem: Given $E^{\mathrm{qm}}(\boldsymbol{X})$, interpolate it with $E(\boldsymbol{X})$
- Issue: no transferability w.r.t. the number of atoms
- Solution: <u>use locality</u>! (An atom interacts only with 10-100 neighboring atoms)

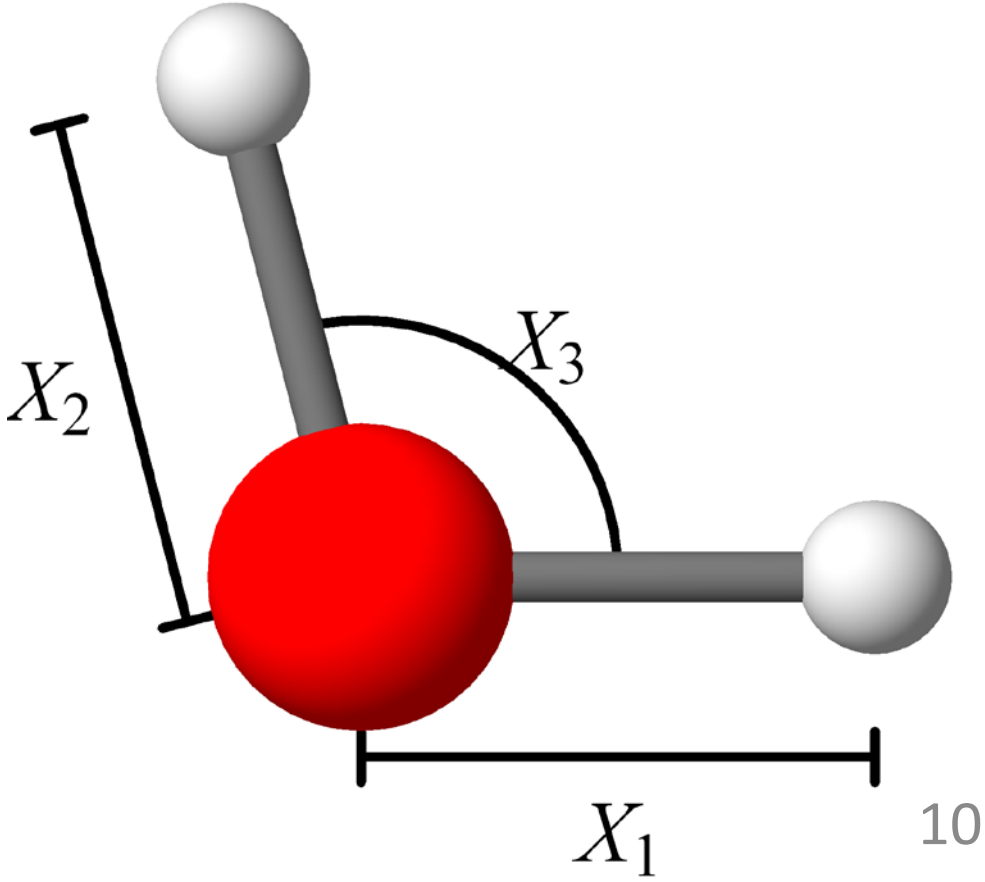

Locality: Energy

$$E = \sum_i V(r_{i1}, r_{i2}, \dots)$$

- Most interatomic potentials are covered. (Coulomb should be added explicitly.)

- Problem: find a good *V.*

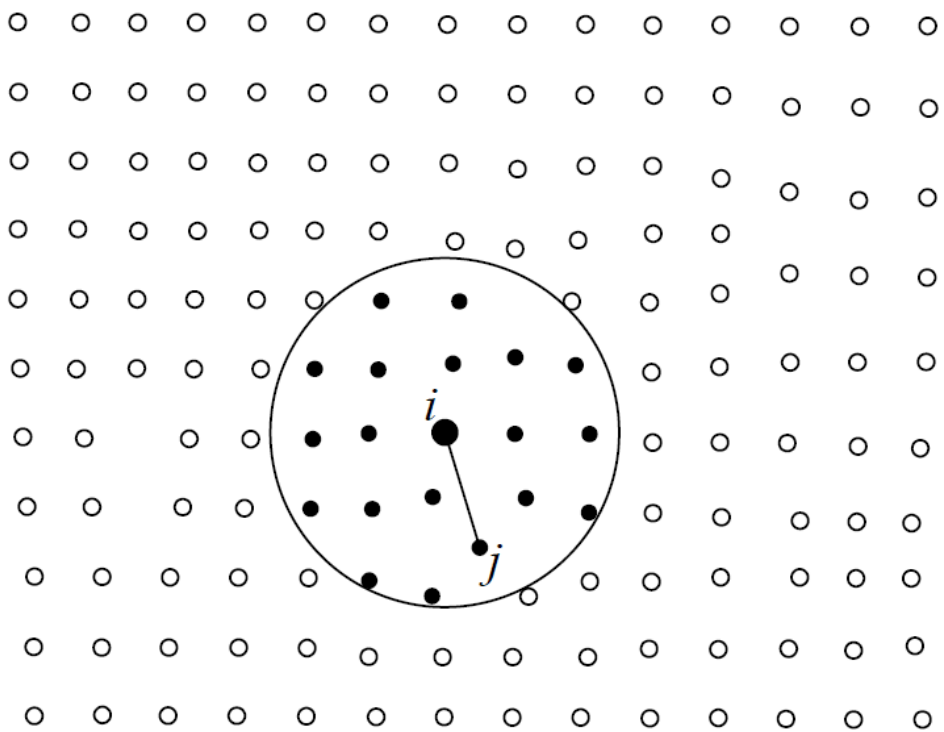

Traditional fitting

- Embedded atom model: $E = \sum_i V(r_{i1}, r_{i2}, \dots)$,
- $V(\boldsymbol{r_i}) = \sum_j \varphi(r_{ij}) + F\left(\sum_j \rho(r_{ij})\right)$.
- Early interatomic potentials (=force fields) had few (three) parameters fitted from few experimental data (elastic constants, defect formation energy, etc.)
- Later potentials have tens of coefficients (e.g., spline coefficients) fitted from the QM data.
- What is different now: <u>there are lots of data</u>!
- So, the question is: *how to incorporate lots of data into the models*?

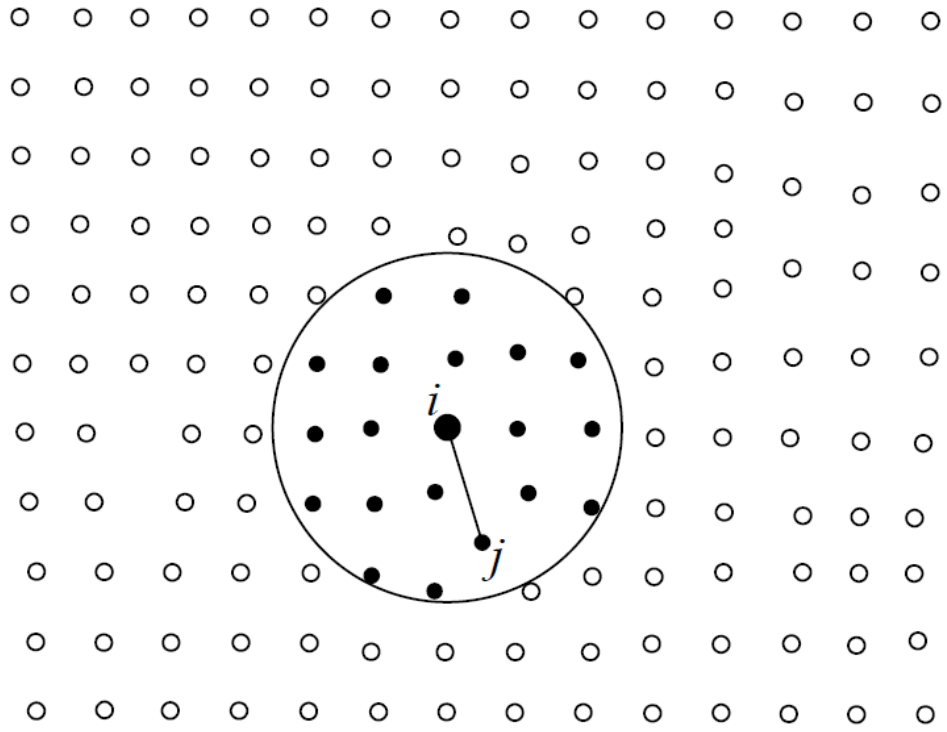

Machine-learning ideology:

1. Choose a (machine-learning) model $E = E(\boldsymbol{x})$
   ($\boldsymbol{x}$ is an atomic configuration)
2. We want to minimize $|E^{\mathrm{qm}} - E|$.
   So we:

- Generate data: $\boldsymbol{x}^{(1)}, \boldsymbol{x}^{(2)}, \ldots; E^{\mathrm{qm}}\left(\boldsymbol{x}^{(1)}\right), E^{\mathrm{qm}}\left(\boldsymbol{x}^{(2)}\right), \ldots, \boldsymbol{f}^{\mathrm{qm}}\left(\boldsymbol{x}^{(1)}\right), \ldots$
- Minimize on data: $\sum_i \left|E\left(x^{(i)}\right) - E^{\mathrm{qm}}\left(x^{(i)}\right)\right|^2 + (\mathrm{forces}) + \ldots$

But what if sampling the right $\boldsymbol{x}^{(i)}$
is a part of the problem?

Illustration: calculating convex hull

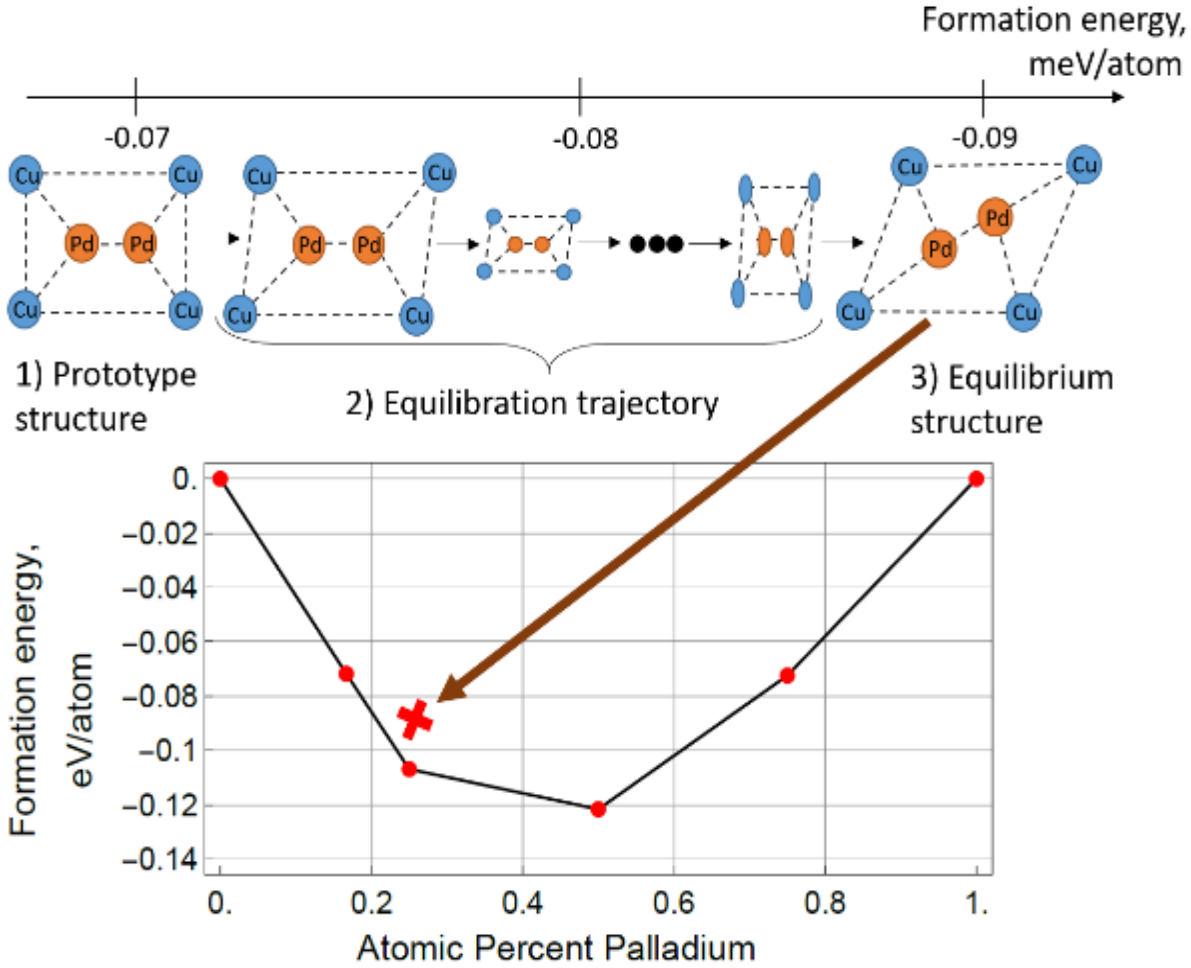

Problem:

- accurate sampling of ground state structures

needs

- accurate approximation of PES

which needs

- accurate sampling of ground state structures

which needs …

Solution: Active learning / Learning on-the-fly

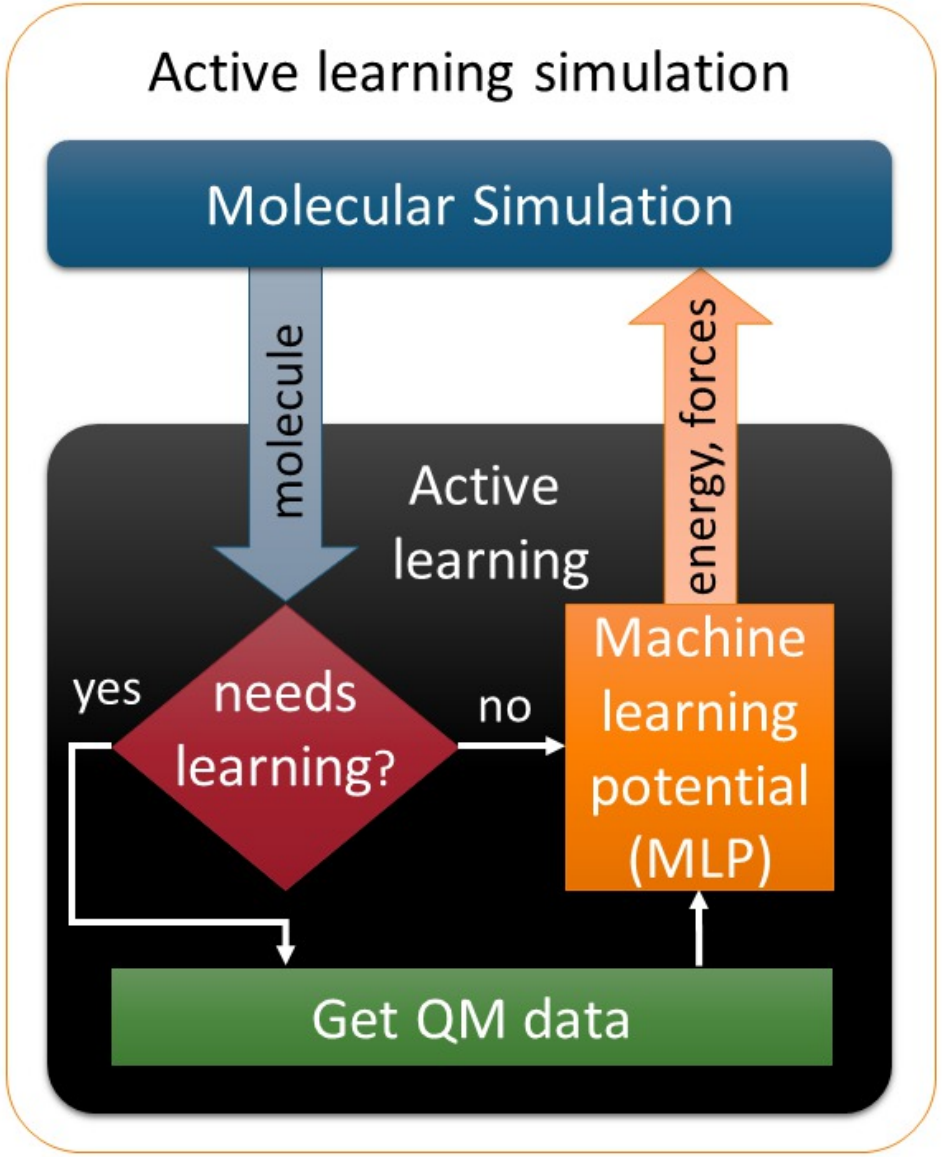

Overview

1. **Overview**
2. **Moment Tensor Potentials**
3. Active learning (how to learn while sampling a PES)
4. Applications

Moment Tensor Potentials: descriptors

Descriptors of atomic environments:

- Moments of inertia of surrounding atoms
- They satisfy the needed symmetries (rotation, permutation, translation, …);
- **Math:**
- $M_{n,m}(\boldsymbol{r}_{\boldsymbol{i}\cdot}) = \sum_j \boxed{f_n(|r_{ij}|)} \boxed{\underbrace{r_{ij} \otimes \cdots \otimes r_{ij}}_{m \text{ times}}}$

Radial term: extracting shells of neighboring atoms

Angular term: shell orientations

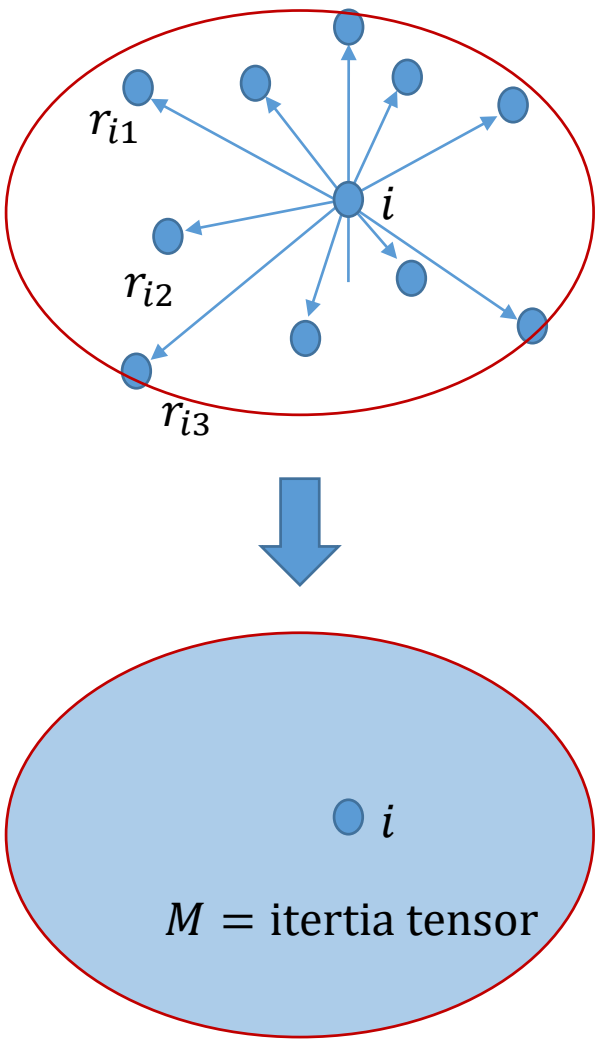

Moment Tensor Potentials, basis functions

- $V(\boldsymbol{u};\theta) = \sum_\alpha \theta_\alpha B_\alpha(\boldsymbol{u})$
- $B_\alpha(\mathbf{u})$ are (all) different multiplications (contractions) of inertia tensors $M_{m,n}(\mathbf{u})$ yielding a scalar.

Theorem:

- $B_\alpha(\mathbf{u})$ is an (over-)complete basis

Equiv. to Atomic Cluster Expansion [*Drautz (2019)*], see

[Bachmayr, Csanyi, Dusson, Etter, van der Oord, Ortner (2020)]

Learning curves

Database (Csanyi, Bartok, Szlachta, 2014)

- Tungsten: uniform and perturbed lattices, vacancies, dislocations

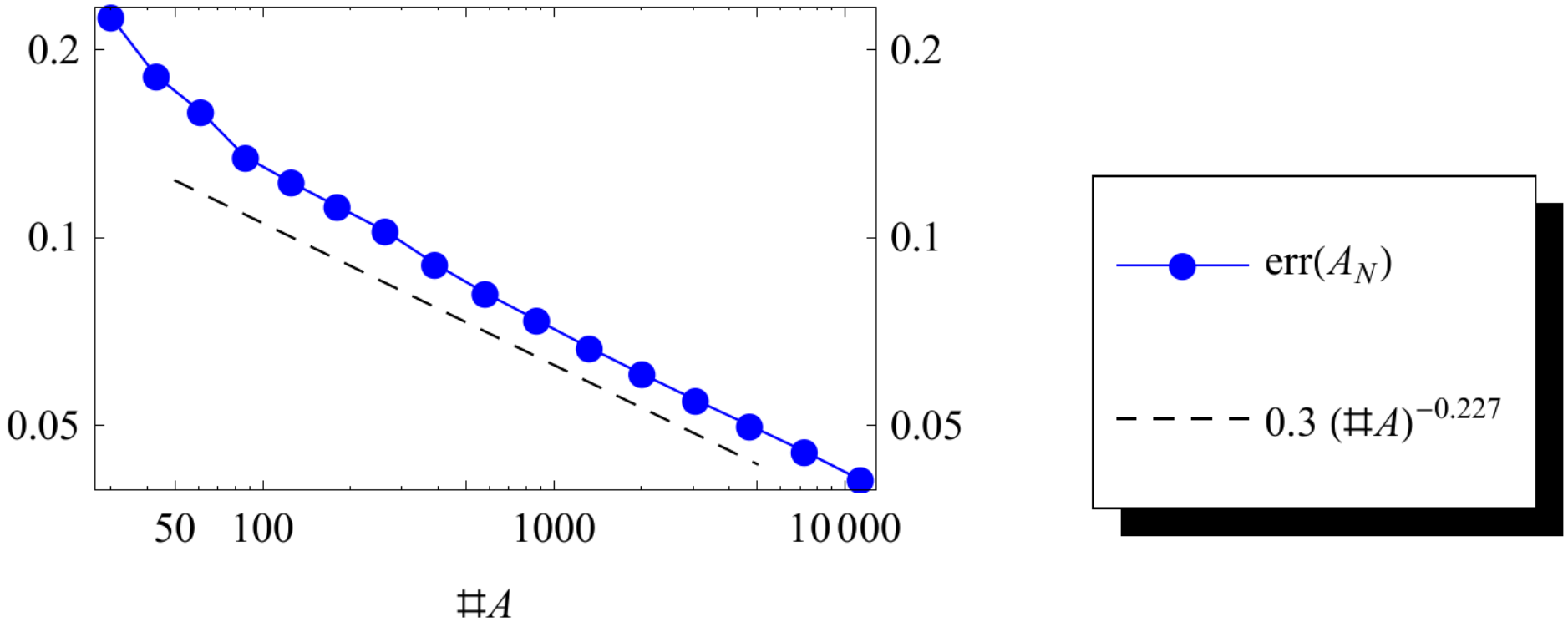

Performance tests

Database (Csanyi, Bartok, Szlachta, 2014)

- Tungsten: uniform and perturbed lattices, vacancies, dislocations

Potential:	GAP	MTP_1	MTP_2
CPU time/atom [ms]:	134	2.9	0.8
basis functions:	10 000	11 133	760
Fit errors:			
force RMS error [eV/Å]:	0.0633	0.0427	0.0633
[%]:	4.2%	2.8%	4.2%
Cross-validation errors:			
force RMS error[eV/Å]:	-	0.0511	0.0642
[%]:	-	3.4%	4.3%

Comparison with more methods

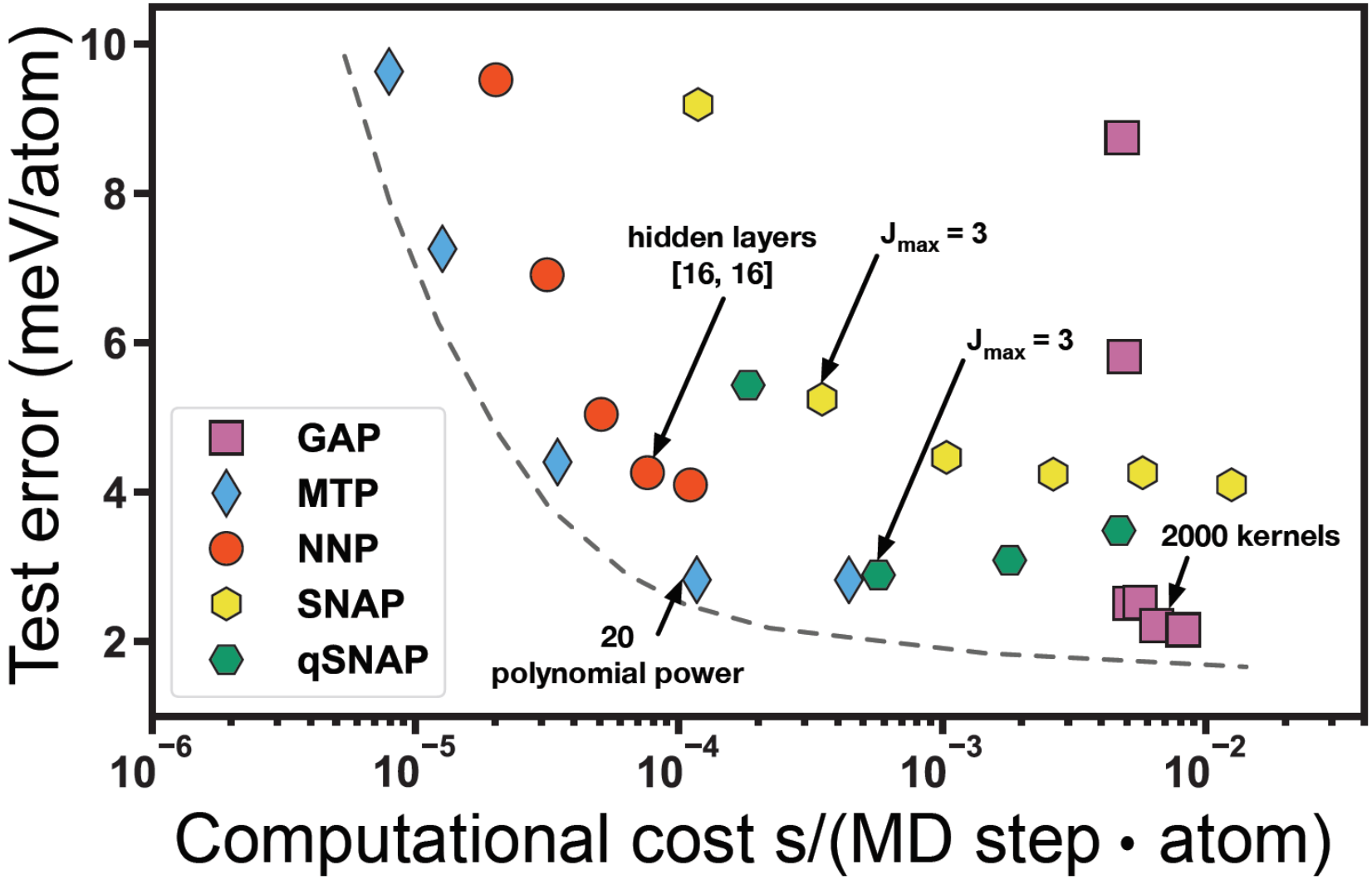

Yunxing Zuo,
Chi Chen,
Xiangguo Li,
Zhi Deng,
Yiming Chen,
Jörg Behler,
Gábor Csányi,
A.S.,
Aidan P. Thompson,
Mitchell A. Wood,
Shyue Ping Ong.
arXiv:1906.08888

Extrapolation, reliability, and active learning

Pathway between two equilibrium AgPd structures

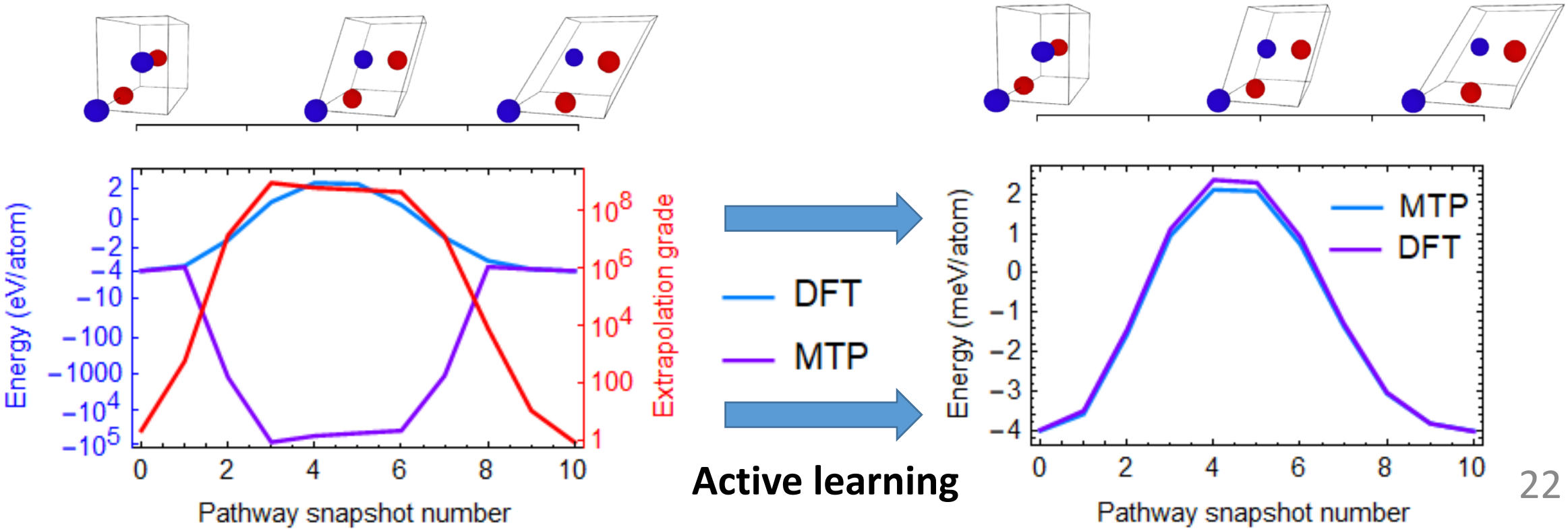

Active Learning of Interatomic Potentials

Active learning

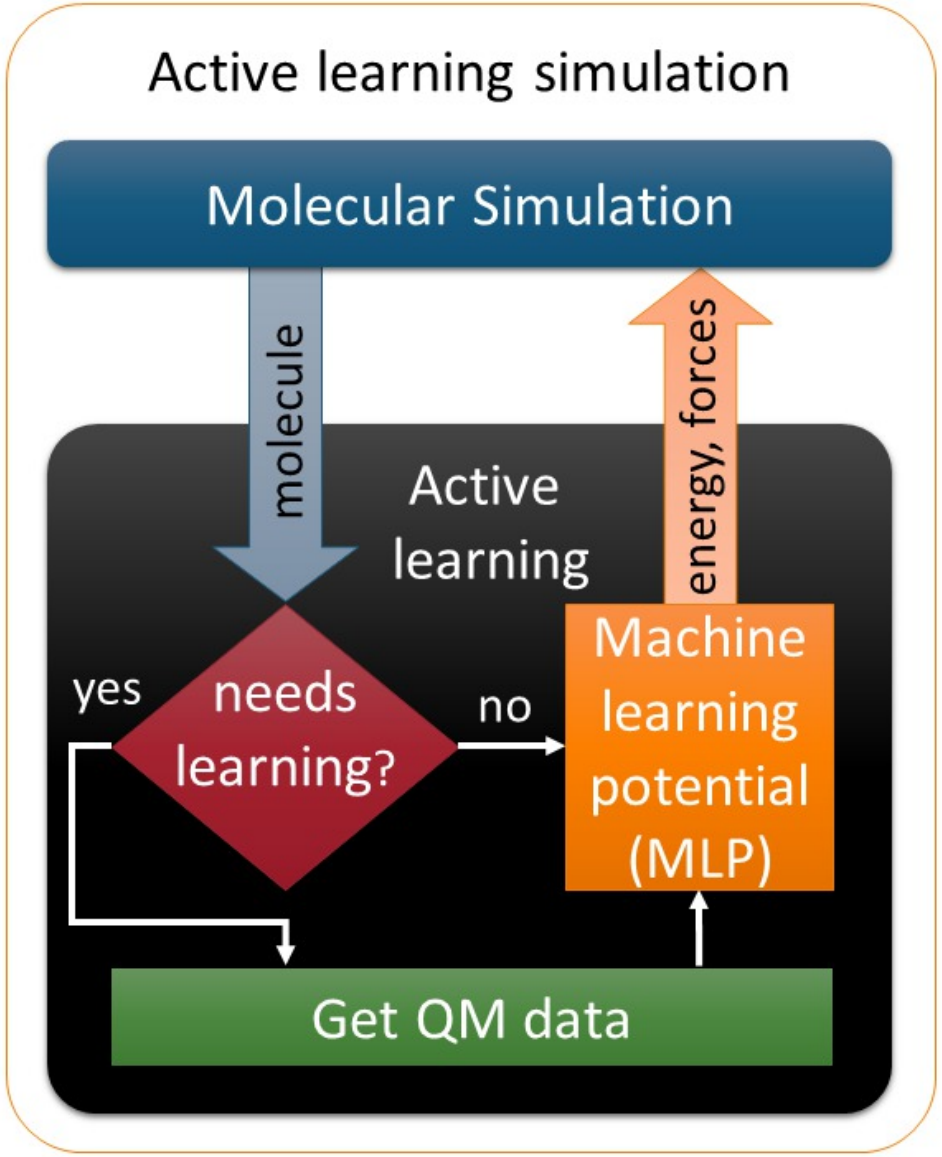

Active Learning of MLIP: Motivation

Higher accuracy => More parameters to fit => Lower transferability

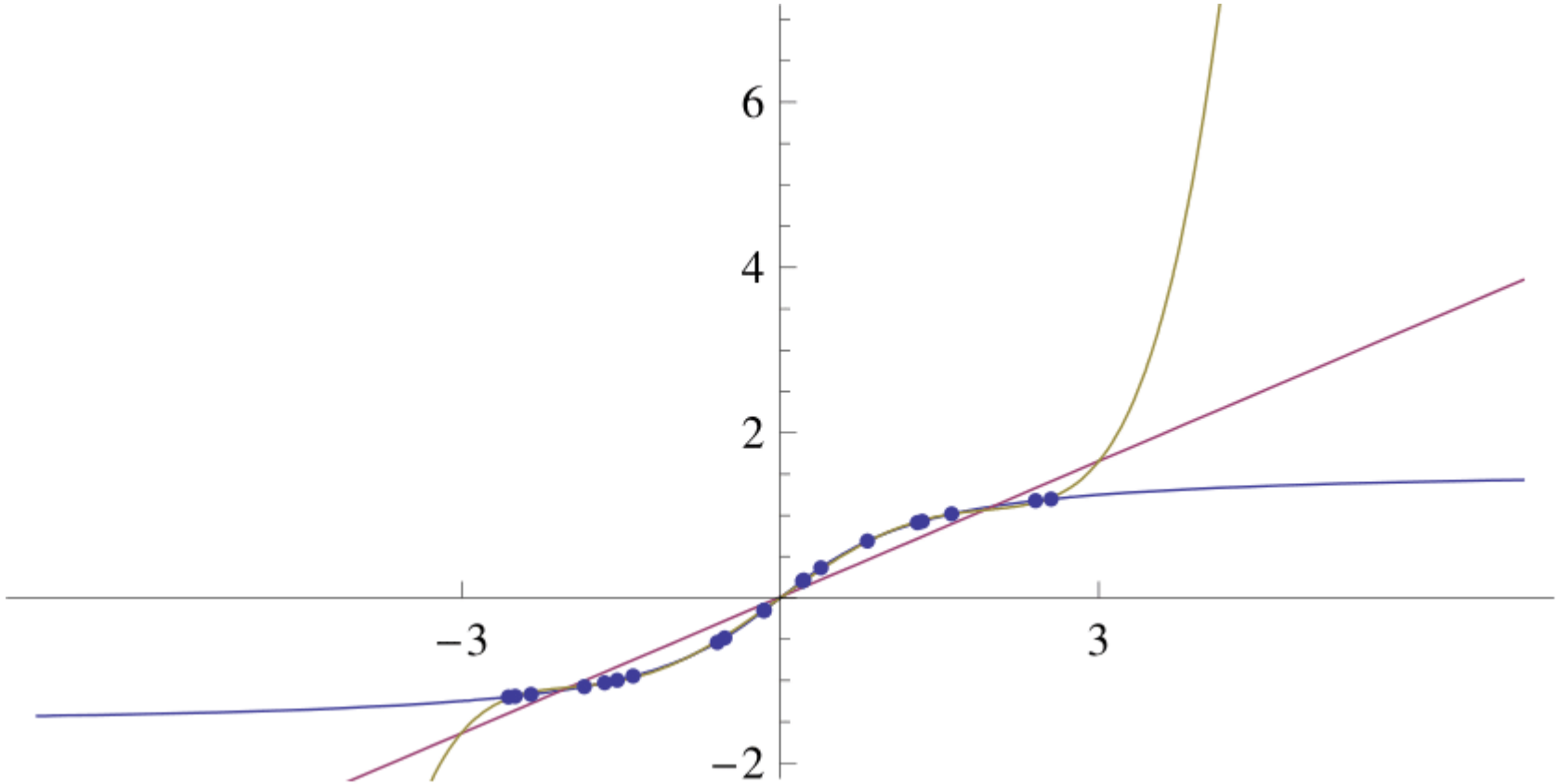

Active learning

Solution: detect when we are extrapolating and switch on learning

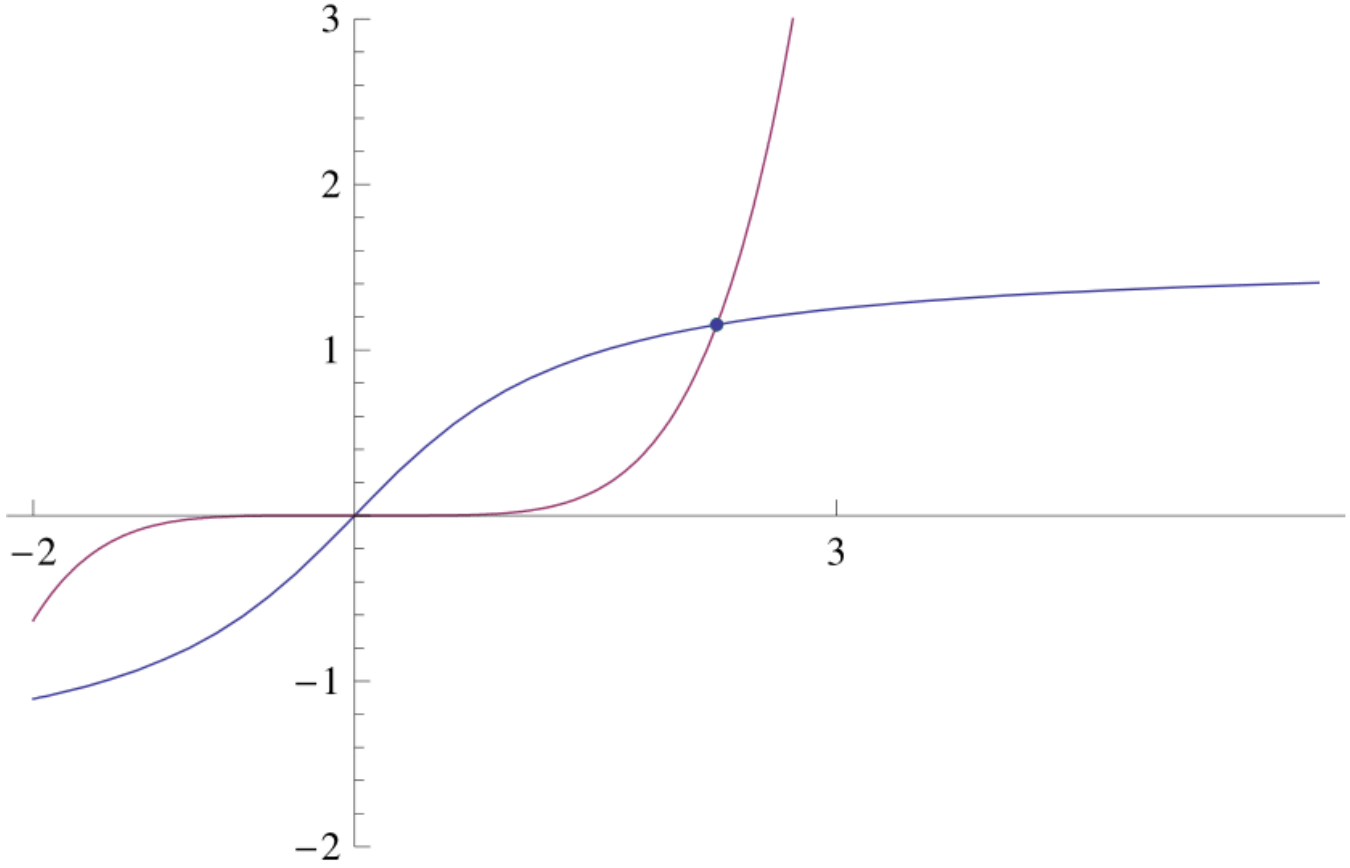

Active learning

Solution: detect when we are extrapolating and switch on learning

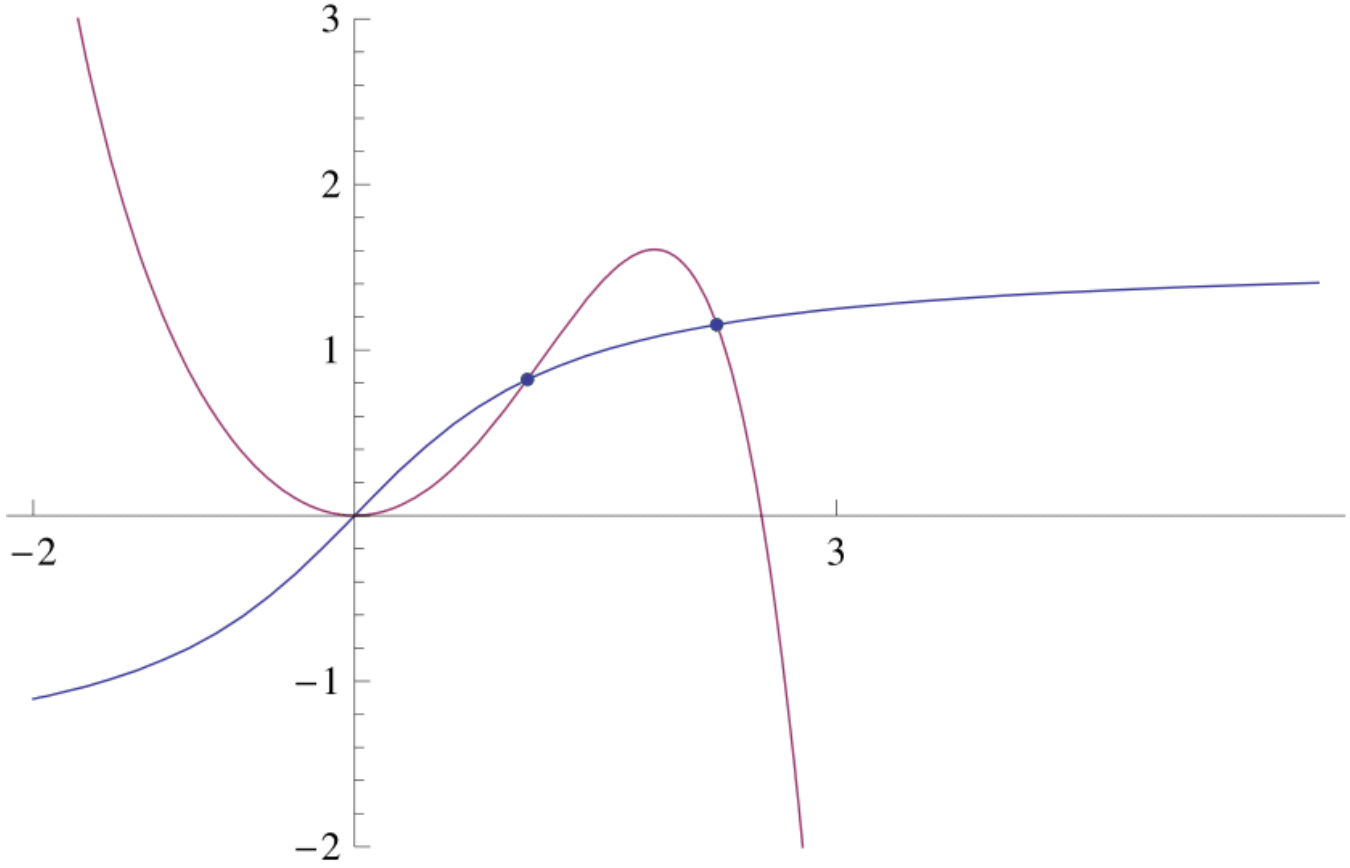

Active learning

Solution: detect when we are extrapolating and switch on learning

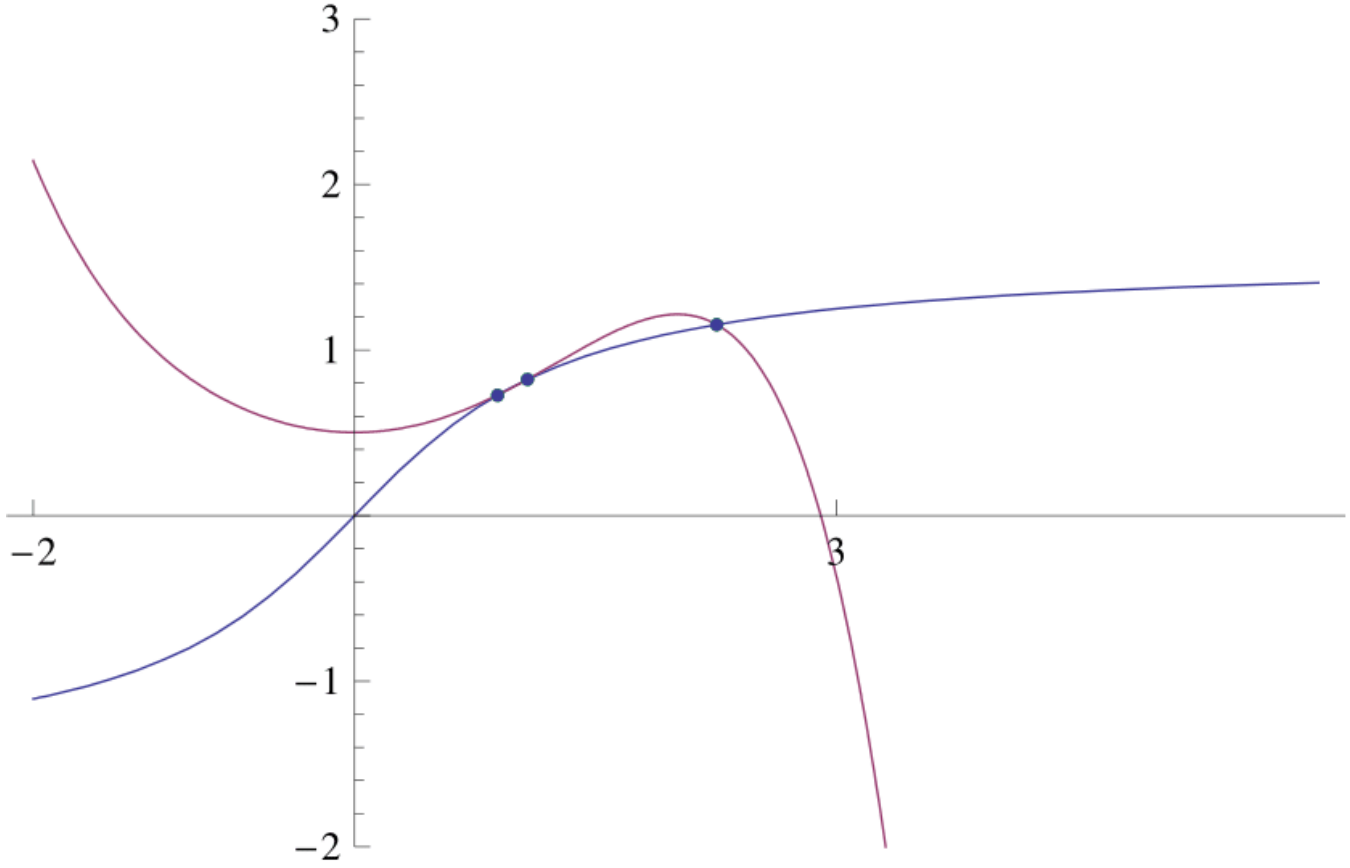

Active learning

Solution: detect when we are extrapolating and switch on learning

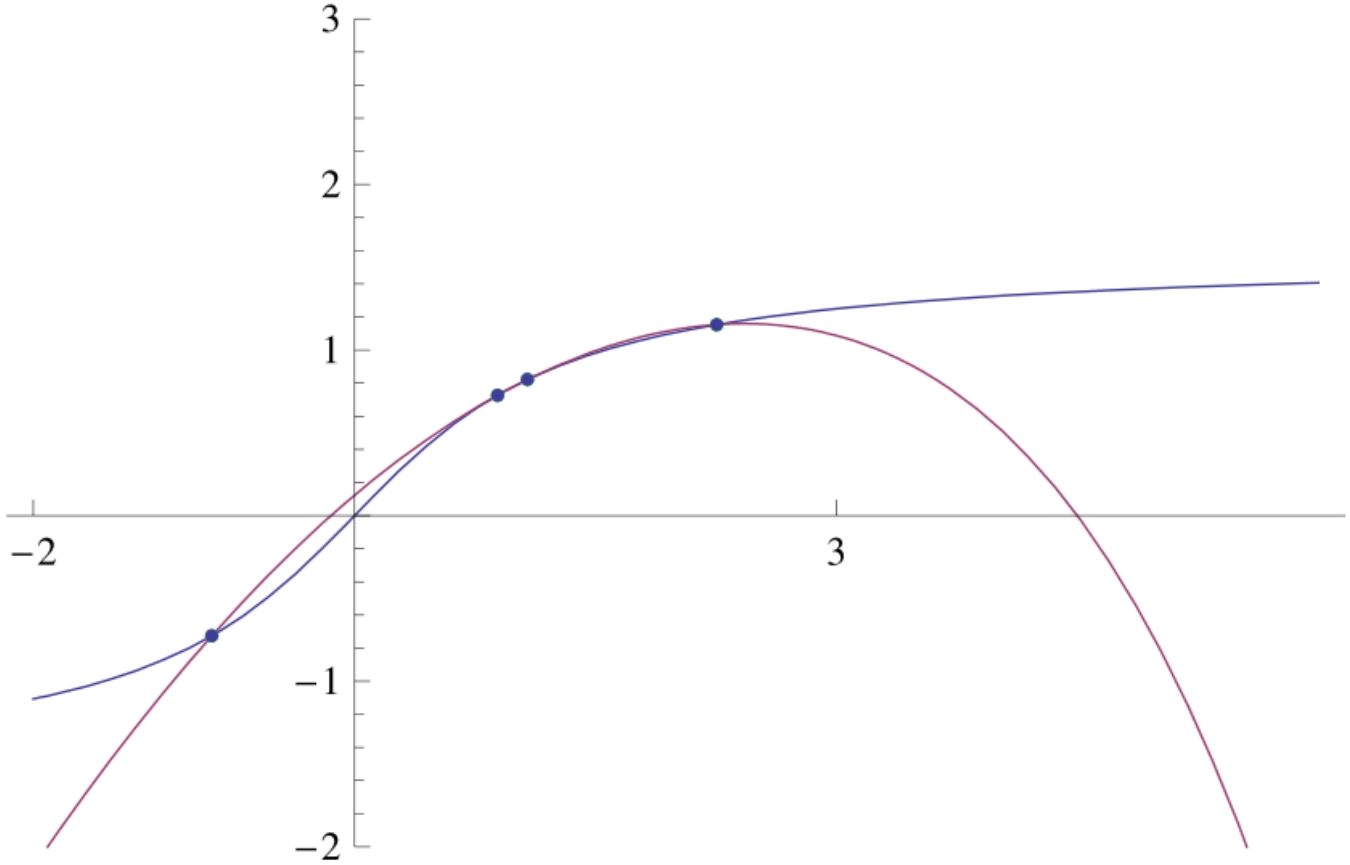

Active learning

Solution: detect when we are extrapolating and switch on learning

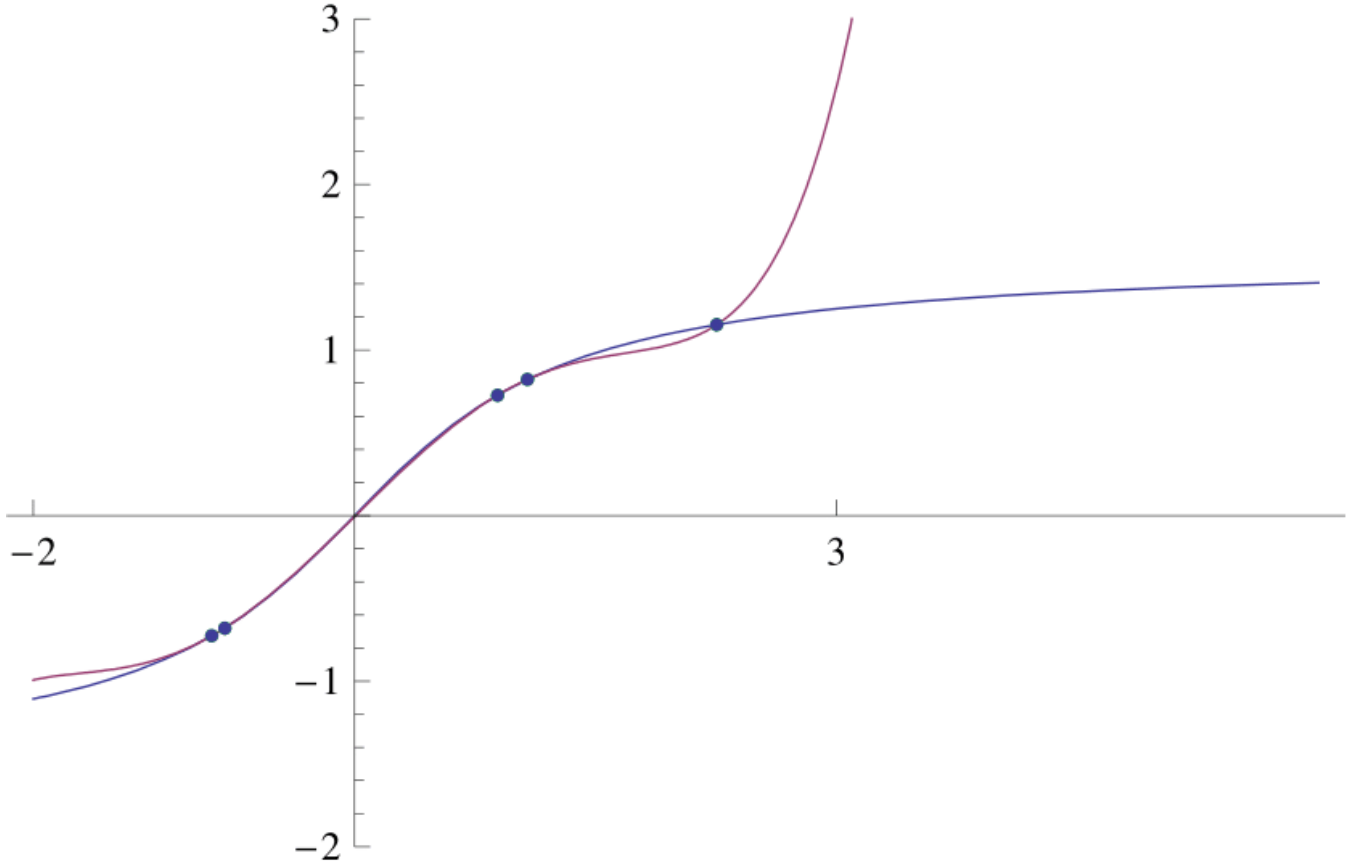

Active learning

Solution: detect when we are extrapolating and switch on learning

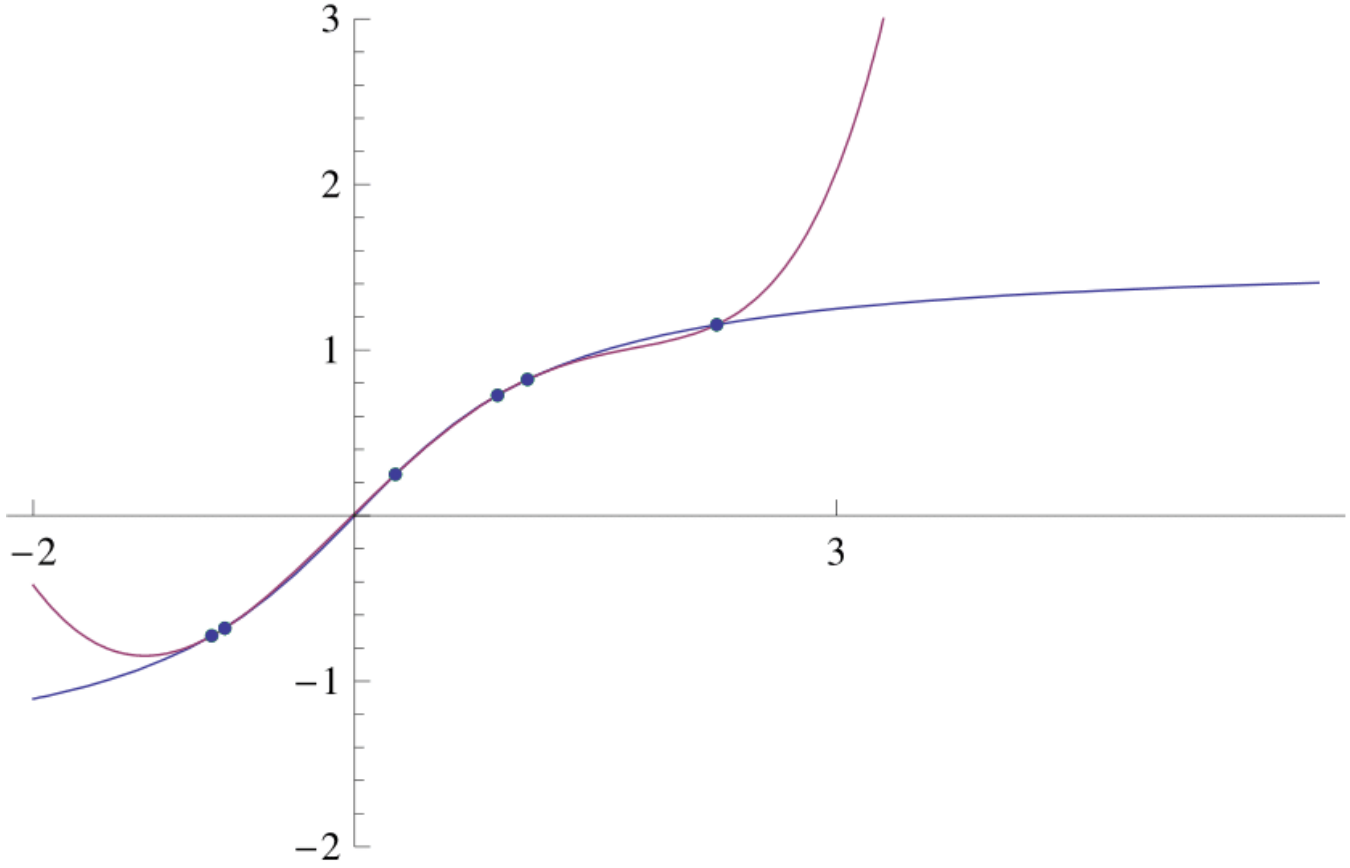

Active learning

Solution: detect when we are extrapolating and switch on learning

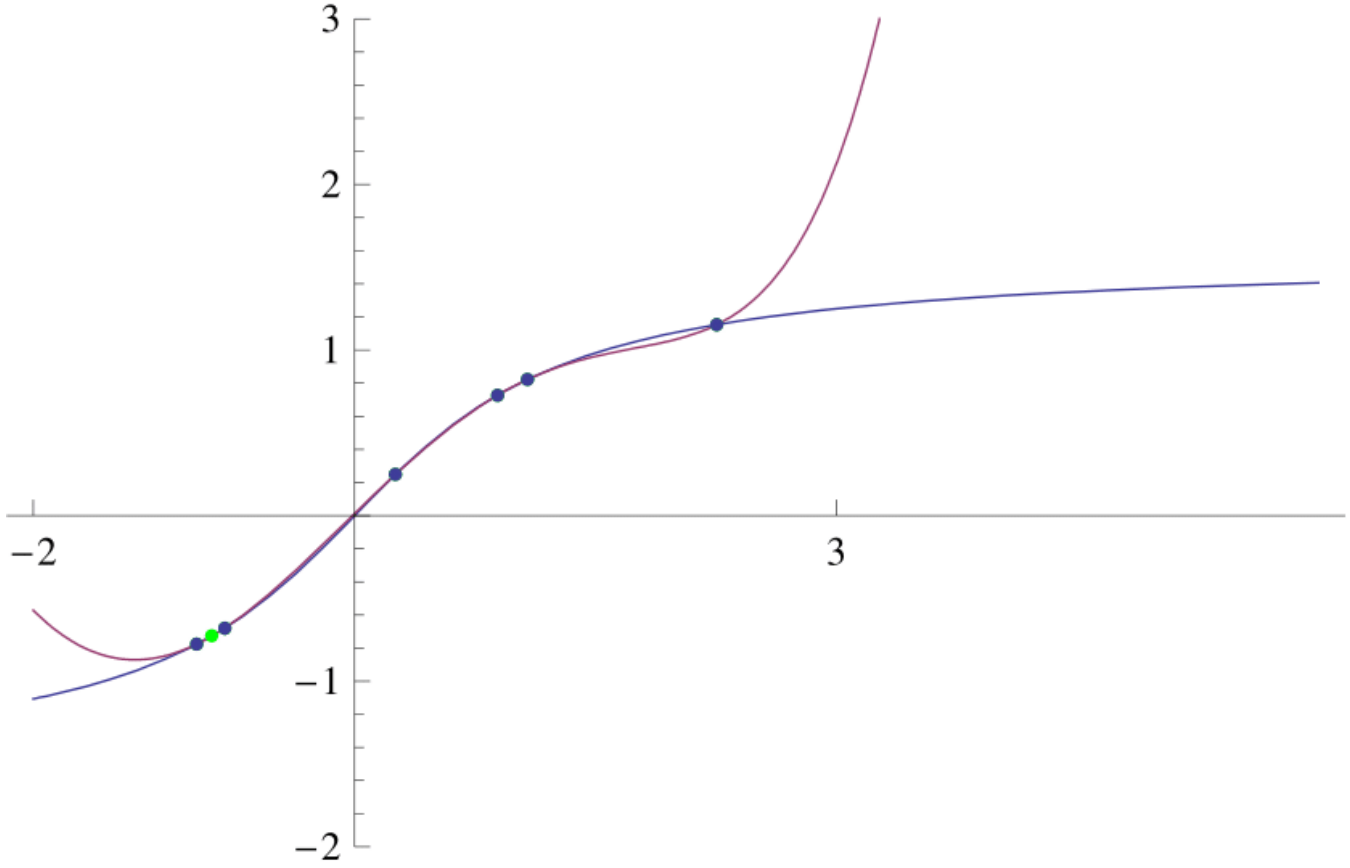

Active learning

Solution: detect when we are extrapolating and switch on learning

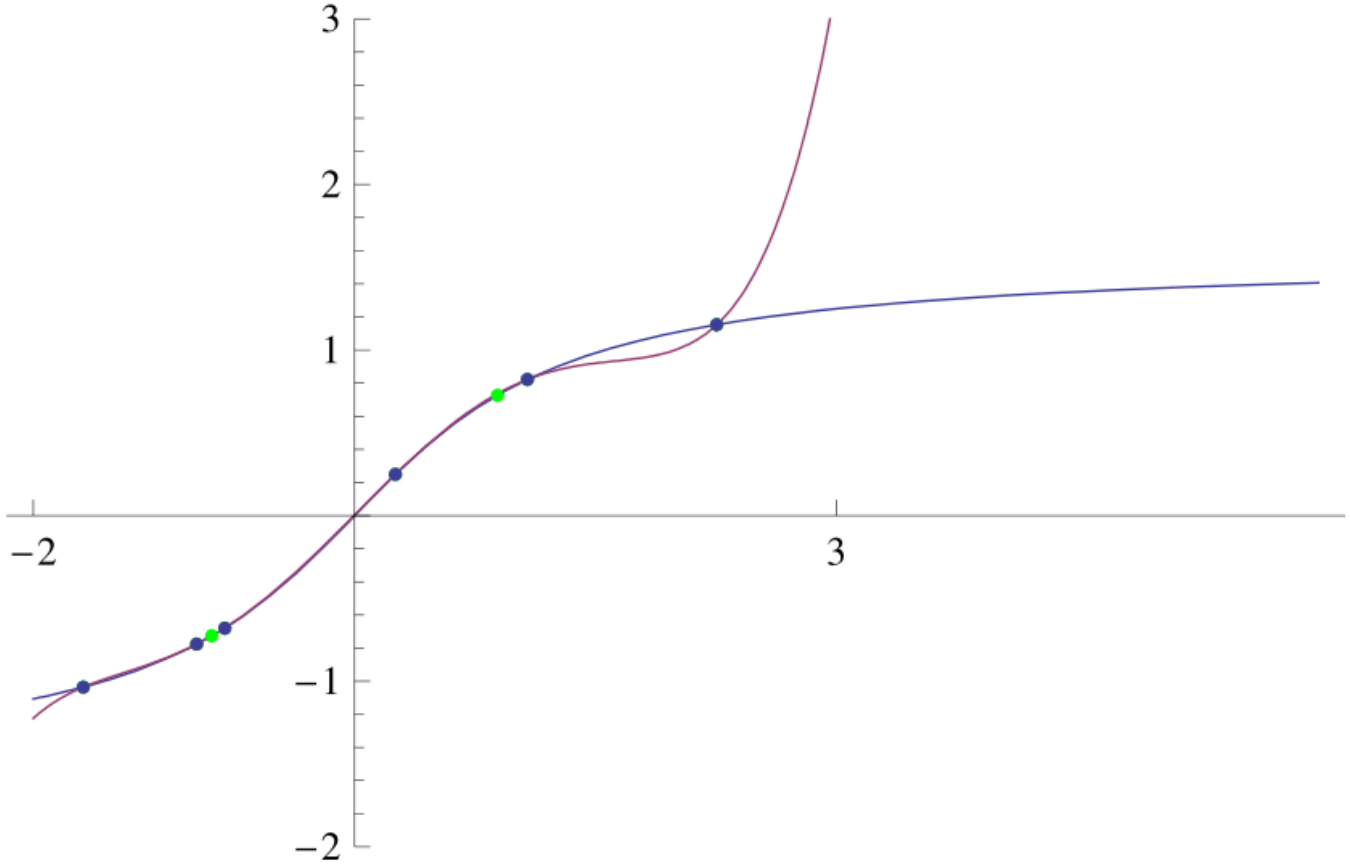

Active learning

Solution: detect when we are extrapolating and switch on learning

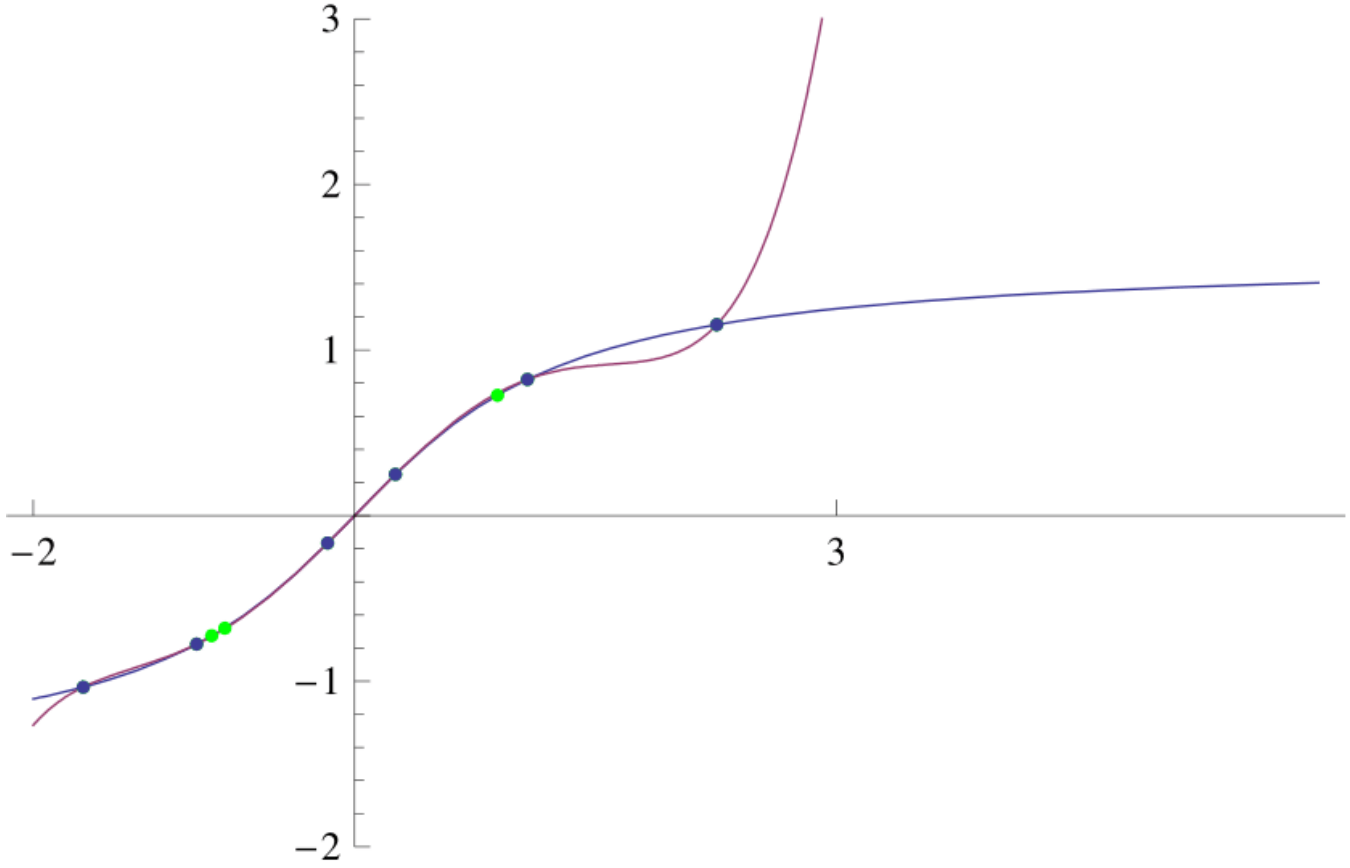

Active learning

Solution: detect when we are extrapolating and switch on learning

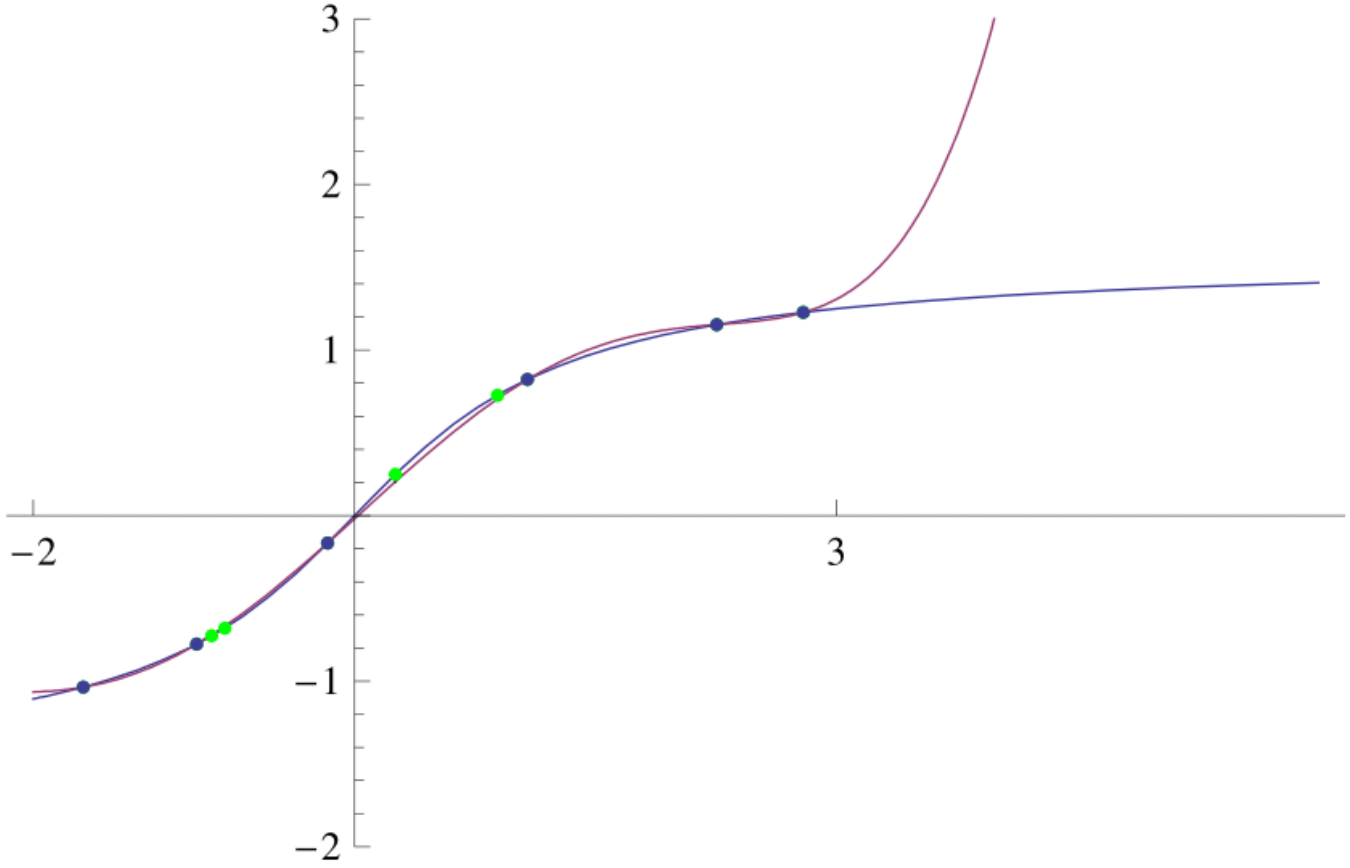

Active learning

Solution: detect when we are extrapolating and switch on learning

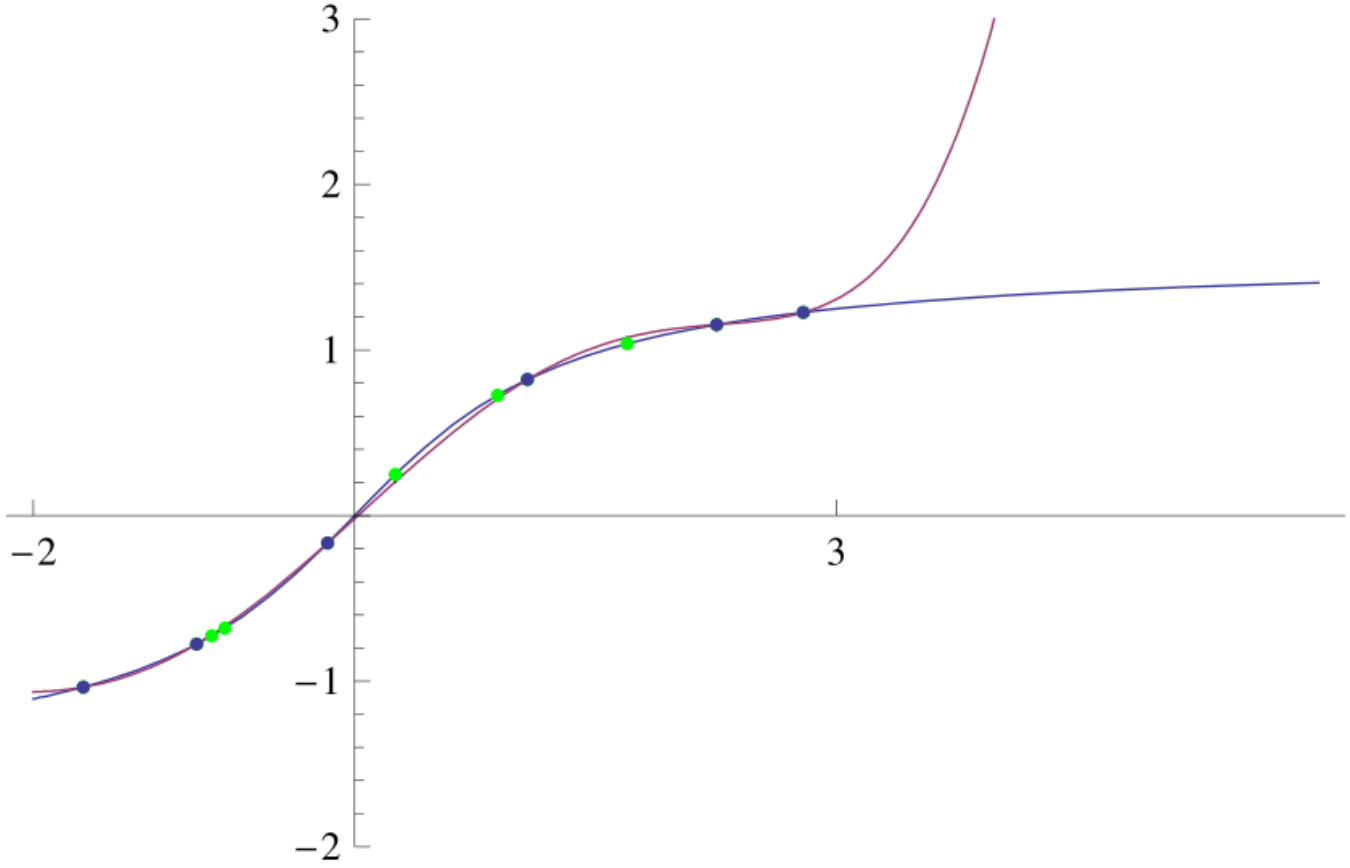

Active learning

Solution: detect when we are extrapolating and switch on learning

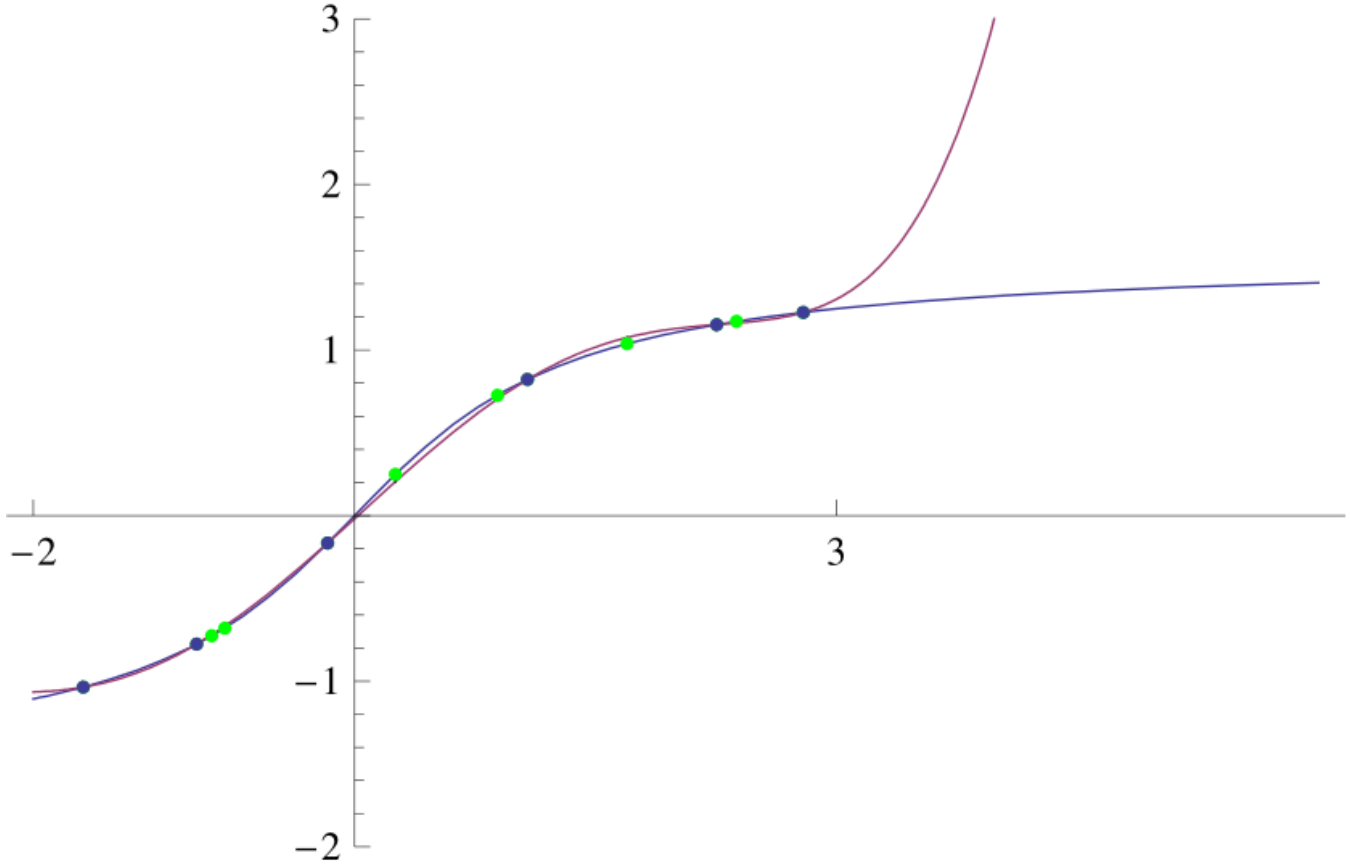

Active learning

Solution: detect when we are extrapolating and switch on learning

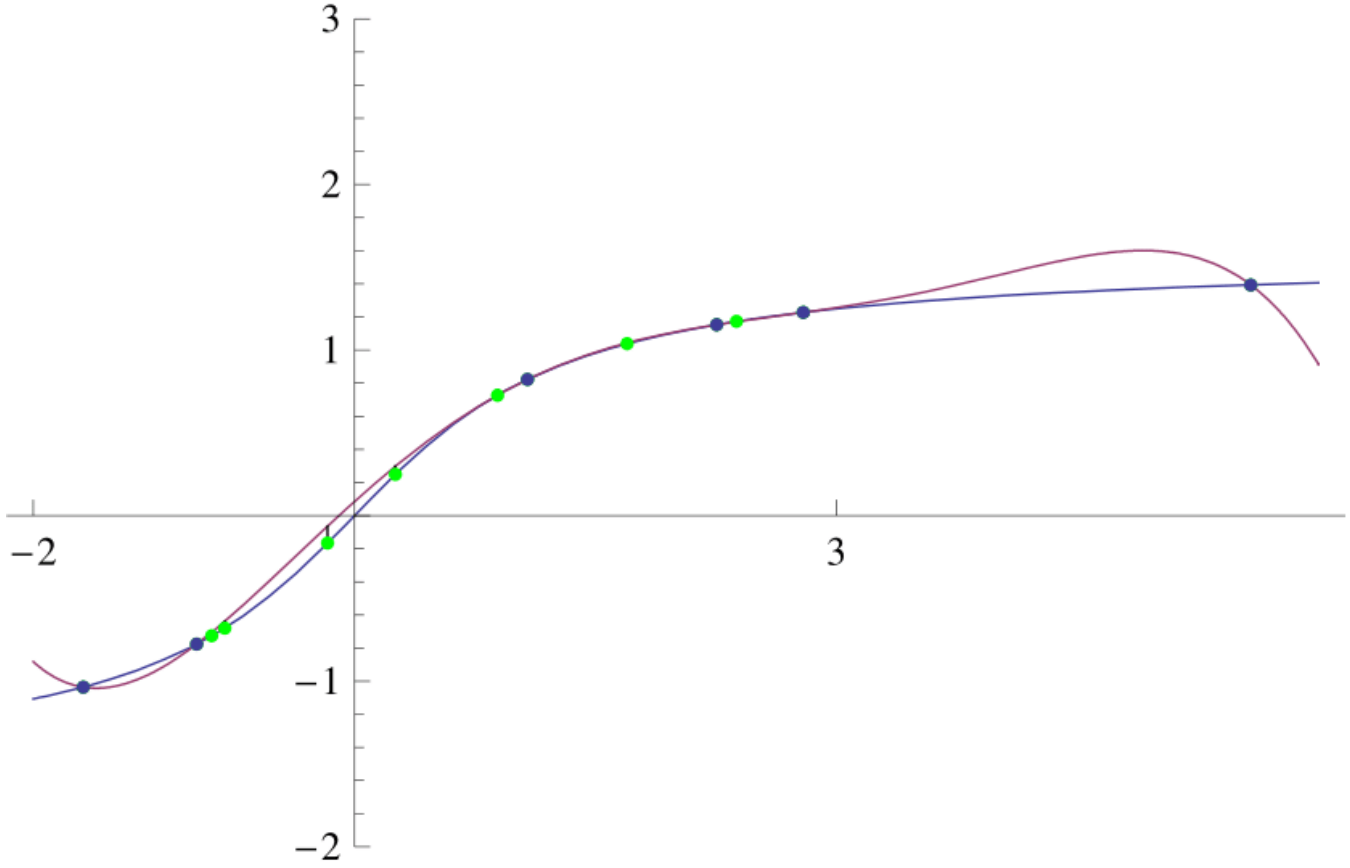

Active learning

Solution: detect when we are extrapolating and switch on learning

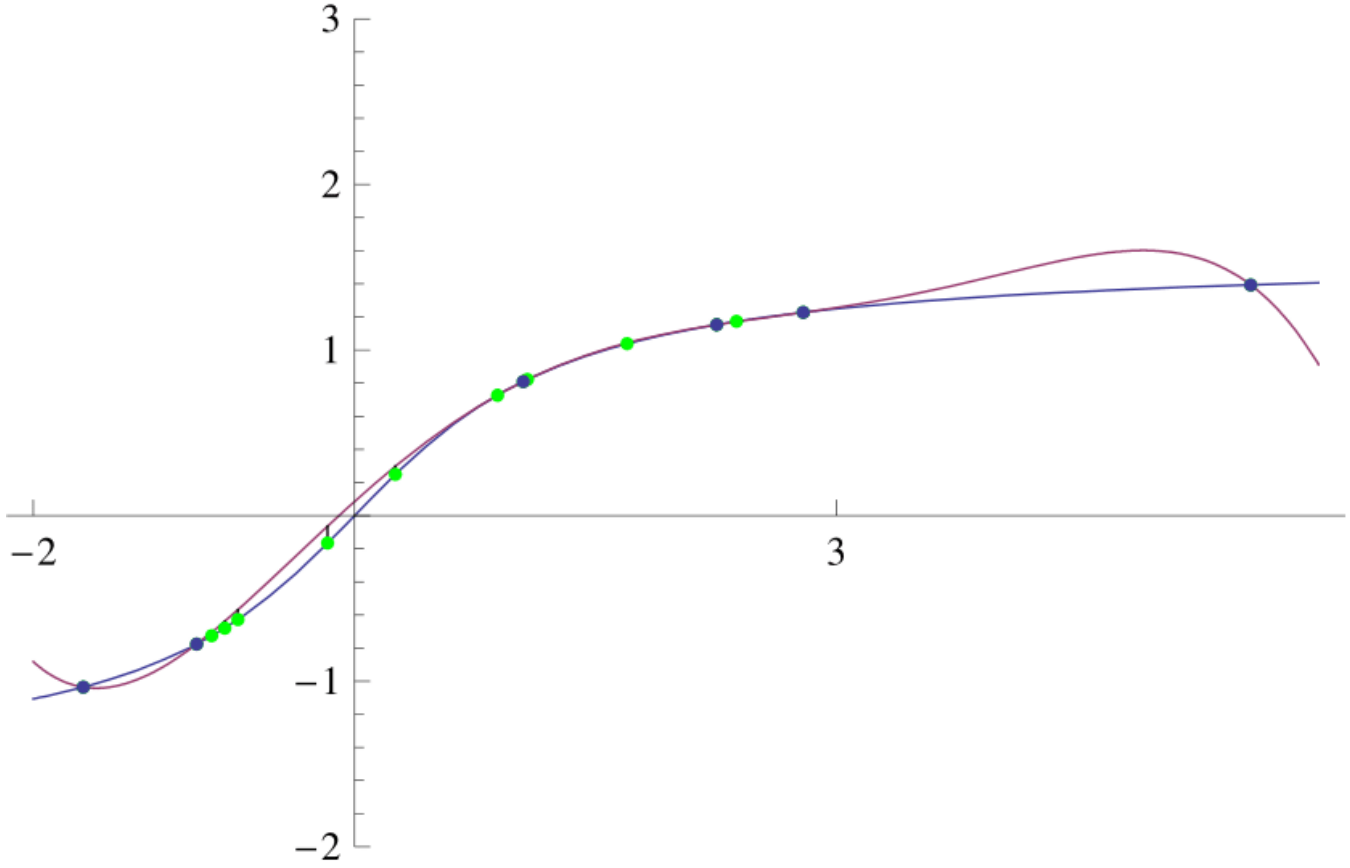

Active learning

Solution: detect when we are extrapolating and switch on learning

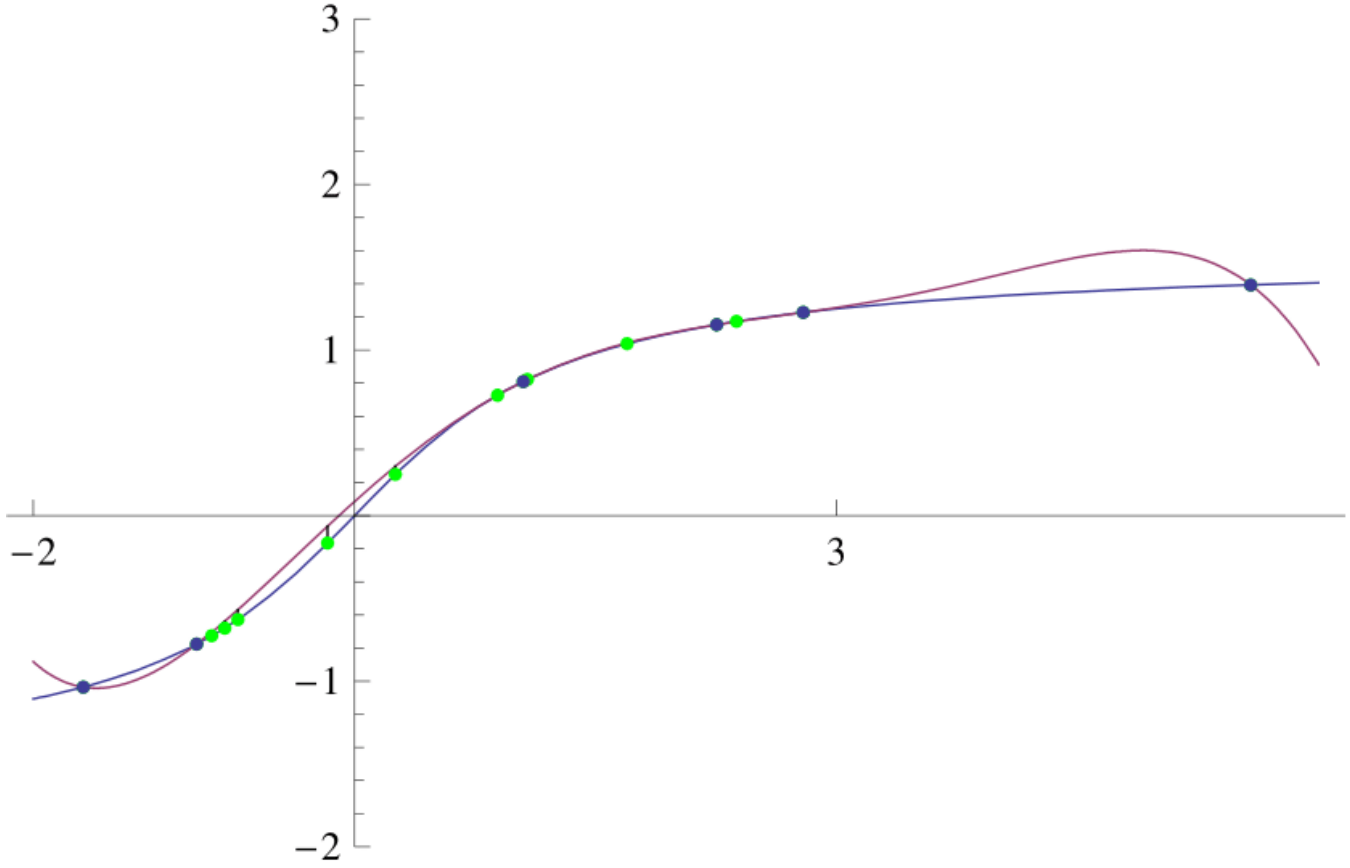

Active learning

Solution: detect when we are extrapolating and switch on learning

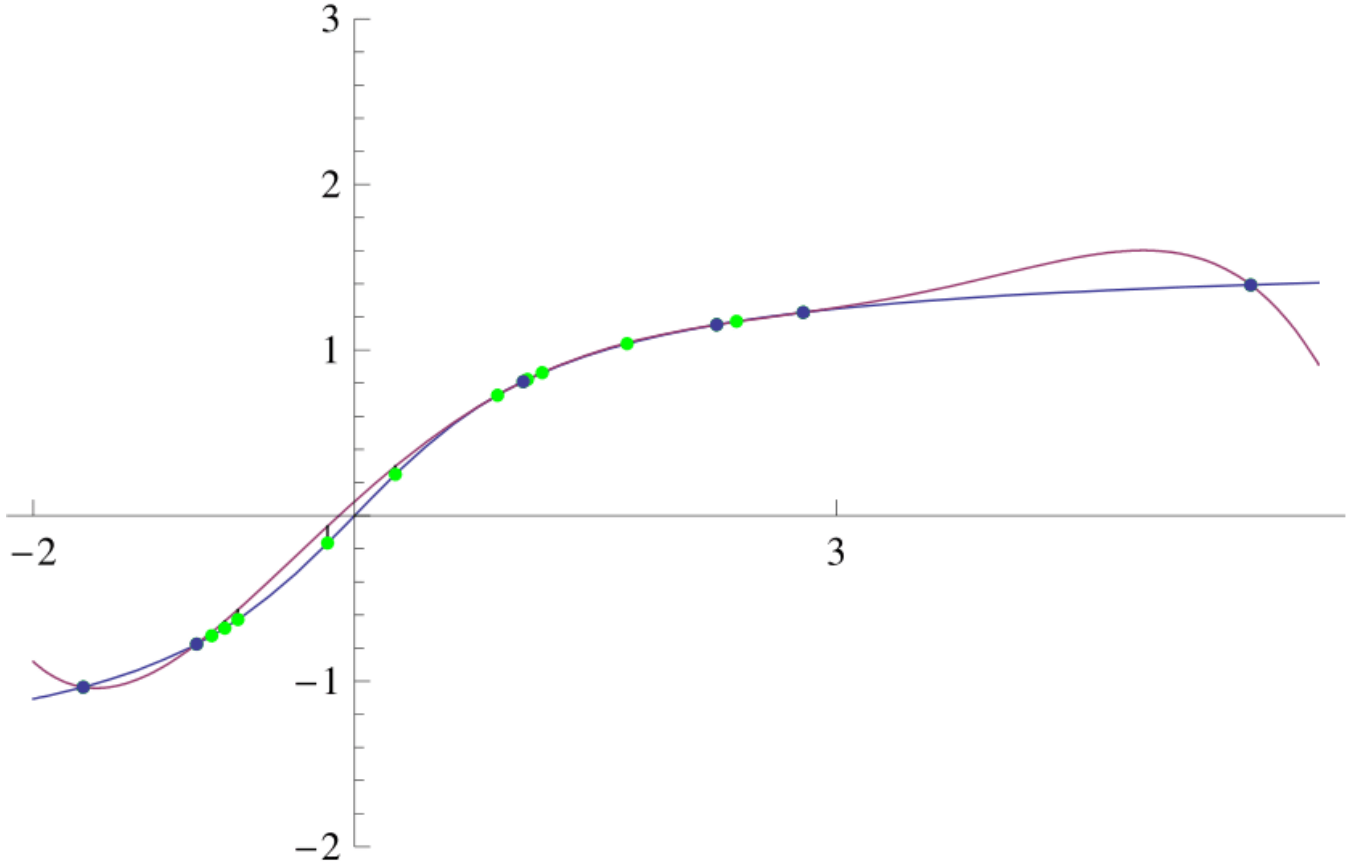

Active learning

Solution: detect when we are extrapolating and switch on learning

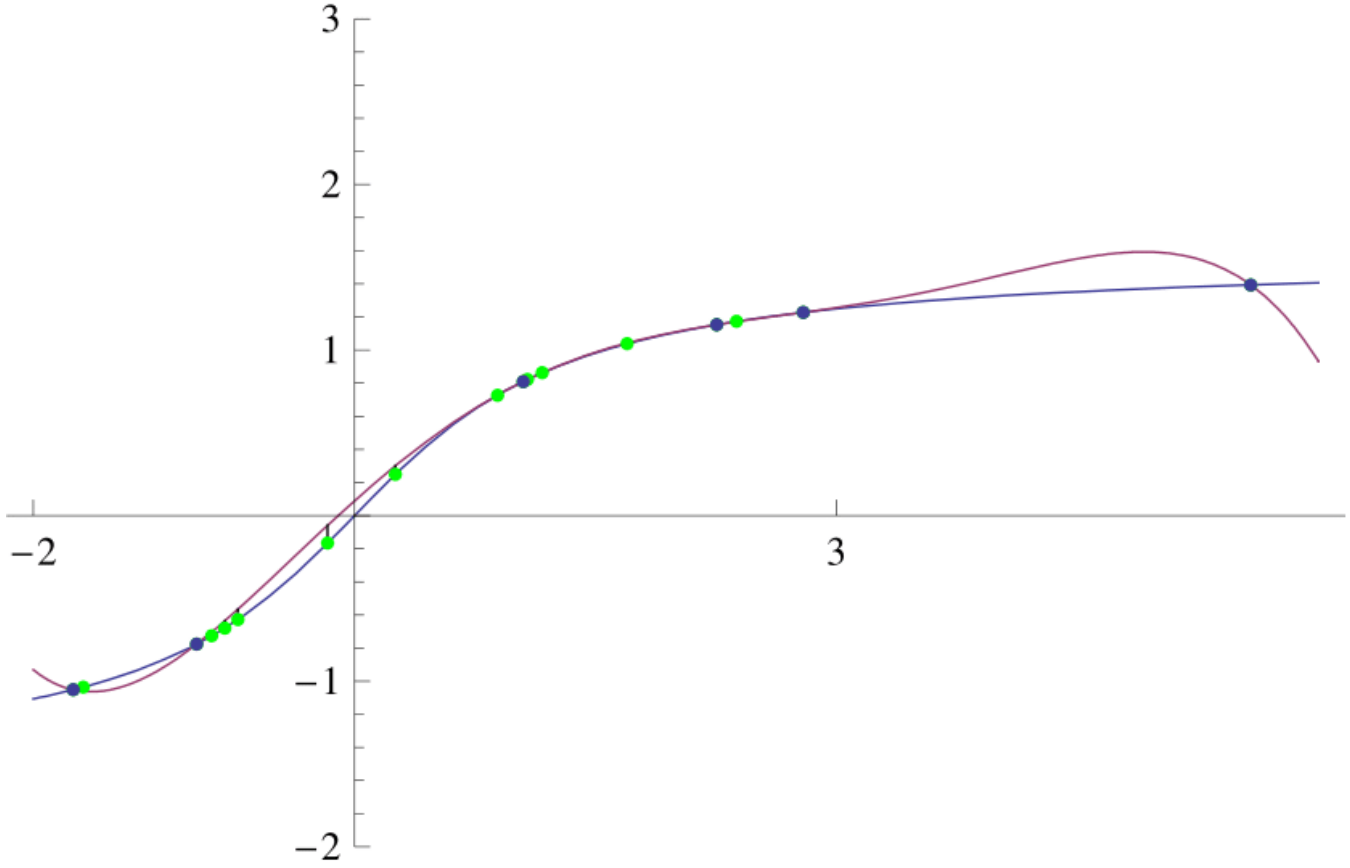

Active learning

Solution: detect when we are extrapolating and switch on learning

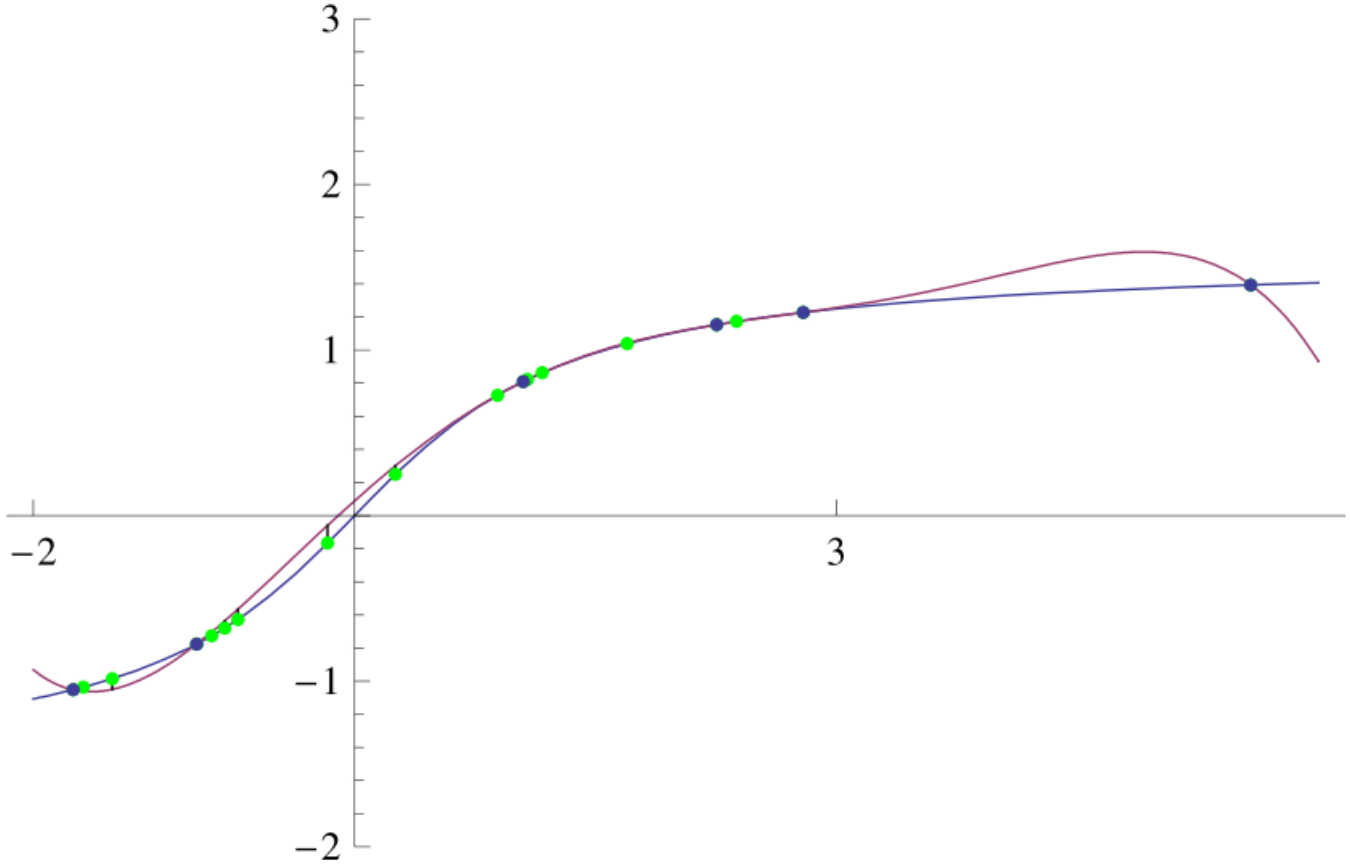

Active learning

Solution: detect when we are extrapolating and switch on learning

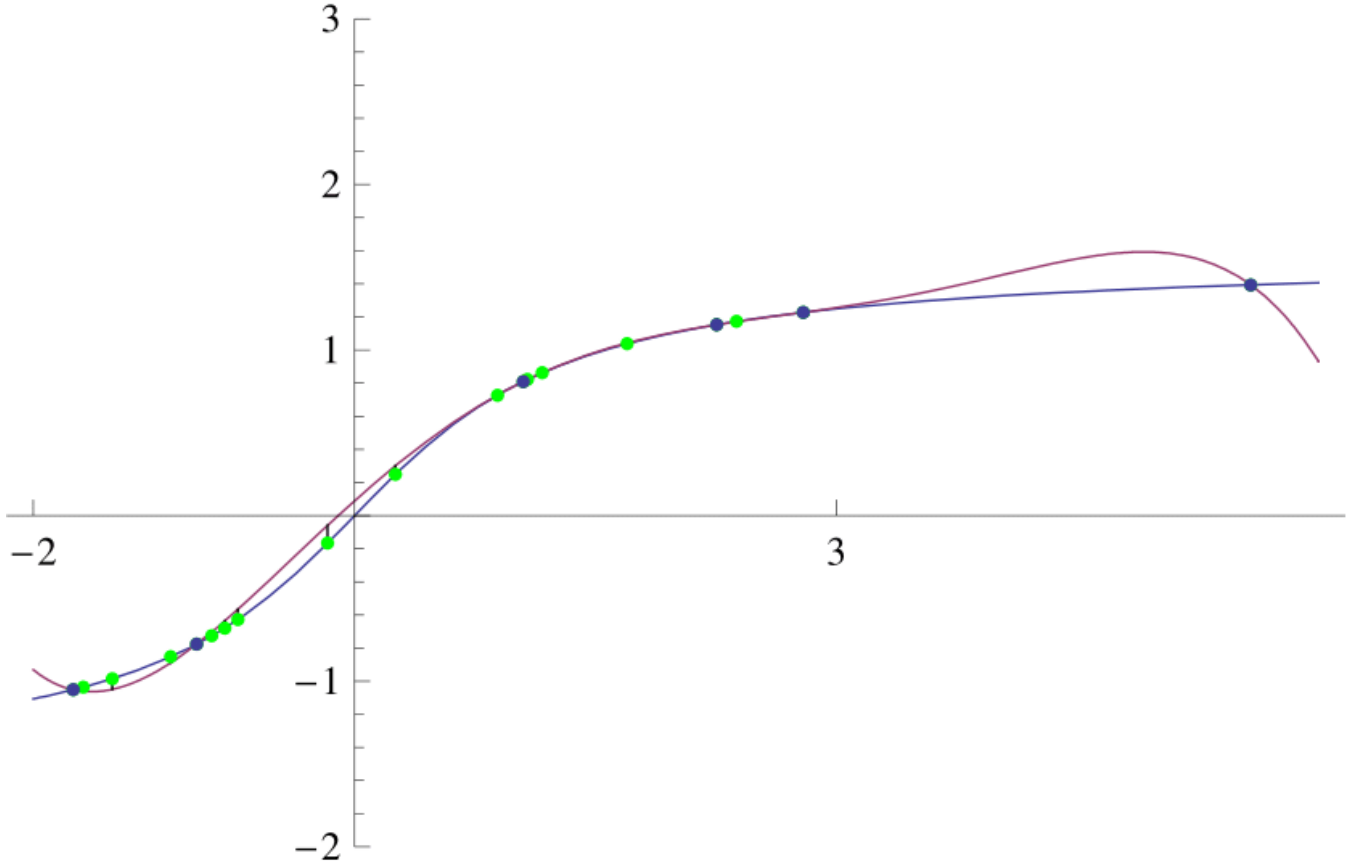

Active learning

Solution: detect when we are extrapolating and switch on learning

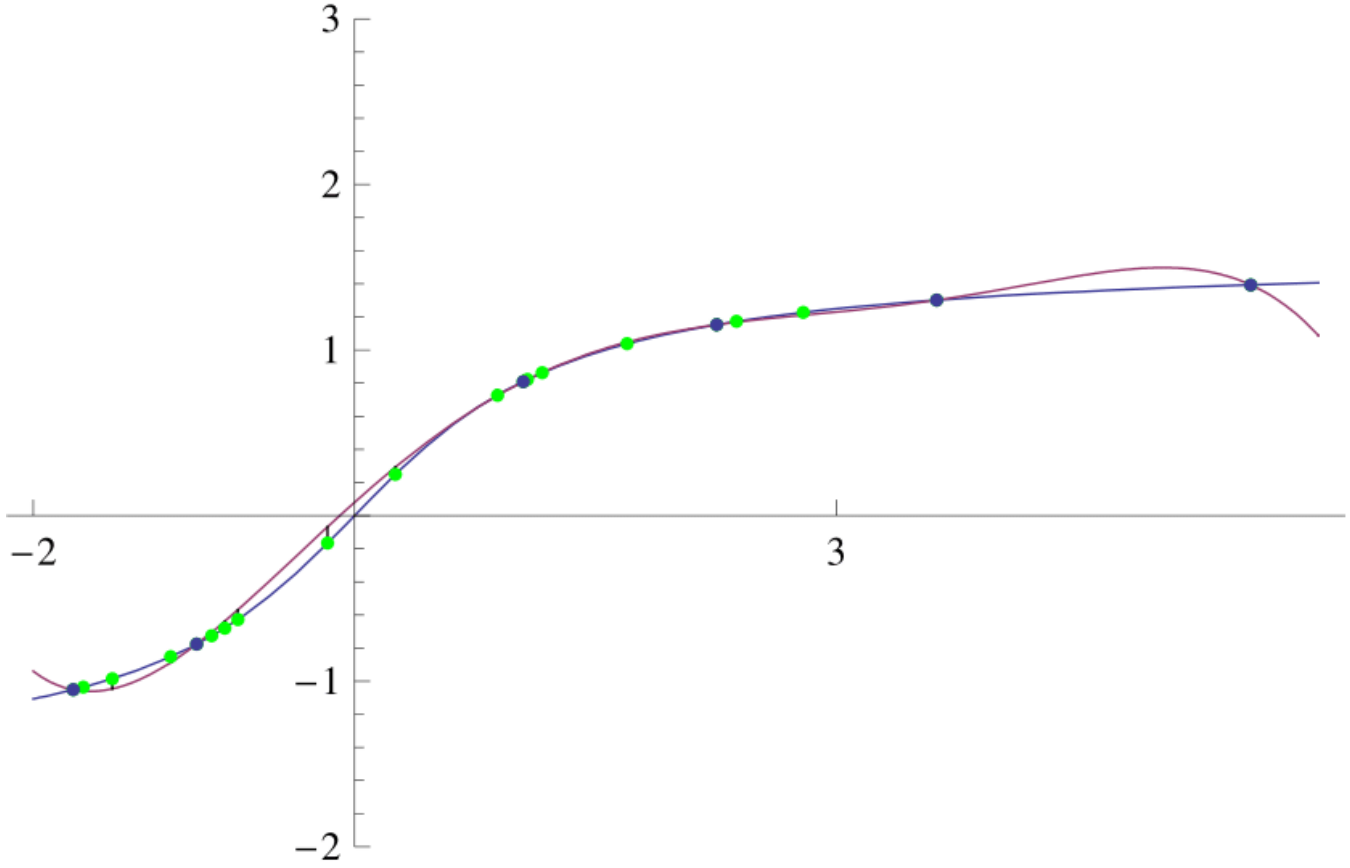

Active learning

Solution: detect when we are extrapolating and switch on learning

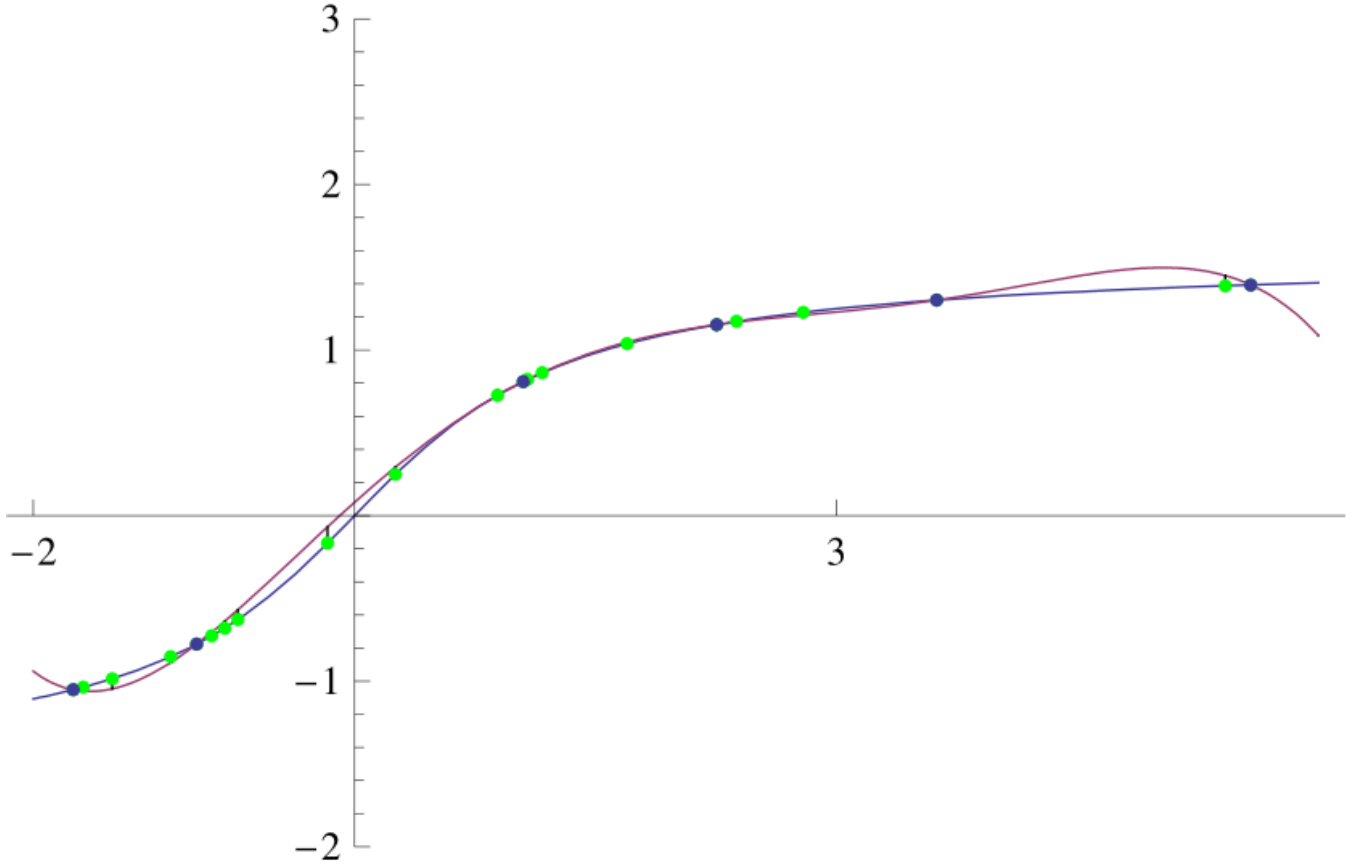

Active learning

Solution: detect when we are extrapolating and switch on learning

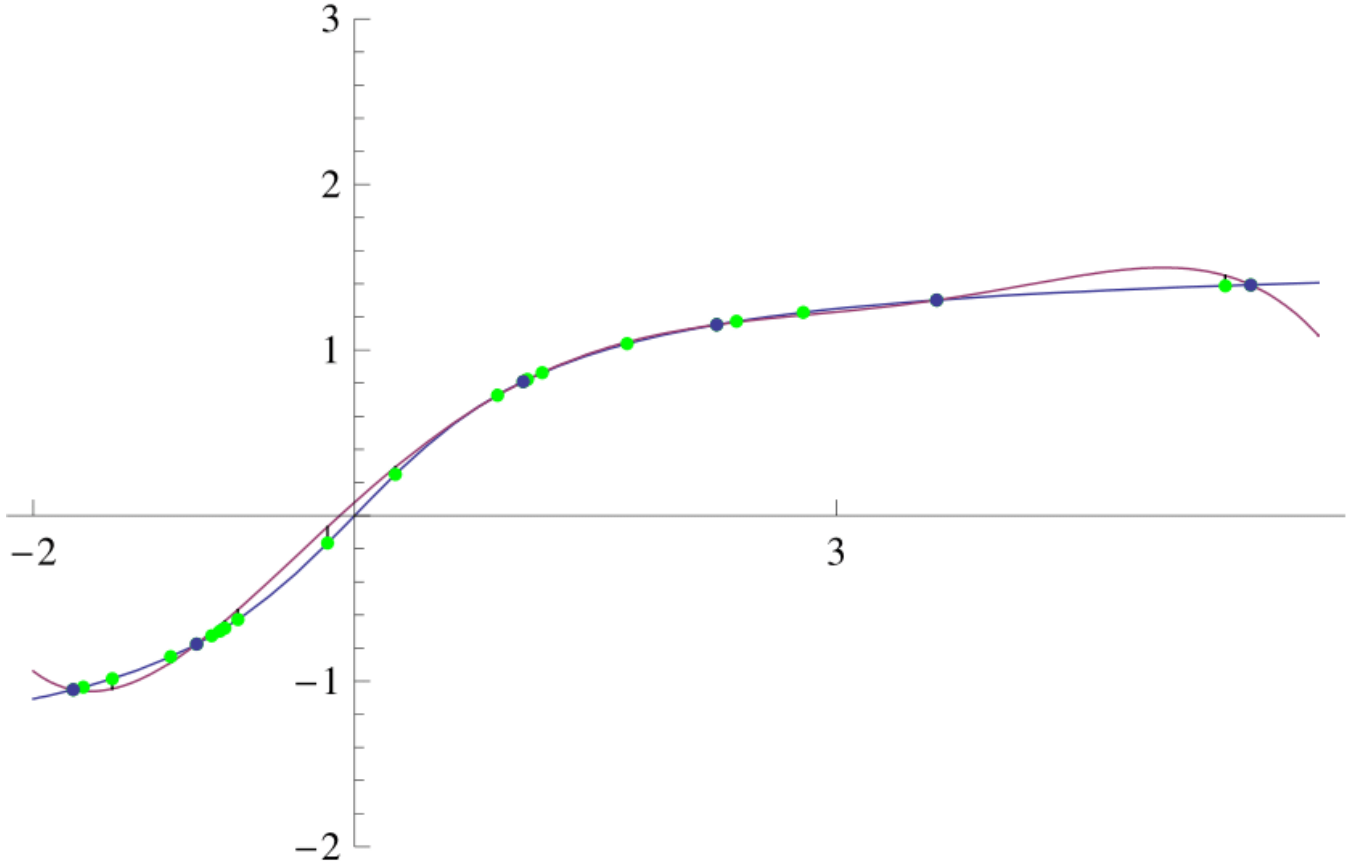

Active learning

Solution: detect when we are extrapolating and switch on learning

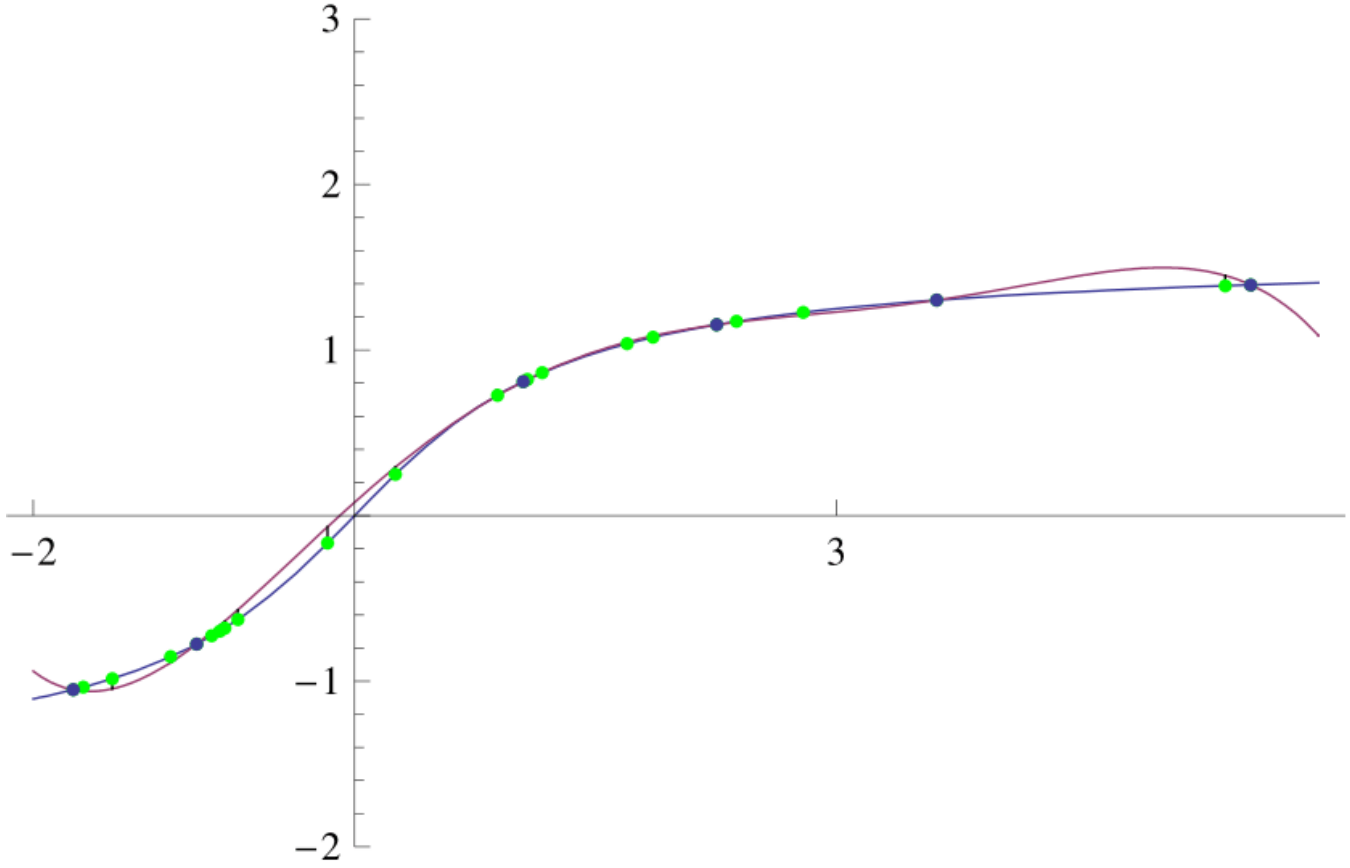

Active learning

Solution: detect when we are extrapolating and switch on learning

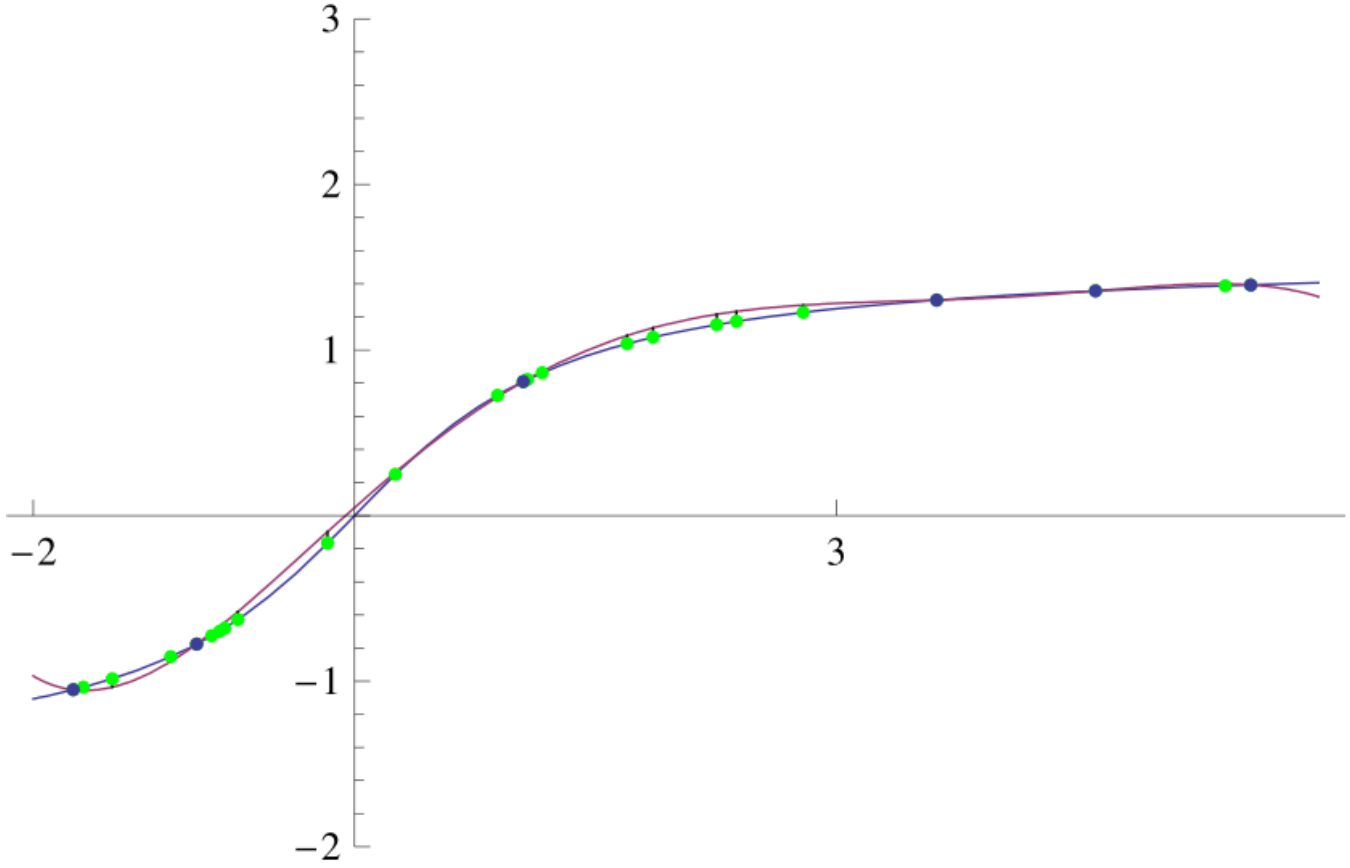

How we do it?

D-optimality

Skip to Applications

D-optimality

essentially

- detects hitting outside a convex hull,

but for linear models

(convex hull -> simplex)

Algorithm: $O(N^2)$

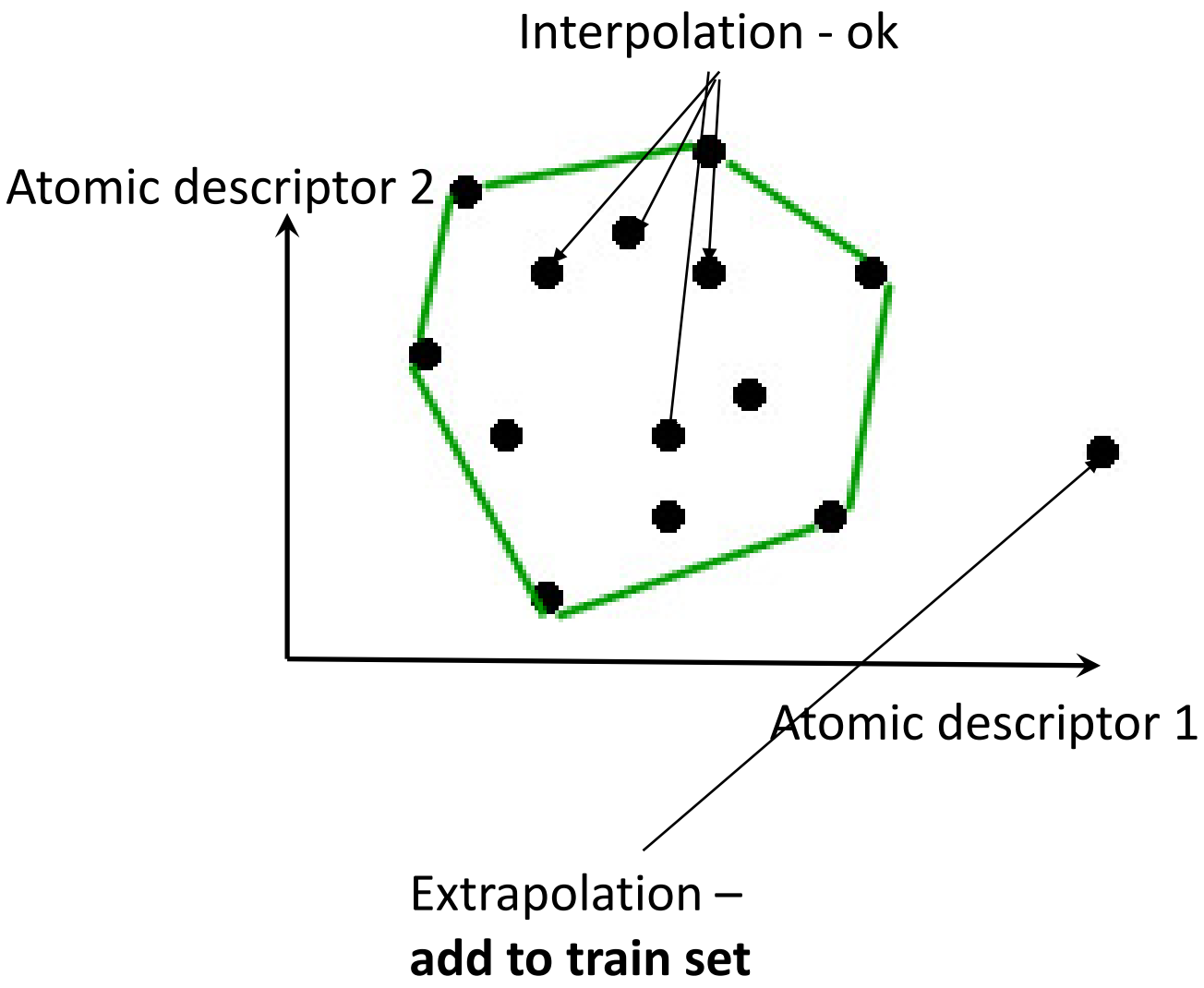

E. Podryabinkin, A. Shapeev (2017)

Applications

Application #1: Learning on the fly

MD with empirical potential

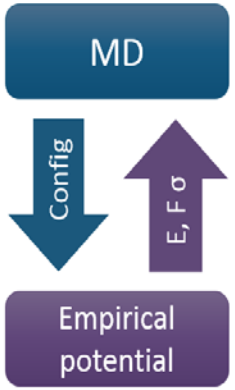

+ Fast
– Qualitative accuracy only

Ab-initio MD

– Time consuming
+ Accurate

Hybrid MD

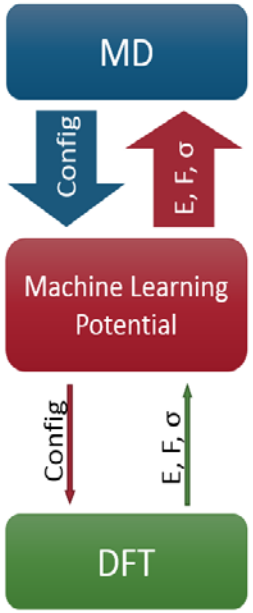

+ Fast
+ Accurate (hopefully)

- Combines training and evaluation of MLIP
- Detects and learns “extrapolative” configurations
- Robust
- Balancing accuracy and amount of QM calcs

Application example #0: Learning on the fly in MD process at NVT-ensemble of 128 BCC-Li atoms

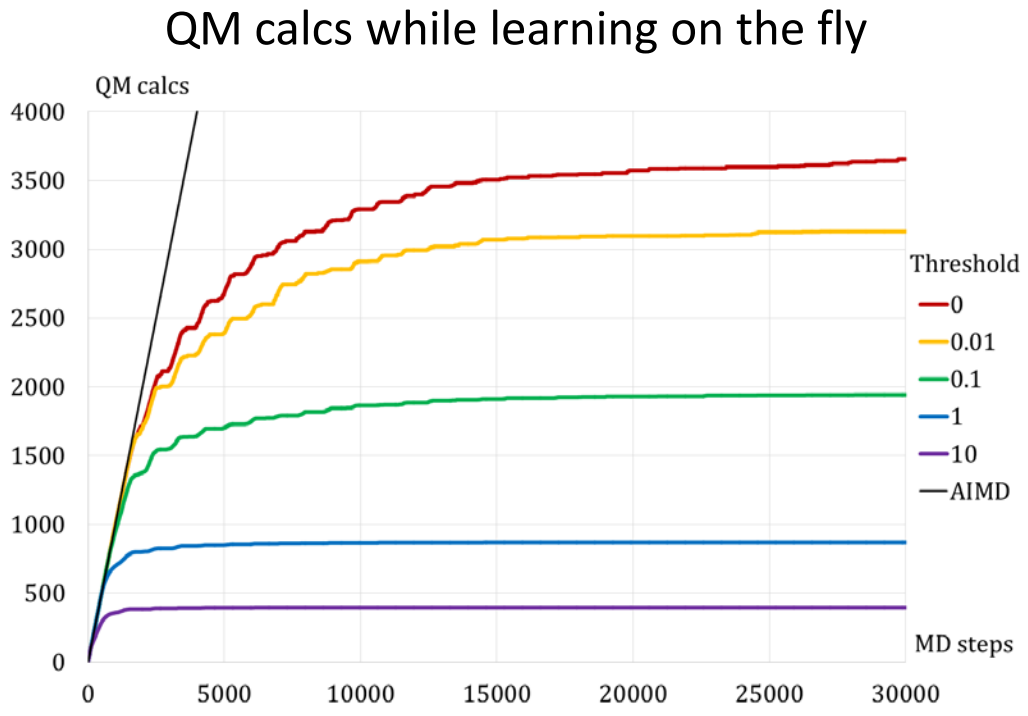

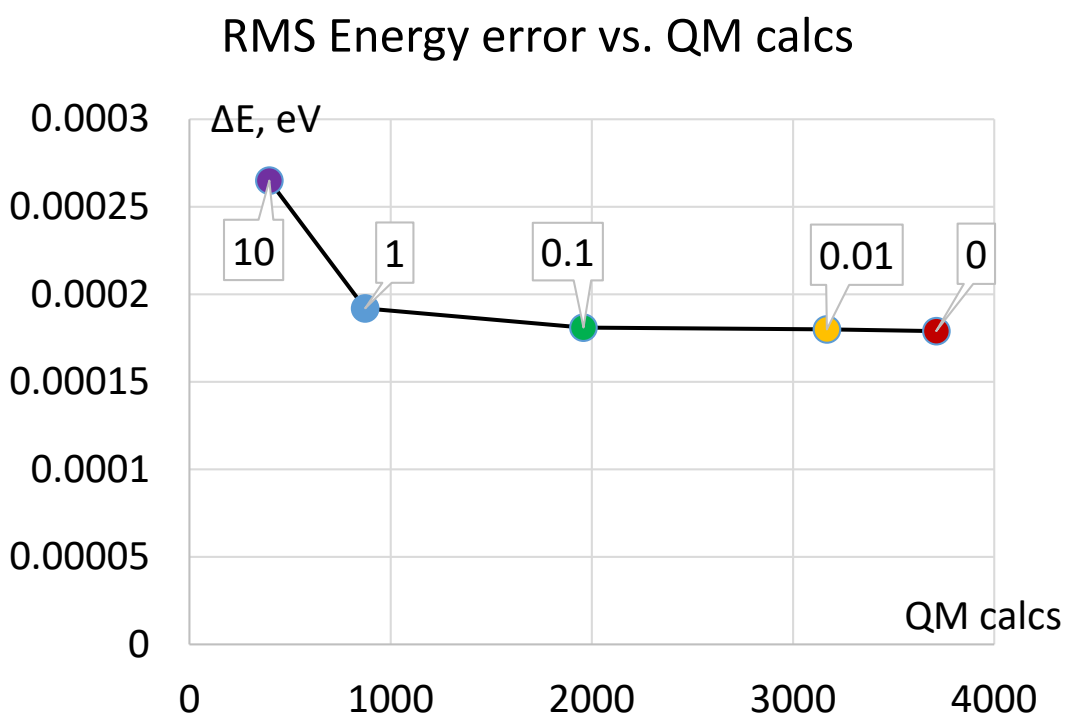

Conclusion: Amount of QM calcs can be reduced several times at the cost of minor losses in accuracy

www.aflowlib.org/superalloys/

46. AlInNi
47. AlIrNi
48. AlLiNi ▲
49. AlMgNi
50. AlMnNi ▲
51. AlMoNi
52. AlNbNi ▲
53. AlNiOs ▲
54. AlNiPd
55. AlNiPt ▲
56. AlNiRe
57. AlNiRh ▲
58. AlNiRu ▲
59. AlNiSb ▲
60. AlNiSc ▲
61. AlNiSi ▲
62. AlNiSn
63. AlNiSr
64. AlNiTa ▲
65. AlNiTc
66. AlNiTi ▲
67. AlNiTl
68. AlNiV ▲
69. AlNiW
70. AlNiY ▲
71. AlNiZn ▲
72. AlNiZr ▲
73. AuBeNi
74. AuCaNi
75. AuCdNi
76. AuCoNi
77. AuCrNi
78. AuCuNi
79. AuFeNi
80. AuGaNi

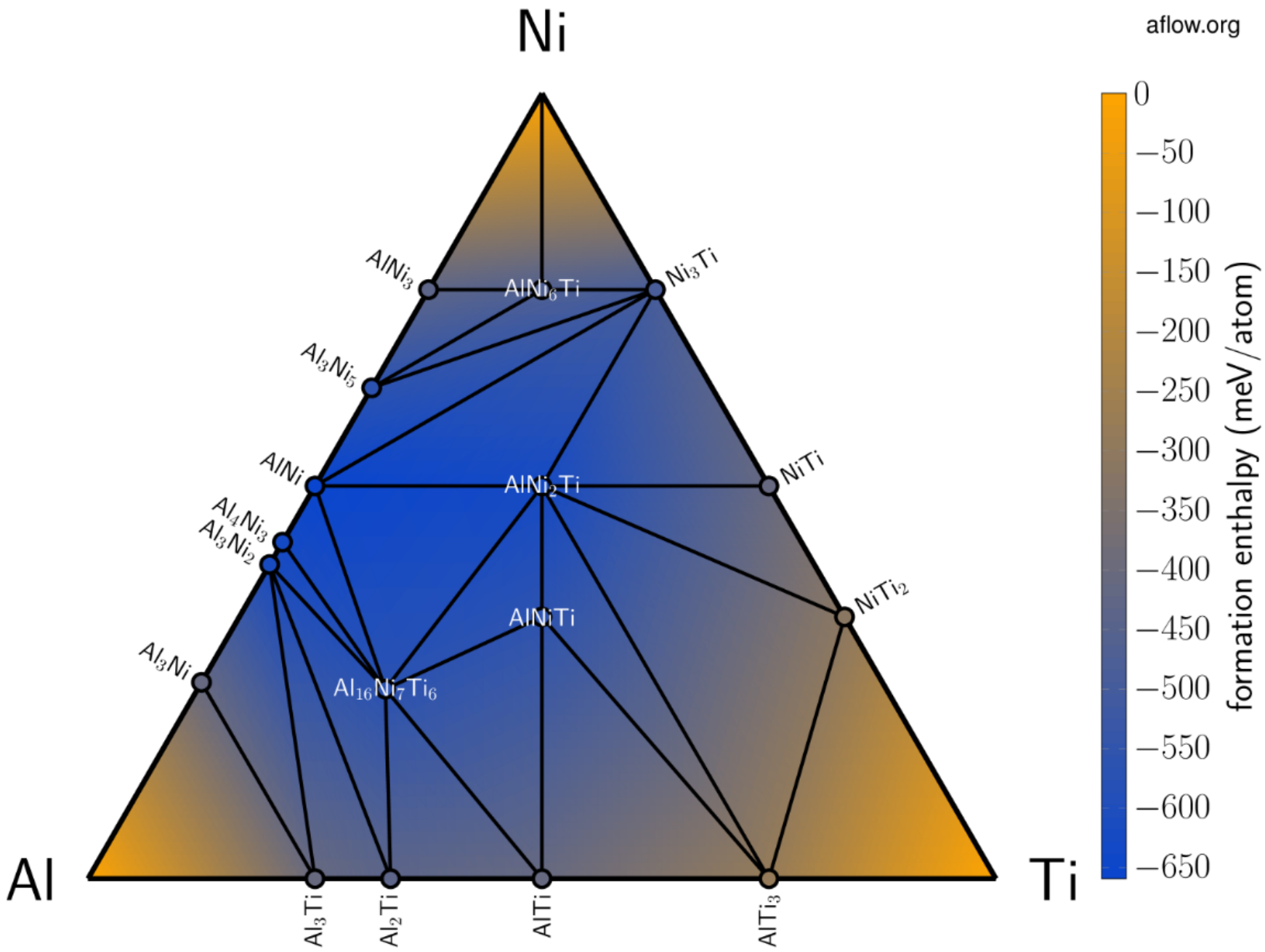

Prediction of convex hull of stable alloys

How it is done:

1. Start with 1500 crystal prototypes (unequilibrated structures)
2. Equilibrate (relax) them with DFT and choose the ones on the convex hull

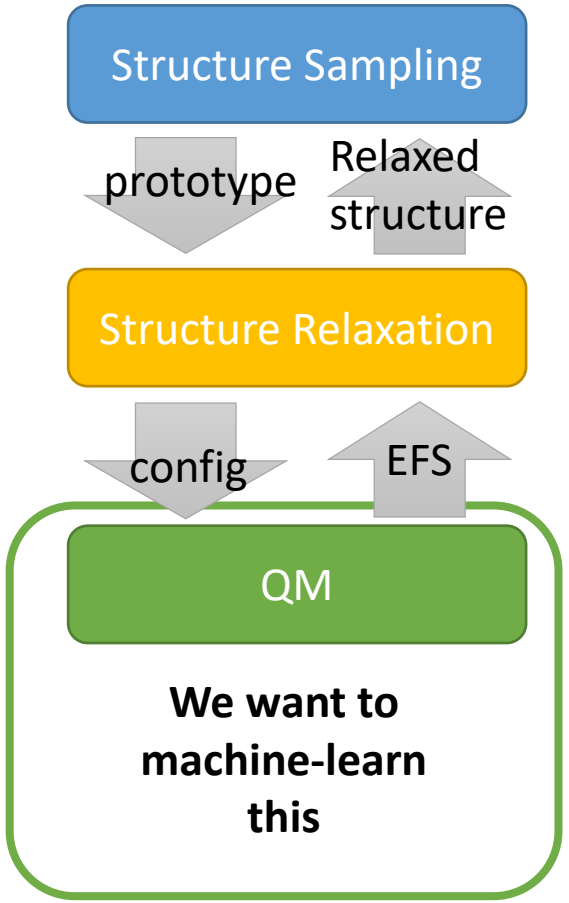

Convex hulls now

K. Gubaev,E. Podryabinkin, Gus L.W. Hart, A.S. (2019)

How it is done:

1. Start with 400K crystal prototypes (unequilibrated structures)
2. Equilibrate (relax) them with MLIP while learning on the fly

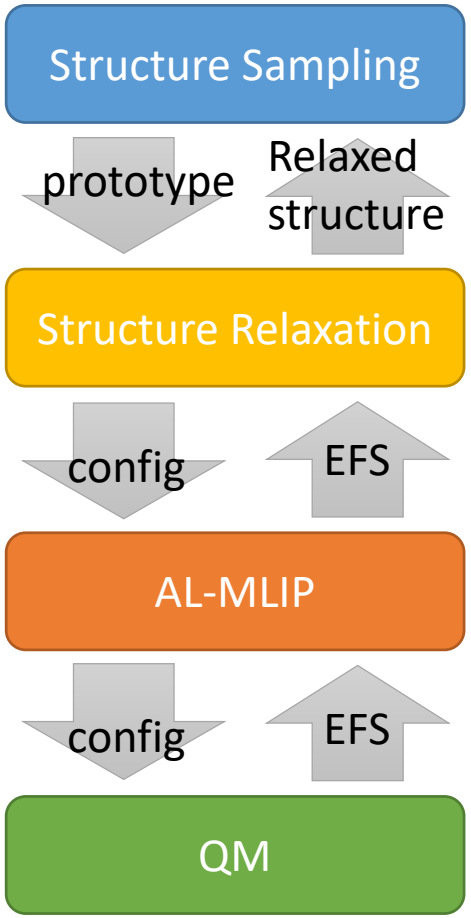

Convex hulls now: details

1. Screen-1:
   1. Start with **400K** structures
   2. Obtain **400K** relaxed structures, with RMSE = **25** meV/atom
   3. Retain **40K** low-energy structures (within 4-σ)
2. Screen-2:
   1. Start with **60K** structures
   2. Obtain **60K** relaxed structures, with RMSE = **9** meV/atom
   3. Retain **7K** low-energy structures (within 4-σ)
3. Final relaxation:
   1. Relax **7K** structures on DFT

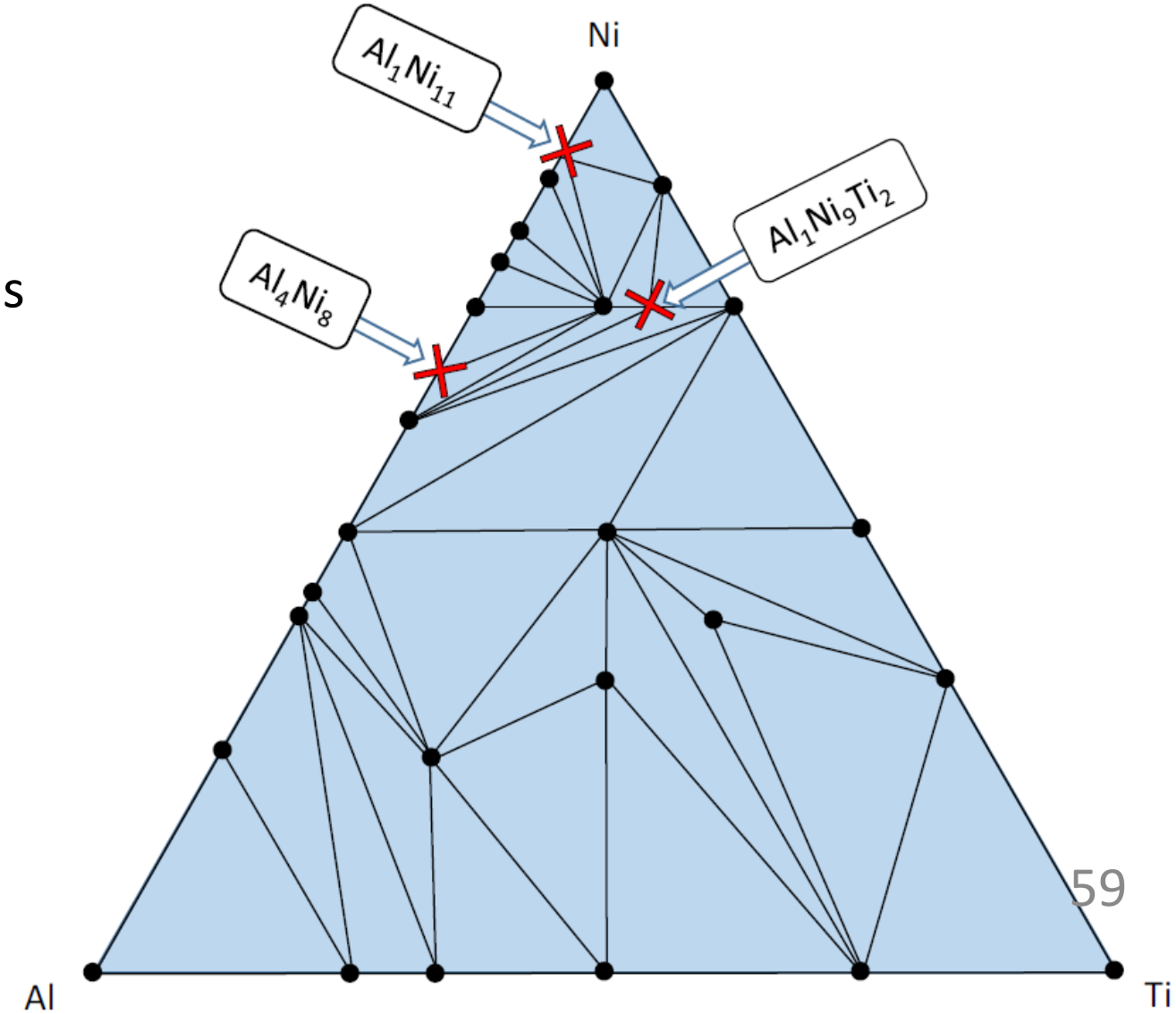

Results

- Some newly discovered structures are hard to “sample passively”:

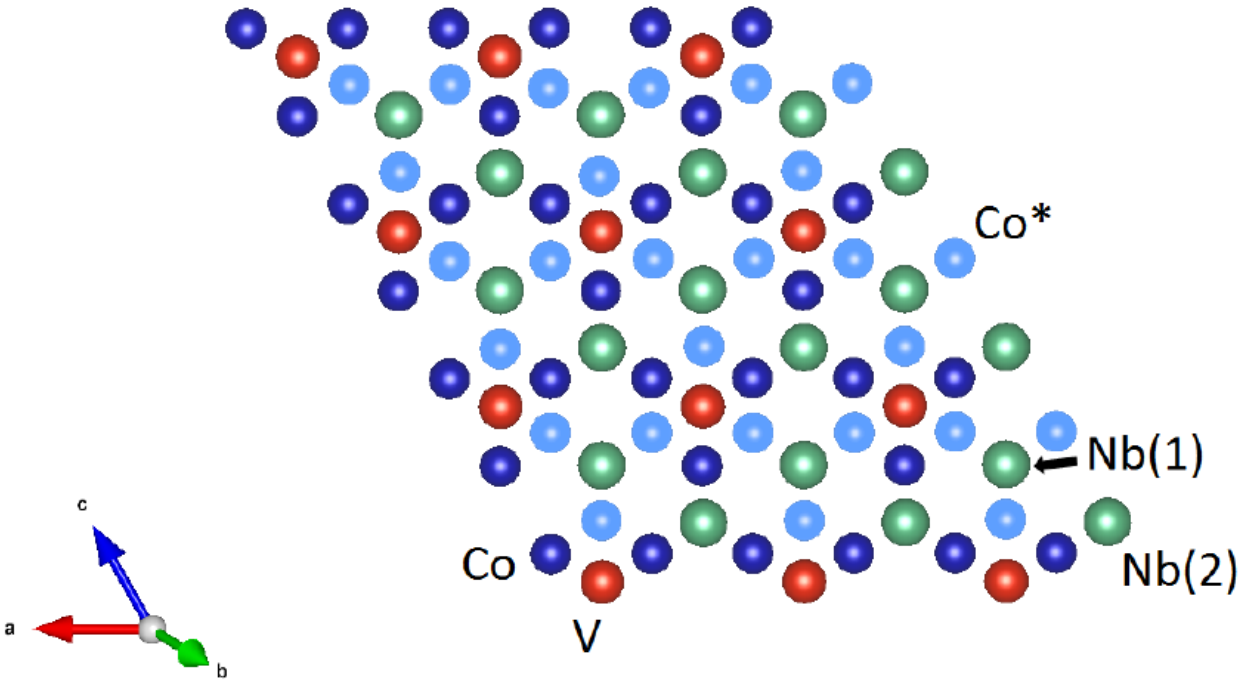

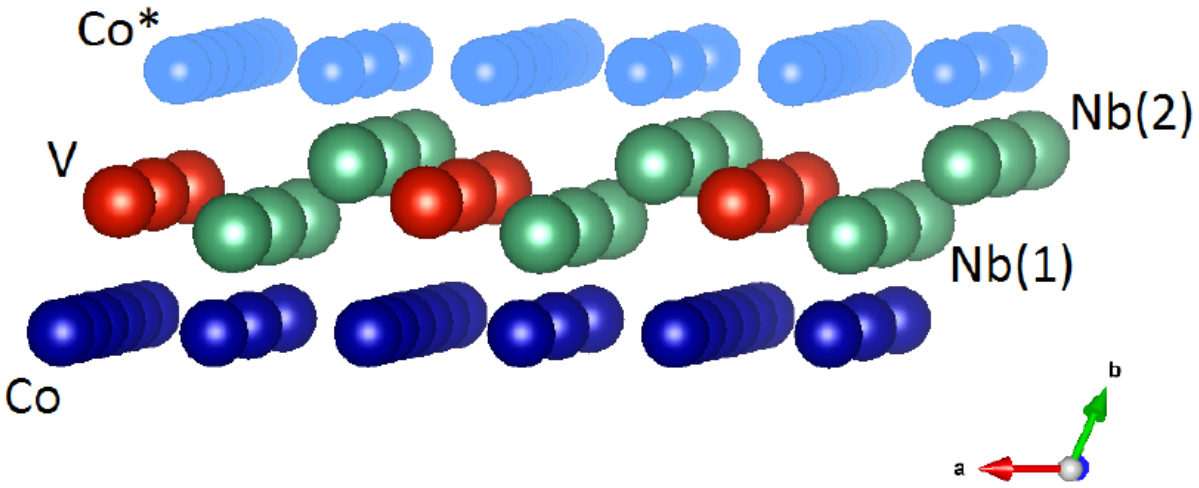

Results and Discussion

- No approximation error in the answer!
  (We only take a risk of missing a structure in the 4-σ interval.)
- 100x speed-up; CPU time:
  1. Final relaxation: 90%
  2. Training set: 9%
  3. Training, Relaxation: 1%
- Main challenge: reduce the 90% $\Leftarrow$ improve accuracy (9 meV/atom):
- Sampling is now the bottleneck, not DFT (we should make friends with Complex High-Dimensional Energy Landscapes)

Application 1b: Boron crystal structure prediction

E. Podryabinkin, E. Tikhonov, A.S., Artem Oganov (2019)

Boron structures prediction challenges:

- A lot of allotropes
- Some allotropes has more than 100 atoms (impossible with DFT)
- Small energy/atom difference between structures with PES minima

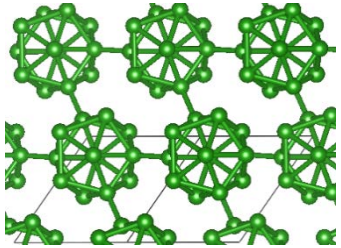

B-12 (6.7058eV/atom)
10 days with DFT
3 days with MLIP

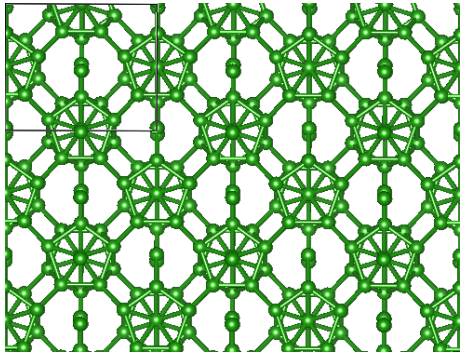

B-28 (6.678eV/atom)
2 months with DFT
5 days with MLIP

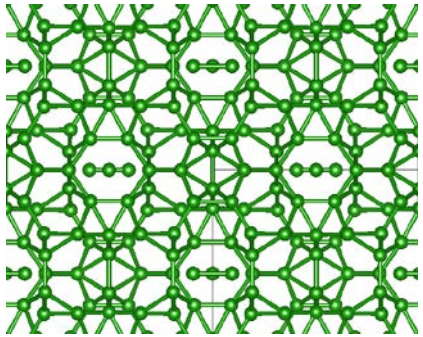

B-54 (6.667eV/atom)
2 year on DFT
8 days on MLIP

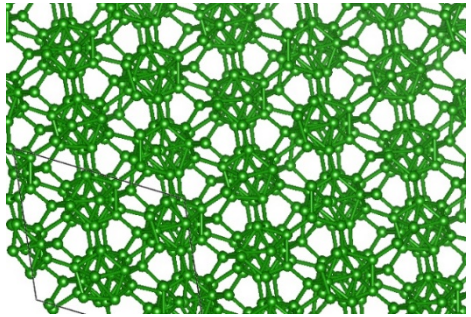

B-106
Best Found on MLIP
within 2 weeks

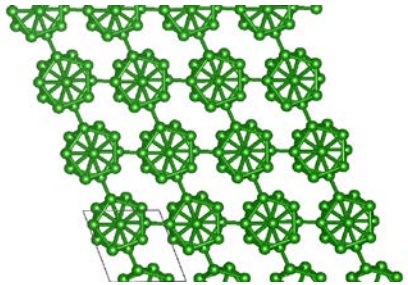

B-108 = B12 x9
10 years with DFT
2 weeks with MLIP

Application #2: thermodynamic integration

- Vibrational entropy of a MoNbTaVW quasi-random structure

Blazej Grabowski, Yuji Ikeda, Fritz Koermann, Christoph Freysoldt, Andrew Duff, A.S., Joerg Neugebauer (2019)

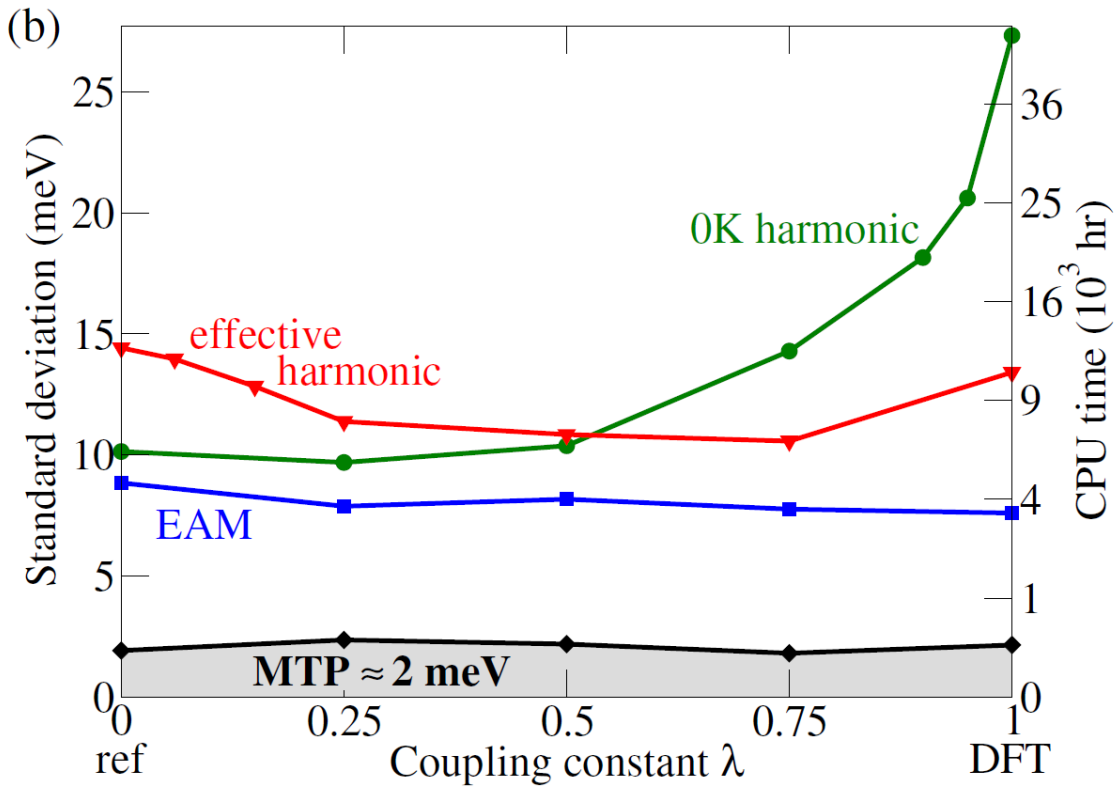

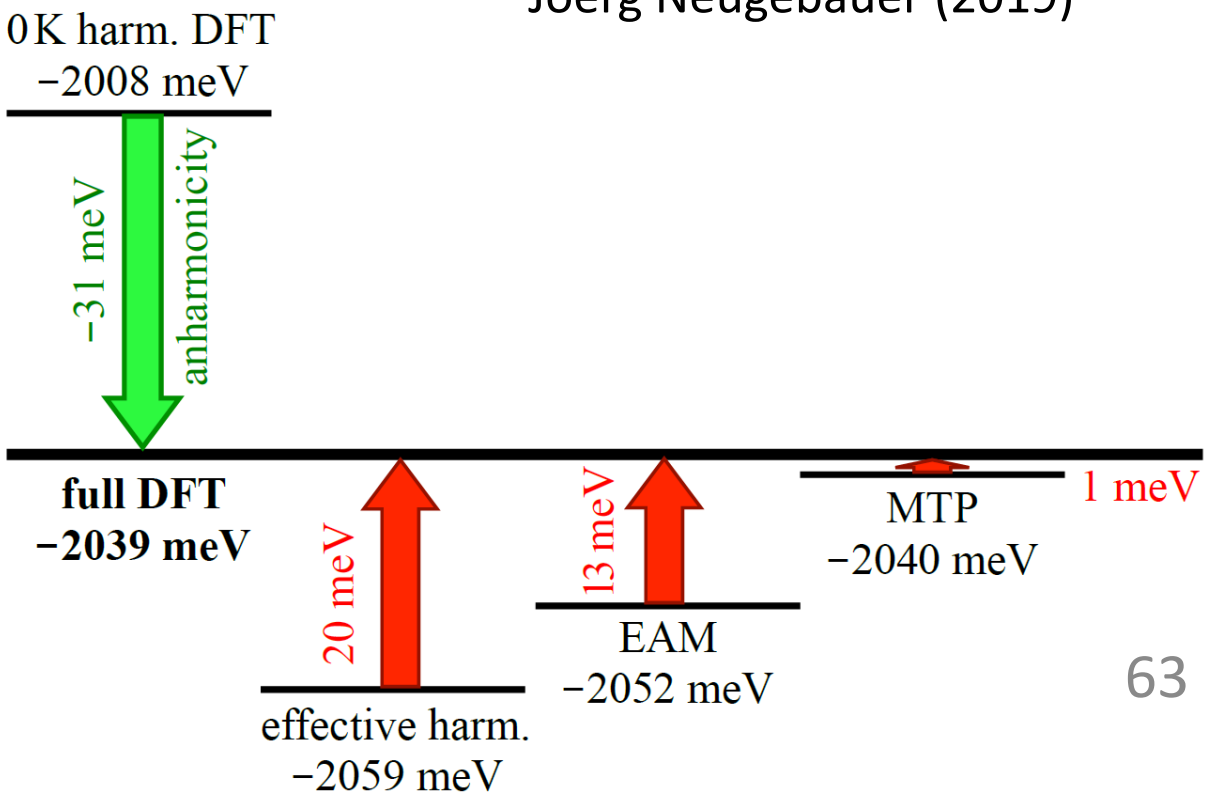

Application #6: automated phase diagrams

(collaboration with Livia Bartok-Partay, Gabor Csanyi, Conrad Rosenbrock and Gus Hart)

- Fitted a potential for Ag-Pd binary system (solid and liquid)

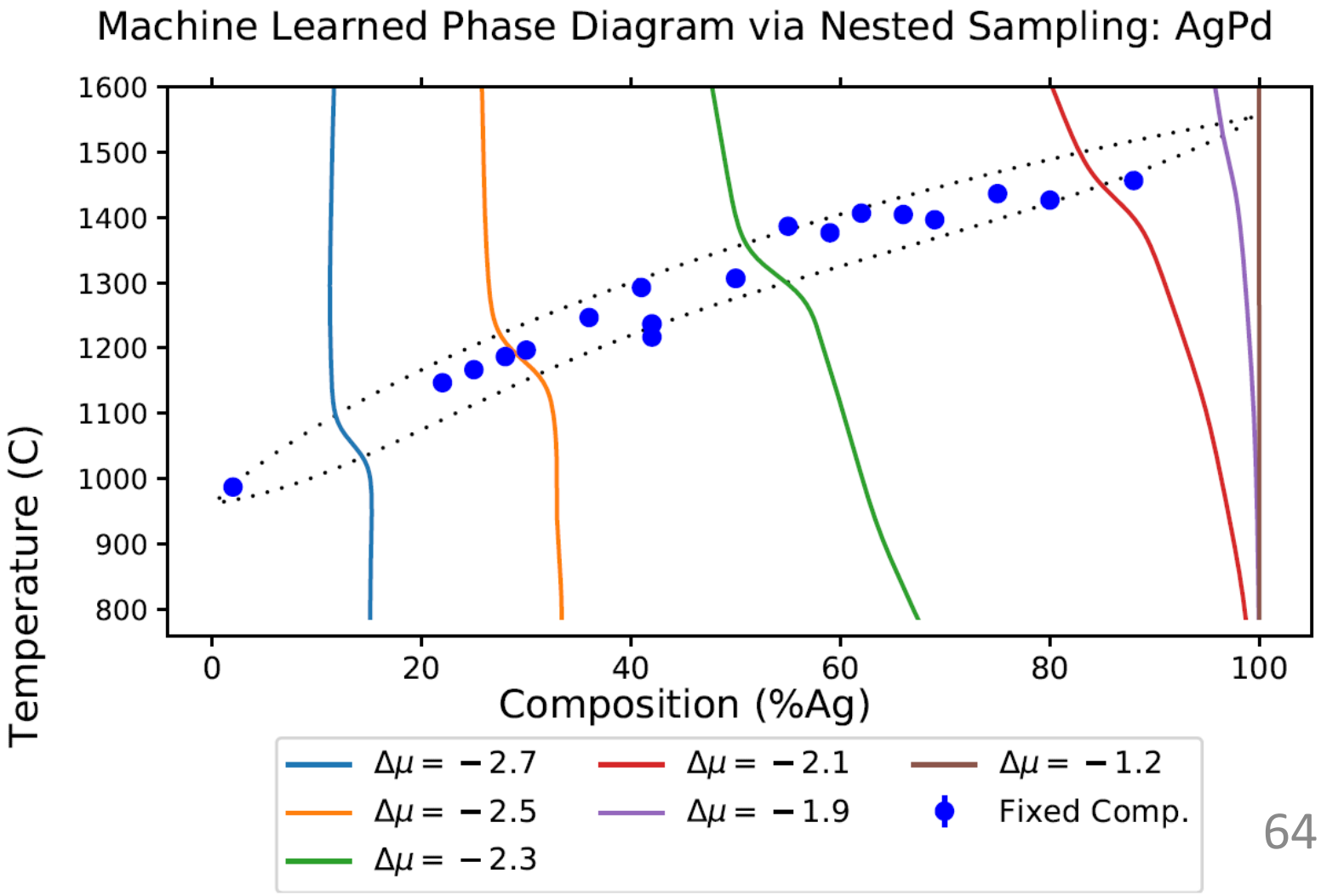

Application #4: elastic properties

A.S., E. Podryabinkin,
K. Gubaev, F. Tasnadi,
Igor Abrikosov (manuscript)

- Elastic constants $C_{11} > C_{12} > C_{44}$ (bcc-Ti)

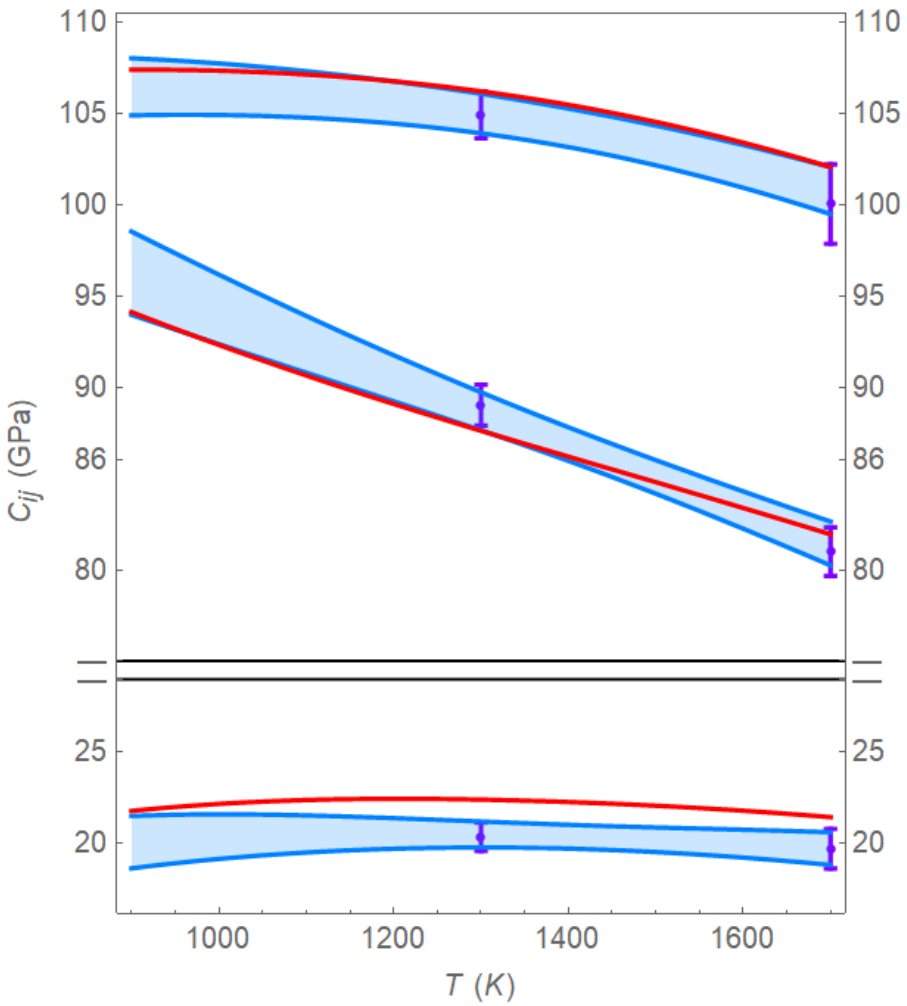

DFT with uncertainty (50 000 DFT-MD time steps)

MTP (negligible statistical uncertainty)

We trade

- 1 GPa statistical error

for

- 1 GPa model error and
- >100x speed-up

First-principles multiscale modeling of thermal conductivity

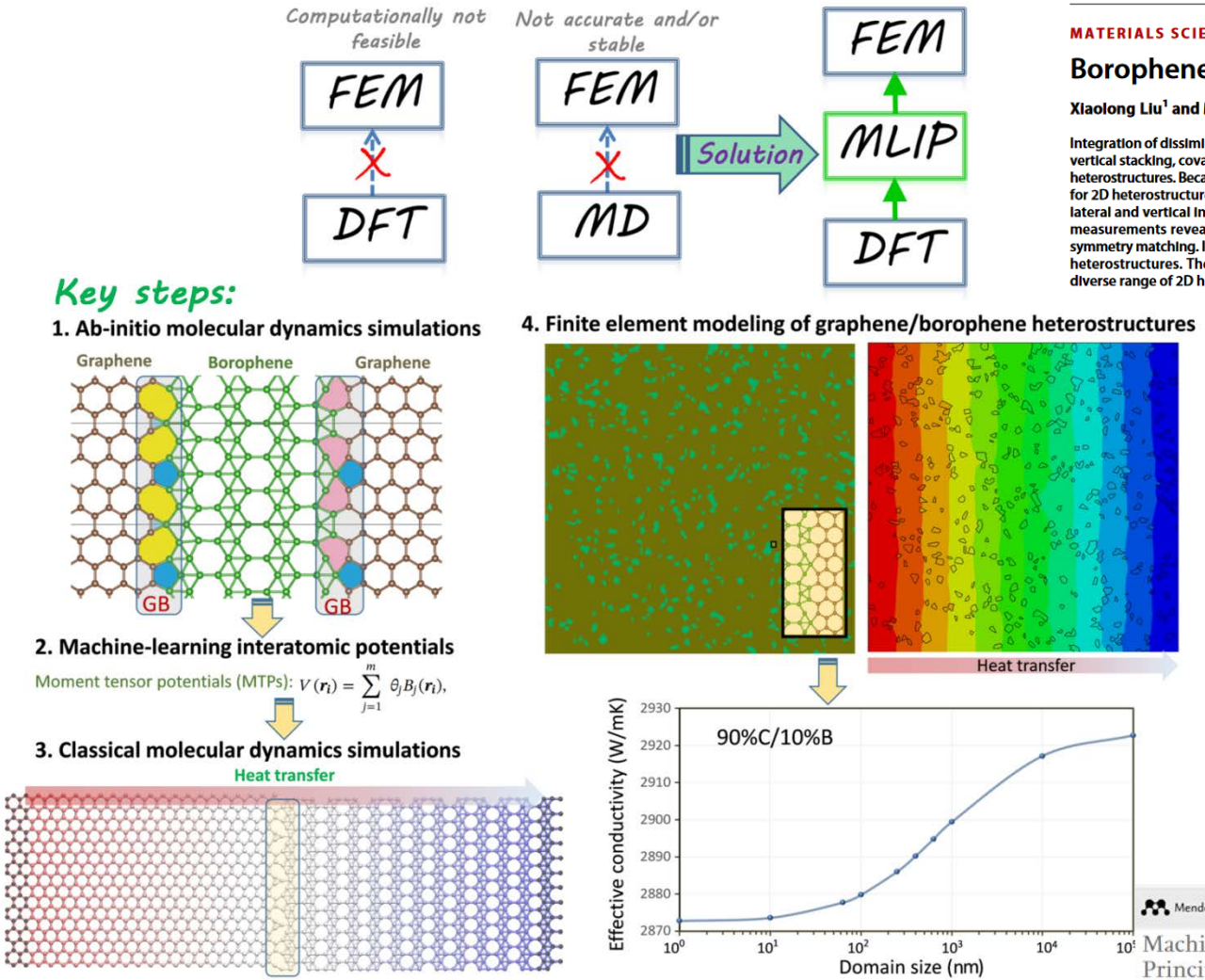

SCIENCE ADVANCES | RESEARCH ARTICLE

MATERIALS SCIENCE

Borophene-graphene heterostructures

Xiaolong Liu[1] and Mark C. Hersam[1,2,3,4]*

Integration of dissimilar two-dimensional (2D) materials is essential for nanoelectronic applications. Compared to vertical stacking, covalent lateral stitching requires bottom-up synthesis, resulting in rare realizations of 2D lateral heterostructures. Because of its polymorphism and diverse bonding geometries, borophene is a promising candidate for 2D heterostructures, although suitable synthesis conditions have not yet been demonstrated. Here, we report lateral and vertical integration of borophene with graphene. Topographic and spatially resolved spectroscopic measurements reveal nearly atomically sharp lateral interfaces despite imperfect crystallographic lattice and symmetry matching. In addition, boron intercalation under graphene results in rotationally commensurate vertical heterostructures. The rich bonding configurations of boron suggest that borophene can be integrated into a diverse range of 2D heterostructures.

Science advances 5 (2019), eaax6444

Mendeley

Machine Learning Interatomic Potentials Enable First-Principles Multiscale Modeling of Lattice Thermal Conductivity in Graphene/Borophene Heterostructures

Published: 10 May 2020 | Version 1 | DOI: 10.17632/pbgscy3ptg.1

Contributor(s): Bohayra Mortazavi, Alexander V. Shapeev, Evgeny V. Podryabinkin

Mater. Horiz., 2020, https://doi.org/10.1039/D0MH00787K

http://dx.doi.org/10.17632/pbgscy3ptg.1

First-principles multiscale modeling of thermal conductivity

Lattice thermal conductivity of pristine crystals

Classical MD simulations

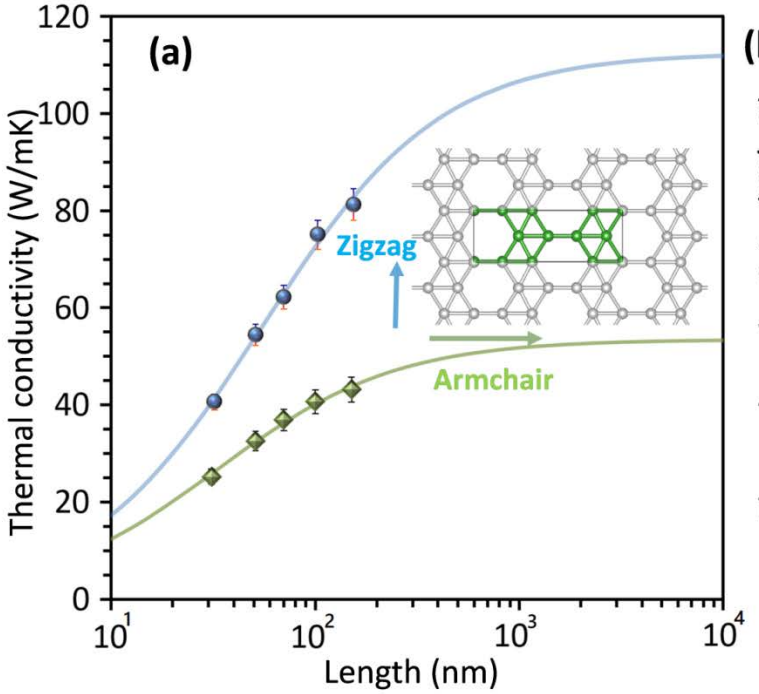

BTE solution of thermal conductivity

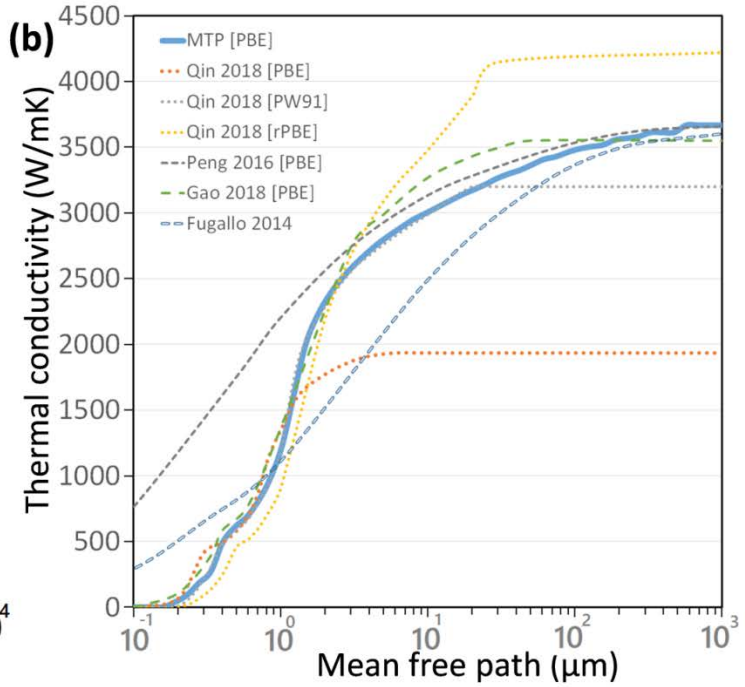

MTP can be employed to estimate the thermal conductivity, either with MD simulations (desirable for low-symmetry structures) or BTE solution.

MTP/ShengBTE: http://dx.doi.org/10.17632/fmkvzbk3nt.1

Mendeley

Accelerating first-principles estimation of thermal conductivity by machine-learning interatomic potentials: A MTP/ShengBTE solution

Published: 8 Jun 2020 | Version 1 | DOI: 10.17632/fmkvzbk3nt.1

Contributor(s): Bohayra Mortazavi, Alexander shapeev, Evgeny Podryabinkin , Xiaoying Zhuang

Mater. Horiz., 2020, https://doi.org/10.1039/D0MH00787K

First-principles multiscale modeling of thermal conductivity

Thermal conductance of grain boundaries

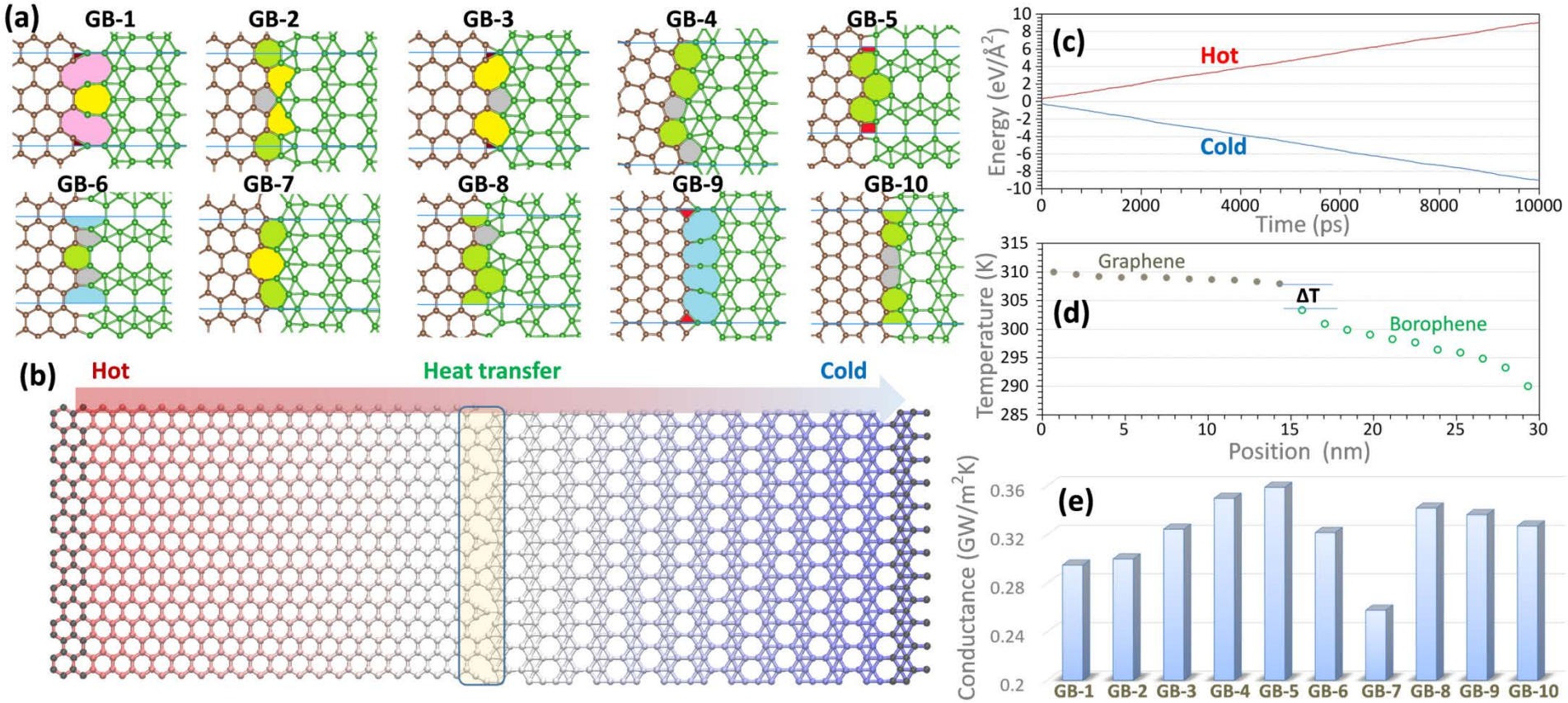

Mater. Horiz., 2020, https://doi.org/10.1039/D0MH00787K

First-principles multiscale modeling of thermal conductivity

Finite element modeling of heterostructures

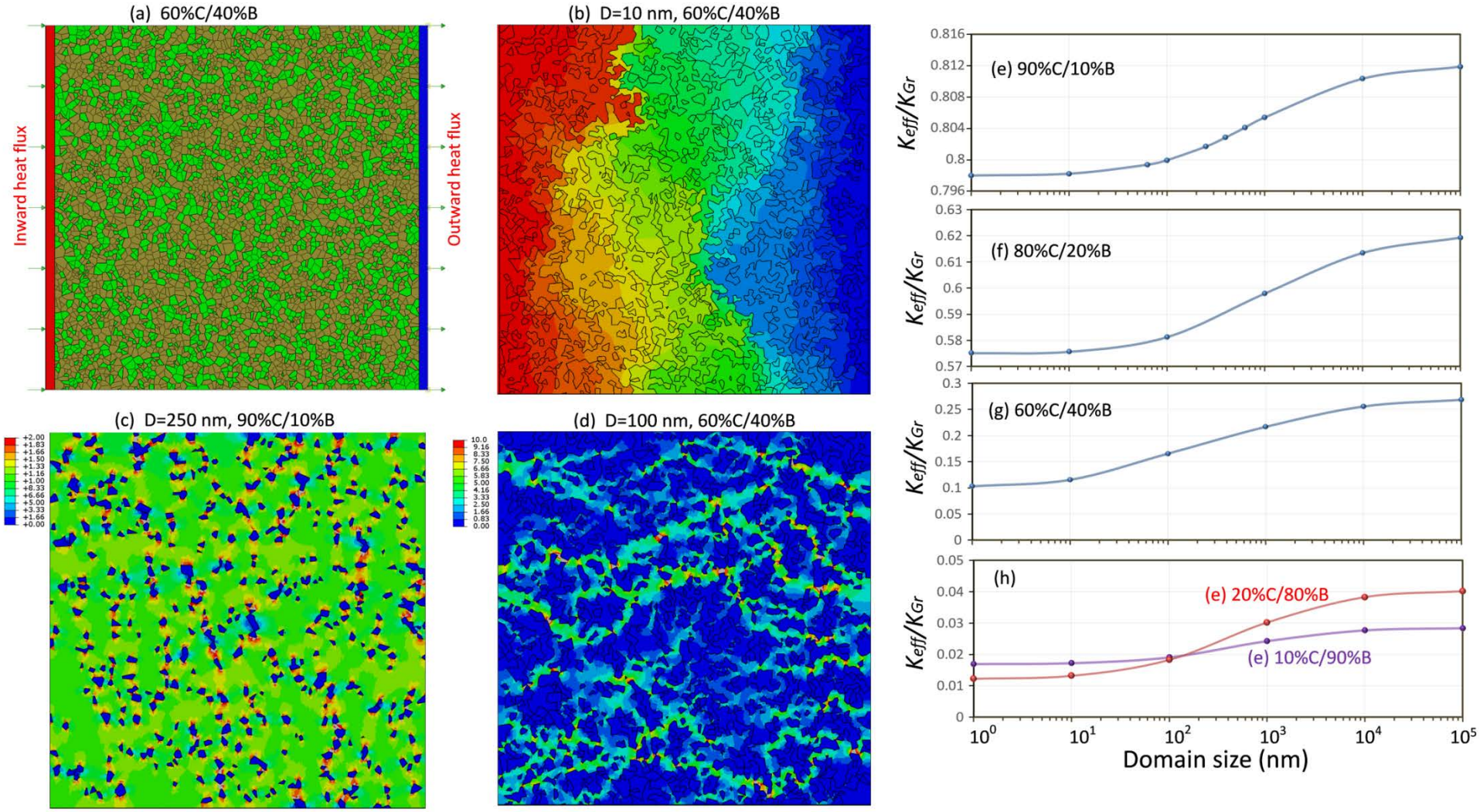

Mater. Horiz., 2020, https://doi.org/10.1039/D0MH00787K

Schematic of the (desired) algorithm

Example for screw dislocation motion in bcc metals

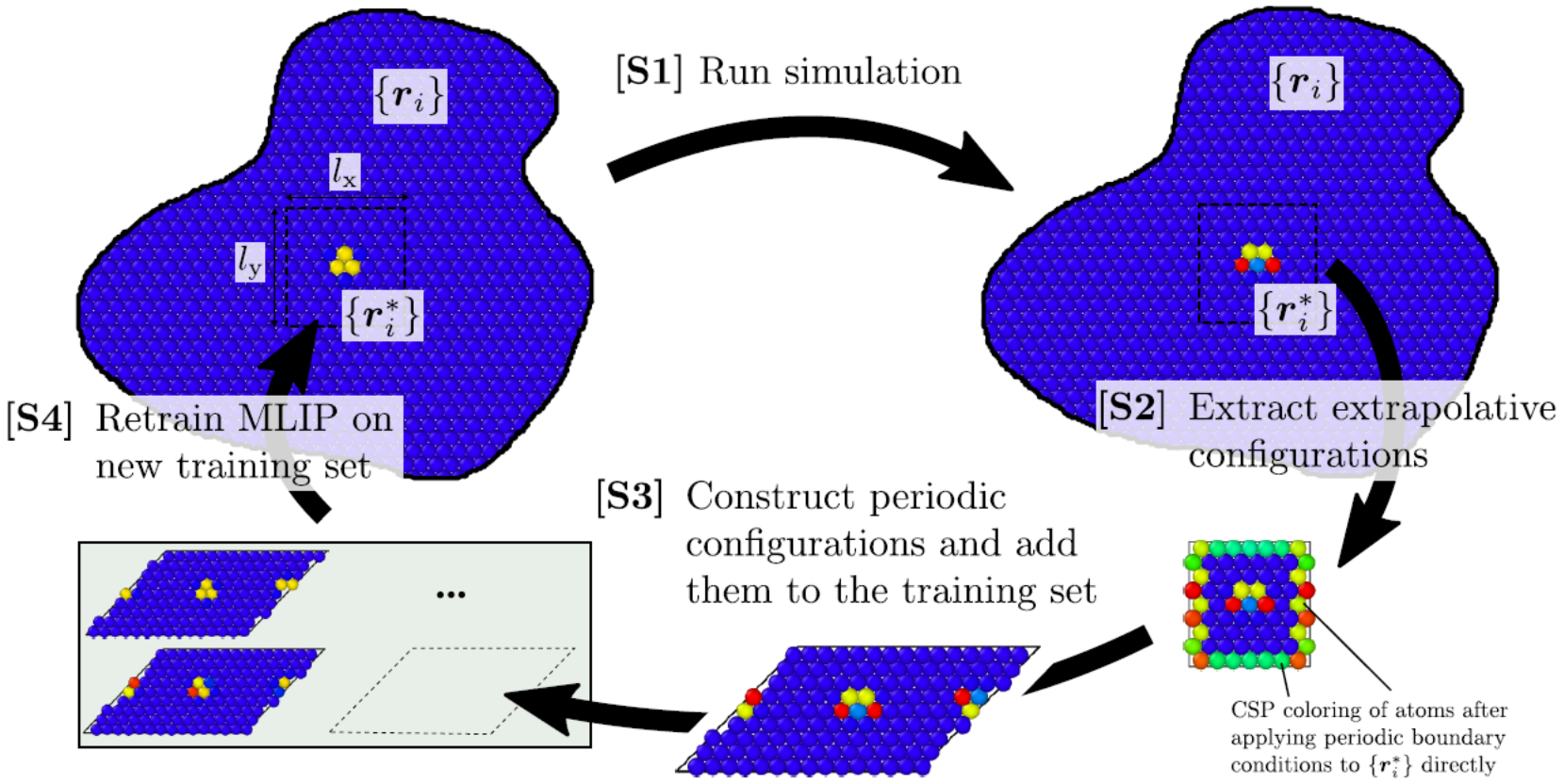

Main difficulty: how to construct these periodic training configurations?

WORK IN PROGRESS: Simulation of nanoindentation for hardness calculation

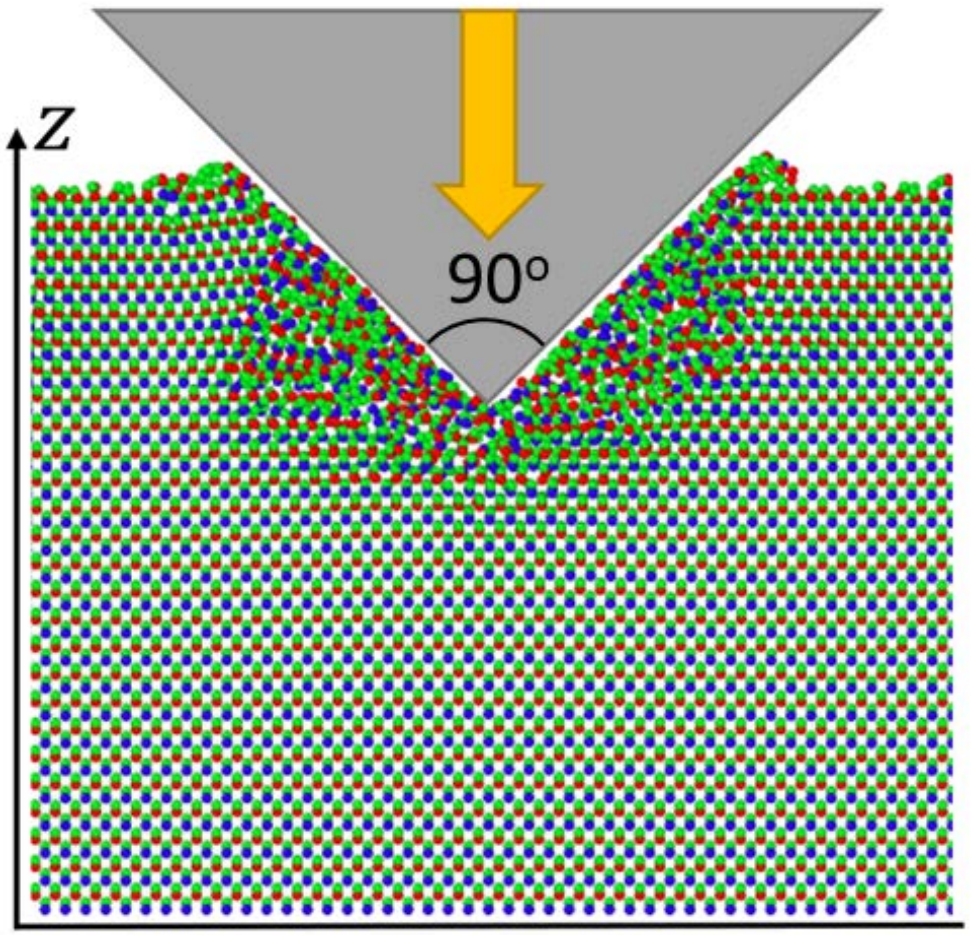

E. Podryabinkin, A. Kvashnin, … A.S.

Calculated hardness vs. measured

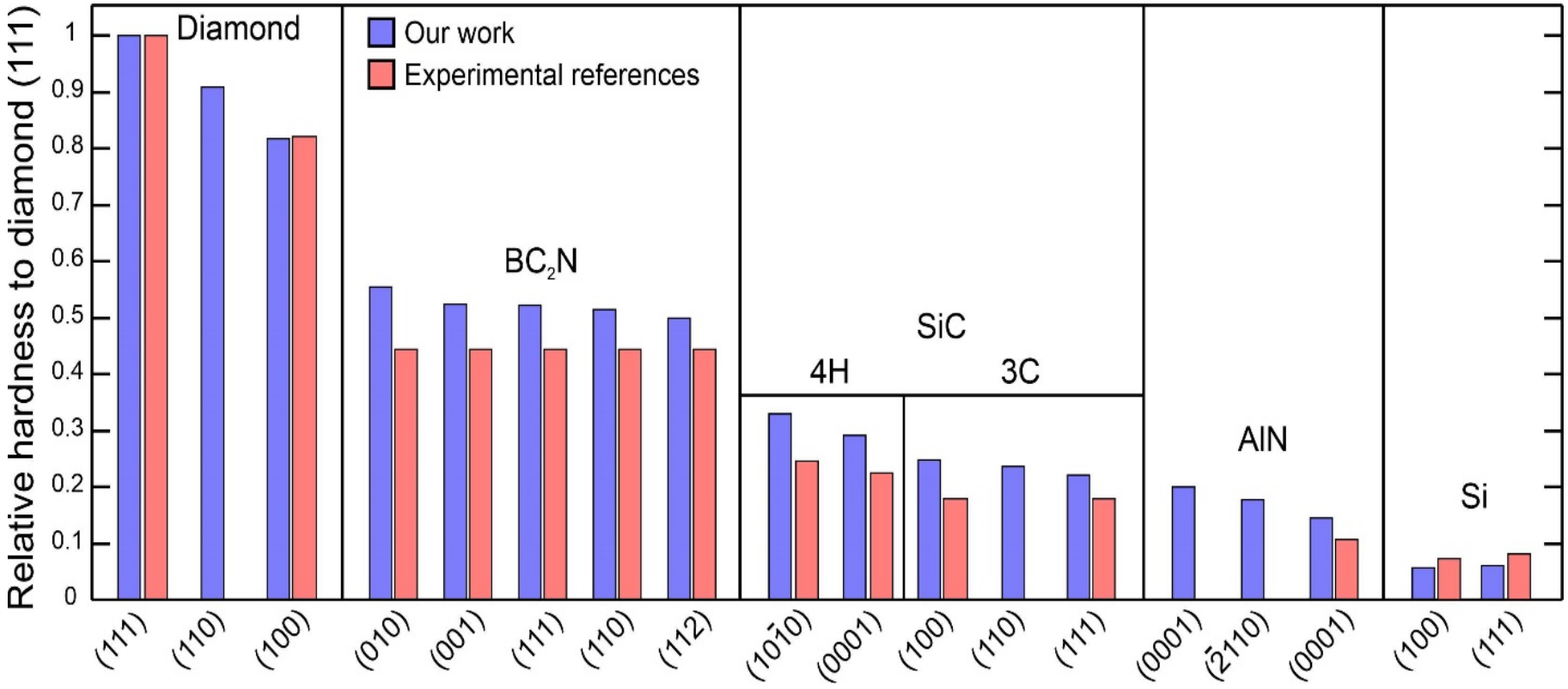

Calculated nanohardness of the considered compounds with respect to the hardest diamond (111) surface in comparison with the available experimental data

On-lattice models: HEAs

T. Kostiuchenko,
Fritz Koermann,
Joerg Neugebauer, A.S. (2019)

- Atoms of different kind sit in the lattice sites.
- Problem: predict the interatomic interaction energy (formation energy, mixing enthalpy)

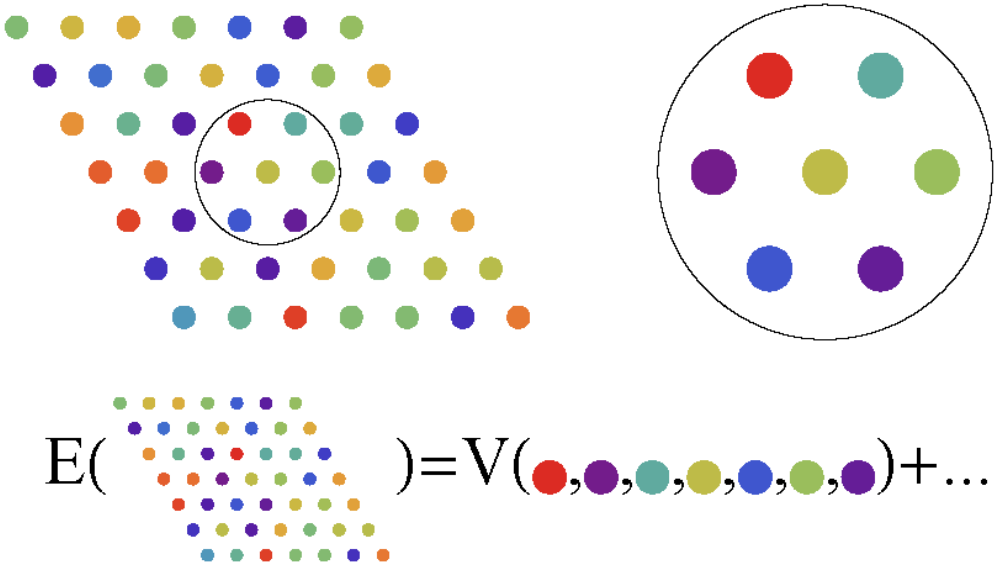

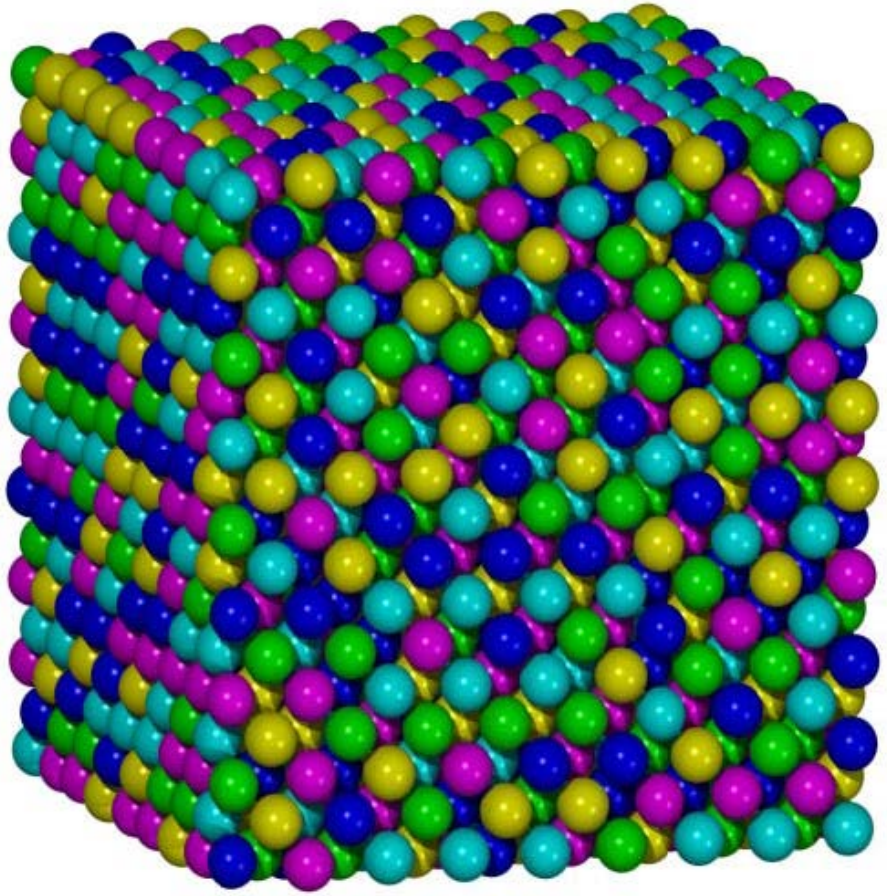

Comparison with existing methods: without local lattice distortions

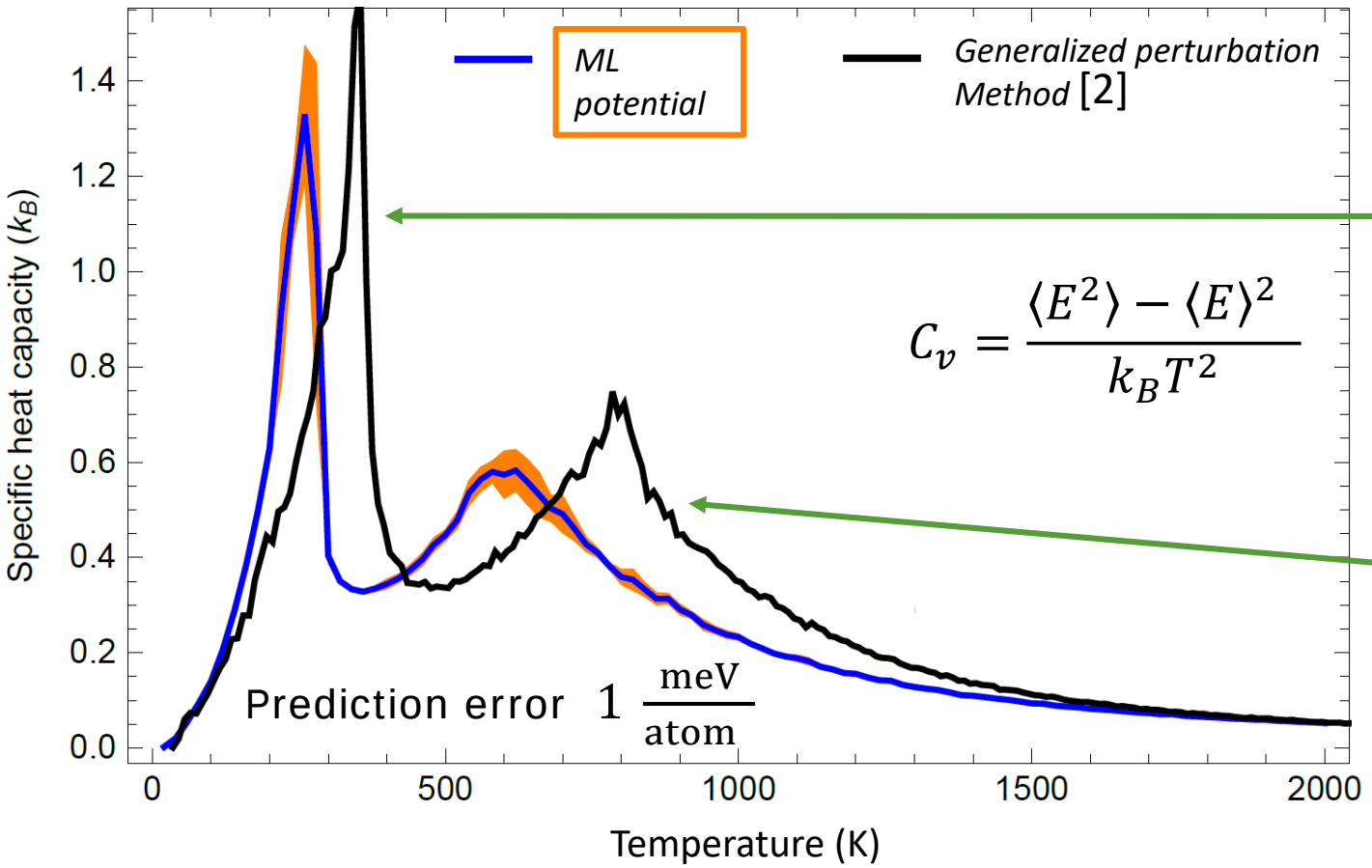

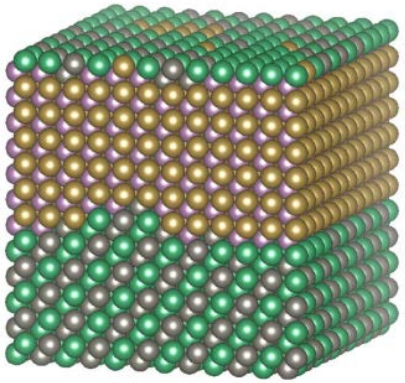

B2(Mo,Ta)

B32(Nb,W)

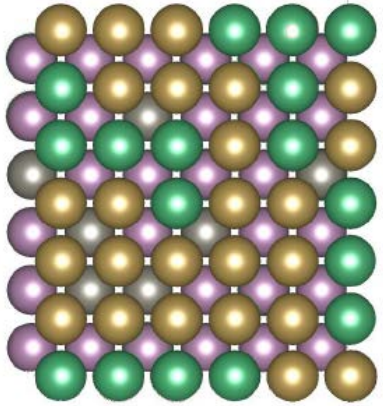

B2(Mo,W;Ta,Nb)

Nb Ta

Mo W

[2] Fritz Körmann, Andrei V Ruban, and Marcel HF Sluiter. Long-ranged interactions in bcc NbMoTaW high-entropy alloys. Materials Research Letters, 5(1):35-40, 2017.

Results & discussion: accounting for local lattice distortions

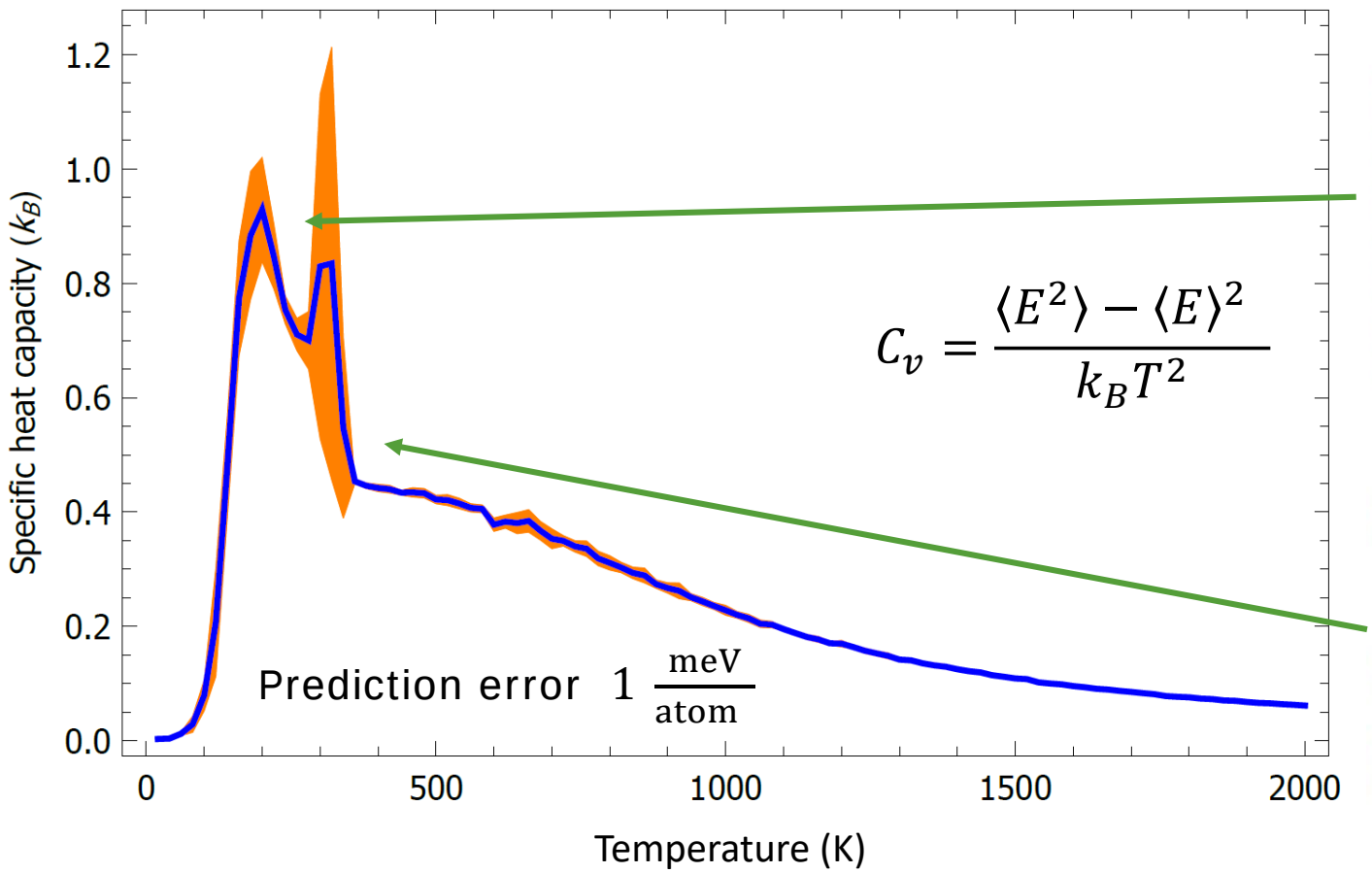

$$C_v = \frac{\langle E^2 \rangle - \langle E \rangle^2}{k_B T^2}$$

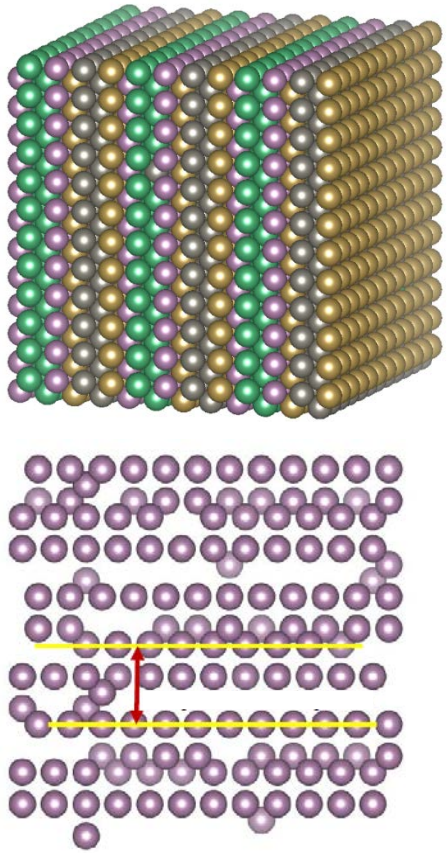

Nb-Mo-Ta-W-W-Ta-Mo-Nb

Semi-ordered lattice structure

$\langle 100 \rangle$

Nb Ta

Mo W

Investigation of complex multicomponent alloys with machine-learning interatomic potentials

Tatiana Kostiuchenko
Andrei V. Ruban
Jörg Neugebauer
A.S.
Fritz Körmann

VCoNi alloy (fcc, magnetic binary alloys)

Short-range order in face-centered cubic VCoNi alloys

Before accounting for local lattice relaxation

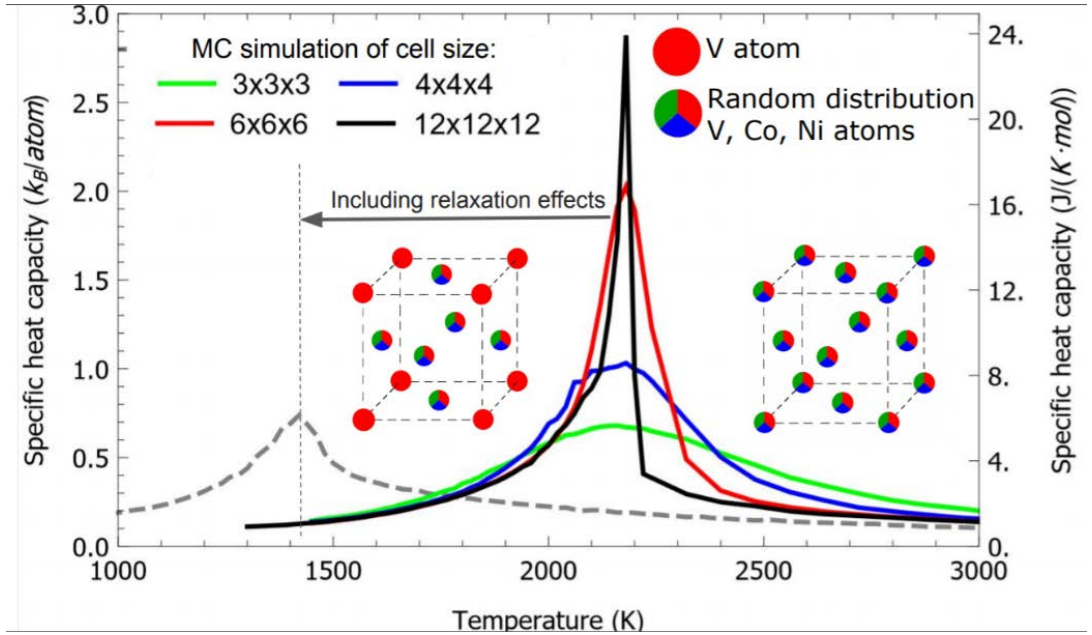

After accounting for local relaxation

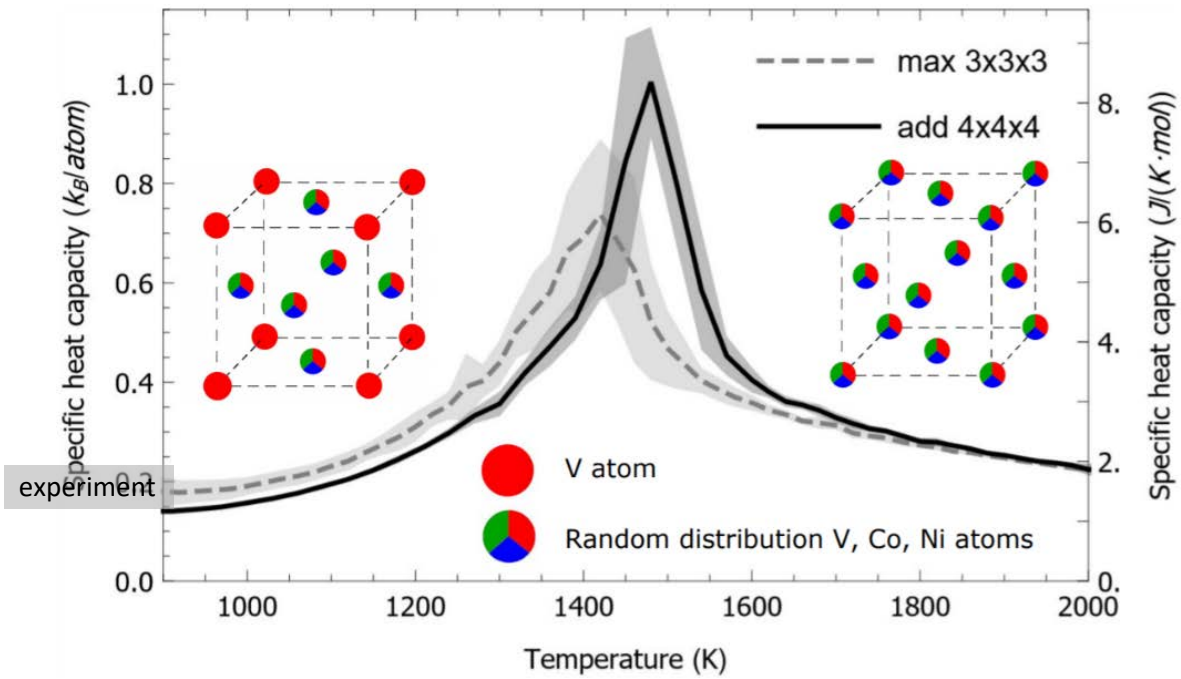

Short-range order in face-centered cubic VCoNi alloys

M3V structure

(Co,Ni)3V

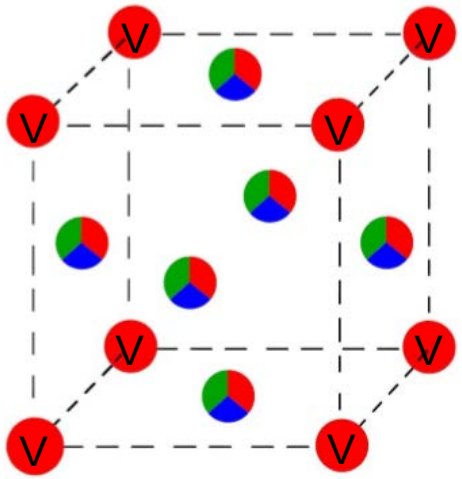

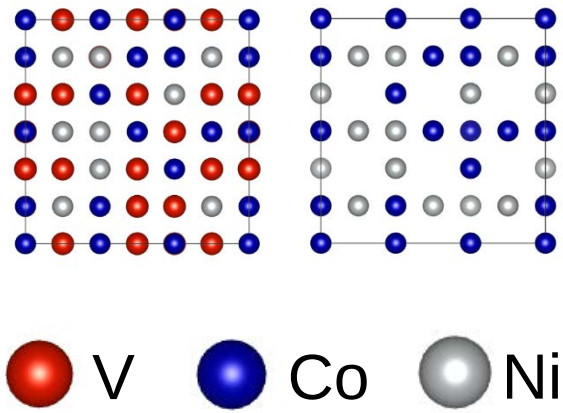

Acta Materialia 194 (2020) 106–117

Contents lists available at ScienceDirect

Acta Materialia

journal homepage: www.elsevier.com/locate/actamat

Full length article

High-rate superplasticity in an equiatomic medium-entropy VCoNi alloy enabled through dynamic recrystallization of a duplex microstructure of ordered phases

Seok Su Sohn[a,*], Dong Geun Kim[b], Yong Hee Jo[b], Alisson Kwiatkowski da Silva[c], Wenjun Lu[c], Andrew John Breen[d,e], Baptiste Gault[c,f], Dirk Ponge[c]

[a] Department of Materials Science and Engineering, Korea University, Seoul 02841, Republic of Korea
[b] Center for High Entropy Alloys, Pohang University of Science and Technology, 37673 Pohang, Republic of Korea
[c] Max–Planck–Institut für Eisenforschung GmbH, Max–Planck–Straße 1, 40237 Düsseldorf, Germany
[d] Australian Centre for Microscopy & Microanalysis, The University of Sydney, Sydney, NSW 2006, Australia
[e] School of Aerospace, Mechanical & Mechatronic Engineering, The University of Sydney, Sydney, NSW 2006, Australia
[f] Department of Materials, Royal School of Mines, Imperial College, Prince Consort Road, London, SW7 2BP, United Kingdom

ARTICLE INFO

Article History:
Received 13 February 2020
Accepted 29 March 2020
Available online 14 May 2020

Keywords:
Multi-principal element alloy
Superplasticity
Ordered phase
Dynamic recrystallization
Dynamic grain coarsening

ABSTRACT

Superplasticity proceeds from fine-grained structures and requires high intrinsic resistance to grain growth at the deformation temperature. Here, we show that a mixture of two kinds of brittle ordered phases enables superplastic behavior through dynamic recrystallization in an equiatomic medium-entropy VCoNi alloy as a model material. The alloy annealed at 900 °C exhibits a face-centered-cubic single phase. However, in-depth characterization at various length scales reveals that the alloy, when annealed at 800 °C, comprises two ordered phases: κ ($(Co_{1.2}Ni_{1.2})V$) and σ ($(Co_{1.2}Ni)V_{1.2}$). As a result of the conventional cold-rolling/annealing process and with the aid of an underlying eutectoid reaction, the alloy exhibits a duplex structure with an average grain size of less than 1 μm, i.e. microduplex structure. The size, morphology, and crystallographic orientation do not substantially change during static isothermal holding at 800 °C, which implies a very high resistance to grain growth. With tensile deformation at 800 °C, however, both phases develop into an equiaxed microstructure with low dislocation density and a dramatic change occurs in the crystallographic texture of the κ phase. These variations result from dynamic recrystallization (DRX), which leads to superplastic elongations of 330–450% at 700–800 °C and at strain rates ranging from 10 to 4 to 10^{-2} s^{-1}. Notably, the superplastic behavior is favorable at the high strain rate due to the enhanced DRX activity, leading to the larger elongation with increasing strain rates. However, deformation-enhanced grain growth occurs concomitantly with dynamic recrystallization; these competitive processes are investigated to elucidate the mechanism of superplasticity in this model material.

1. Introduction

Superplasticity is defined as the capability to exhibit large elongation to failure of over 300% without necking or fracture at elevated temperatures and low stresses in many numerous metals, alloys, intermetallics, and ceramics [1,2]. In metallic materials it is enabled through their fine grains, which are typically smaller than 10 μm, and high resistance to grain growth at the deformation temperature where superplastic forming occurs. Those microstructures are suitable for grain-boundary sliding, which is an essential mechanism to exhibit prolonged extensions and reduce effective stress levels. Although superplasticity occurs in single-phase alloys, it is typically associated with multiple secondary phases hindering grain-boundary migration. In this respect, various eutectic or eutectoid alloys have been investigated in efforts to achieve superplasticity through control of the alloying composition and thermomechanical processing conditions [3–6].

Multi-principal element alloys (MPEAs), also known as high- or medium-entropy alloys (HEAs or MEAs), have attracted extensive attention because of their promising mechanical responses and functional properties [7–11]. The formation of disordered single-phase solid solutions (either face-centered cubic (fcc), body-centered cubic (bcc), or hexagonal closed-packed (hcp), instead of intermetallics or multiphase alloys, is the major defining characteristic of such alloying strategies. The high configurational entropy significantly contributes to the total free energy by overcoming the enthalpies of compound formation and phase separation. According to the prerequisite for

* Corresponding author.
E-mail address: ssohn@korea.ac.kr (S.S. Sohn).

https://doi.org/10.1016/j.actamat.2020.03.048
1359-6454/ 2020 Acta Materialia Inc. Published by Elsevier Ltd. All rights reserved.

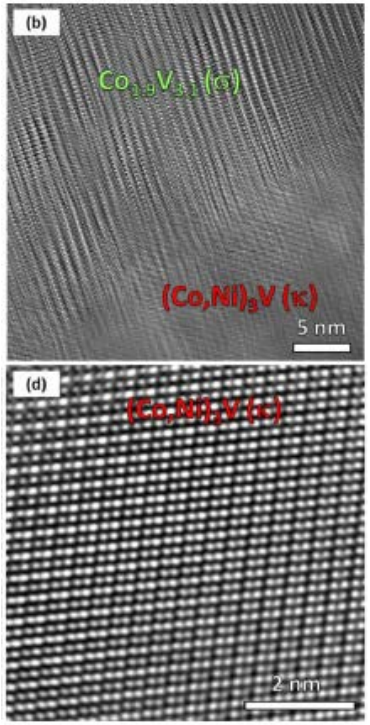

Summary: MLIP Code

- Public version: http://mlip.skoltech.ru/
  - developer's version (incl. unpublished capabilities) by request
- QM model interfaces:
  - VASP, Gaussian (DFT)
- Atomistic Driver interfaces:
  - LAMMPS, serial and parallel (but no learning on the fly)
  - USPEX
  - ASE
  - RPMDrate
- Active learning / Learning on the fly